



universität
wien

MASTERARBEIT

Titel der Masterarbeit

„The Role of HDAC1 and HDAC2 in Transcription and Induced
Pluripotency“

Verfasser

Simon Weissmann, BSc

angestrebter akademischer Grad

Master of Science (MSc)

Wien, 2013

Studienkennzahl lt. Studienblatt: A 066 834

Studienrichtung lt. Studienblatt: Masterstudium Molekulare Biologie

Betreuer: Ao. Univ.-Prof. Dr. Christian Seiser

Abstract

The tight regulation of gene expression by transcriptional control is one of the key mechanisms used by multicellular organisms to determine cell fate identity during development or to respond to environmental stimuli. The inability to establish, maintain or alter gene regulatory networks in a coordinated fashion causes developmental defects and various pathological conditions including cancer. One mechanism by which eukaryotic cells regulate the rate of transcription is the reversible addition of small chemical moieties to histones which influences the DNA accessibility for the transcriptional machinery. Among these histone modifications, acetylation of lysine residues is the most extensively studied and represents a dynamic and reversible histone mark that is generally associated with transcriptional activation. The two groups of enzymes which add and remove this mark are the histone acetyl transferases (HATs) and histone deacetylases (HDACs) respectively.

In this project we used a combination of *in vitro* and *in vivo* models to investigate the role of the two highly homologous enzymes HDAC1 and HDAC2. We looked into their importance during transcription on a genome-wide level by combining large-scale expression analysis of HDAC1 and HDAC2 knockdown or HDAC inhibitor treated F9 teratocarcinoma cells to global binding patterns of HDAC1, obtained by chromatin immunoprecipitation followed by next generation sequencing (ChIP-seq). One important part of this study was to optimize technical parameters of the ChIP protocol focusing on the aspects of antibody quality and protein to DNA crosslinking. Here we could show that dual crosslinking by alternative crosslinkers can greatly enhance signal to noise ratios, especially in HDAC1 ChIP-qPCR experiments, and significantly improve the quality of HDAC1 ChIP-seq data. The combinatorial approach of expression and ChIP-seq data revealed a high presence of HDAC1 at active genes and a surprisingly low number of transcriptional changes of HDAC1 bound genes induced by knockdowns or HDAC inhibitor treatment, suggesting an involvement of HDAC1 at different steps of transcriptional regulation. Furthermore, the improved ChIP method was used to describe the molecular binding dynamics of HDAC1 and HDAC2 in the developmental processes in the murine brain and epidermis. To this end, we looked at genes that were deregulated in conditional knockout tissue and we could identify several genes which are important in epidermal and brain development and which show a dynamic recruitment of HDAC1 and HDAC2 that could partly explain the observed phenotypes.

Finally, we tried to elucidate the importance of HDAC1 and HDAC2 during the process of reprogramming somatic to induced pluripotent cells. Therefore, we generated HDAC1 and HDAC2 deficient mouse embryonic fibroblasts (MEFs) by the delivery of a retroviral vector containing a Cre-recombinase and an EGFP-reporter gene. We could show that a direct transduction of freshly isolated MEFs resulted in highly specific knockouts which, unlike HDAC inhibitor treatment, did not improve the reprogramming capacity leading to the conclusion that the deletion of one HDAC does not mimic the effect of global deacetylase inhibition.

Zusammenfassung

Die genaue Regulation der Genexpression durch transkriptionelle Kontrolle ist einer der wichtigsten Mechanismen, die multizelluläre Organismen verwenden um ihre Zellidentität in der Entwicklung zu definieren oder um auf Umweltreize zu reagieren. Das Unvermögen genregulatorische Netzwerke zu etablieren, aufrechtzuerhalten oder koordiniert zu verändern verursacht Entwicklungsdefekte und verschiedene pathologische Erscheinungsformen, unter anderem Krebs. Ein Mechanismus mit dem eukaryotische Zellen Transkription regulieren, ist das reversible Hinzufügen von kleinen chemischen Gruppen, welches die Zugänglichkeit der DNA durch die transkriptionelle Maschinerie beeinflusst. Unter diesen Histonmodifikationen ist Histonazetylierung die am besten erforschte und repräsentiert eine dynamische und reversible Histonmarkierung, welche generell mit transkriptioneller Aktivierung assoziiert ist. Die zwei Enzymgruppen, die diese Markierung hinzufügen und wieder entfernen, sind die Histonazetyltransferasen (HATs) beziehungsweise Histondeazetylasen (HDACs).

In diesem Projekt verwendeten wir eine Kombination aus *in vitro* und *in vivo* Modellen, um die Rolle der zwei homologen Enzyme, HDAC1 und HDAC2, zu untersuchen. Wir analysierten ihre Bedeutung in der Transkription auf einem genomweiten Level, indem wir groß-angelegte Expressionsanalysen von HDAC1 und HDAC2 knockdown oder HDAC Inhibitor (HDI) behandelten F9 Teratokarzinom Zellen, mit globalen Bindemustern von HDAC1 verglichen, welche wir durch Chromatinimmunpräzipitation, gefolgt durch genomweites Sequenzierung, (ChIP-seq) generierten. Ein wichtiger Teil dieser Studie war die Optimierung der technischen Parameter während des ChIP Vorgangs, besonders die Aspekte der Antikörperqualität und des Crosslinkens von Protein zu DNA. Zu diesem Punkt konnten wir zeigen, dass duales Crosslinken das Verhältnis von Signal zu Hintergrund verstärkt, besonders in HDAC1 ChIP-qPCR Experimenten und die Qualität von HDAC1 ChIP-seq Daten signifikant verbessern kann. Das Kombinieren von Expressions- und ChIP-seq Daten zeigte eine starke Präsenz von HDAC1 an aktiven Genen und eine überraschend niedrige Zahl an transkriptionellen Änderungen von HDAC1 gebundenen Genen, die durch Knockdown oder Behandlung mit HDAC Inhibitoren verursacht wurden. Dies lässt eine Beteiligung von HDAC1 an verschiedenen Schritten der transkriptionellen Kontrolle vermuten. Weiters wurde die verbesserte ChIP Technik verwendet um das dynamische Bindeverhalten von HDAC1 und HDAC2 in Entwicklungsprozessen des Mäusehirns und der -epidermis zu charakterisieren. Dazu analysierten wir Gene, welche in knockout Geweben dereguliert waren und konnten dabei mehrere Gene identifizieren, die wichtig für Hirnbeziehungsweise Epidermisentwicklung waren und welche eine dynamische Rekrutierung von HDAC1 und HDAC2 zeigten, die die beobachteten Phenotypen beschreiben könnte. Letztlich, versuchten wir die Bedeutung von HDAC1 und HDAC2 während des Reprogrammierens von somatischen zu iPS Zellen zu ergründen. Dazu generierten wir HDAC1 und HDAC2 defiziente embryonische Fibroblasten, durch das Einbringen eines retroviralen Vektors, welcher eine Cre-Rekombinase und ein EGFP-Reporter Gen enthielt. Wir konnten zeigen, dass die direkte Transduktion von frisch isolierten Fibroblasten höchst spezifische Knockouts erzeugte, welche aber, im Unterschied zur Behandlung durch HDIs, keine Erhöhung des Reprogrammierungspotential erwirkten. Dies führte zu dem Schluss, dass die Deletion einer HDAC nicht den Effekt von globaler Histondeazetylasehemmung rekonstituieren kann.

Contents

Contents	1
1 Introduction	3
1.1 Eukaryotic chromatin organization	3
1.2 Promoter-architecture and transcriptional initiation	4
1.3 Transcriptional regulation and chromatin	5
1.3.1 Epigenetics	5
1.3.2 The histone code hypothesis	6
1.3.3 Lysine acetylation	6
1.3.4 Histone acetyltransferases	8
1.3.5 Histone deacetylases (HDACs)	9
1.3.6 HDAC inhibitors	11
1.4 Chromatin in pluripotency and reprogramming	12
1.4.1 The embryonic stem cell state	12
1.4.2 Reprogramming of somatic cells by defined factors	13
1.4.3 Small molecules in reprogramming	15
1.5 The epidermis	16
1.5.1 Epidermal structure, self renewal and differentiation	16
1.5.2 The epidermal differentiation complex	17
1.5.3 The role of HDAC1 and HDAC2 in epidermal development	17
1.6 Histone acetylation in neural cell-type specification	18
1.6.1 HATs and HDACs in brain development	18
2 Materials and Methods	20
2.1 Cell Culture	20
2.1.1 Media and solutions	20
2.1.2 Culturing teratocarcinoma cells	20
2.1.3 Culturing a human osteosarcoma (U2OS) cell line	21
2.1.4 Culturing embryonic stem cells (ESCs) on gelatin	21
2.1.5 Generation of irradiated feeder cells for ESC culture	21
2.1.6 Culturing ESCs on a layer of irradiated feeder cells	21
2.1.7 Inhibitor treatment	22
2.2 Handling RNA	22
2.3 Chromatin Immunoprecipitation	23
2.3.1 Solutions and Buffers	23
2.3.2 Crosslinking and harvesting of <i>in vitro</i> cultured cells	24
2.3.3 Crosslinking and harvesting of tissue samples	24
2.3.4 Chromatin shearing	25
2.3.5 Setting the IP	26
2.3.6 Washing the IP	27
2.3.7 DNA Precipitation	27

2.3.8	Quantitative PCR (qPCR)	28
2.3.9	DNA purification and RNase treatment for sequencing	30
2.4	Protein analysis	30
2.4.1	Whole Cell Protein extraction (Hunt Extraction)	30
2.4.2	Histone isolation	30
2.4.3	SDS-PAGE and Western Blots	31
2.5	Antibody purification	32
2.5.1	Heterologous expression and purification of His-tagged HDAC1 and HDAC2	32
2.5.2	Purification of polyclonal antibodies	34
2.5.3	Enrichment of monoclonal antibodies from hybridoma supernatant	35
2.6	Generation of HDAC1 and HDAC2 deficient Mouse Embryonic Fibroblasts (MEFs)	35
2.6.1	Plasmid production	35
2.6.2	Extraction and direct transduction of unfrozen Mouse Embryonic Fibroblasts	36
2.6.3	Genotyping PCR	38
2.6.4	Detection of HDAC1 and HDAC2 knockouts	39
3	Results	40
3.1	Expression and HDAC1 ChIP-seq data can be validated by site-directed ChIP and qPCR in F9 teratocarcinoma	40
3.2	The HDAC1 ChIP in ESCs does not show reproducible results	44
3.3	Antibody purification	45
3.4	HDAC1 and HDAC2 ChIPs can be improved with the alternative crosslinker DSG	47
3.5	The alternative crosslinker DSG improves the results in HDAC1 ChIP-seq experiments	50
3.6	HDAC1 may dissociate from the promoter of the <i>Cdkn1a</i> (p21) gene during its activation	57
3.7	Molecular characterization of conditional HDAC1 and HDAC2 knockout models in murine epidermis	60
3.8	Molecular characterization of conditional HDAC1 and HDAC2 knockout models in the murine nervous system	65
3.9	Generation of HDAC1 and HDAC2 deficient Mouse Embryonic Fibroblasts	69
4	Discussion	77
4.1	Preliminary HDAC1 binding data and response to HDIs suggests three models of action	77
4.2	Optimization of HDAC1 and HDAC2 ChIPs	78
4.3	Transcriptional regulation by HDAC1 and HDAC2	79
4.4	HDAC1 and HDAC2 in epidermal knockout mouse models	83
4.5	HDAC1 and HDAC2 in brain development	84
4.6	HDAC1 and HDAC2 in reprogramming	85
	References	87
	CURRICULUM VITAE	93

1 Introduction

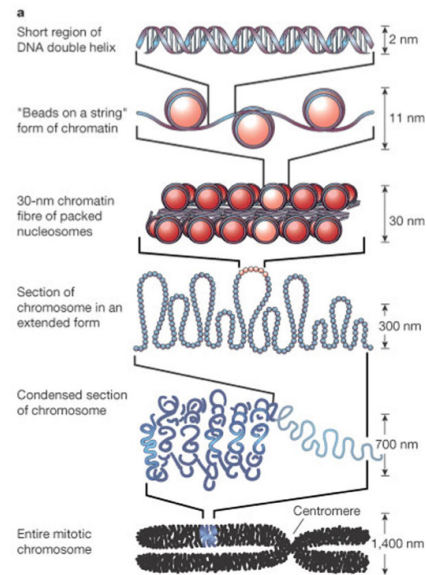
1.1 Eukaryotic chromatin organization

Due to the immense length, eukaryotic DNA has to be organized and tightly folded in order to fit into the nucleus. The DNA is packed onto scaffolding histone and non-histone proteins forming a polymer called chromatin. The basic subunit, the nucleosome, consists of the core histone octamer (one tetramer of H3 and H4 and two dimers of H2A and H2B) which are highly conserved among various species. These core histones are highly basic which allows for a tight association with acidic DNA. Together with a stretch of roughly 147 bp of DNA that is wrapped around this octamer and together with a linker DNA the so called “beads on a string” structure is formed. This structure can be tightened by the evolutionary less conserved H1 linker histone into a filament called 30 nm fibre. From this structure the packaging complexity can be increased up to the dense mitotic chromosomes (Figure 1). The process of further compaction is not entirely understood yet since several structural models already exist for lower degrees of packaging suggesting that the 30 nm fibre is highly dependent on the size of the linker DNA [1]. Eukaryotic chromatin can occur in a condensed and highly compact form, called heterochromatin and in an open structure called euchromatin. These different states are characterized by the degree of interaction between DNA and histones as well as the presence of binding proteins, chromatin remodelers and histone modifications which allow the chromatin to switch between these forms.

Core histones consist of a globular C-terminal part residing in the center of the nucleosome and flexible N-terminal parts, which are also referred as histone tails. These tails protrude out of the nucleosomes and can interact with other nucleosomes or are involved in the recruitment of non-histone proteins which makes them a hub for binding proteins. Furthermore, the amino acids within these tails (but also within the central globular domain) are often targeted by post-translational modifications.

Apart from the subset of major histones other histone variants exist (with the exception of H4) which share a high percentage of sequence identity with their canonical counterparts. These variants can get incorporated into the nucleosomes, which leads to alteration of the chromatin structure. Histone variants and their modifications, can play different roles in a variety of cellular processes. For example H2A.Z is incorporated around the transcriptional start site (TSS) and its acetylated version is associated with active genes [2]. Whereas another protein CENP-A, a histone H3 variant, is associated with centromeric DNA [3].

Figure 1: Eukaryotic chromatin is organized in different packaging modes. The 11 nm fibre is DNA wrapped around the histone core, whereas the 30 nm fibre results by the addition of H1 in a structure which is not yet fully understood. 300 and 700 nm structures represents a higher compaction by looping. The 1.4 nm structure exists only in metaphase during chromosome segregation. Adapted from Felsenfeld and Groudine, 2003 [4].



1.2 Promoter-architecture and transcriptional initiation

Transcription is the process of generating RNA molecules from a given DNA sequence. This is done by DNA-dependent RNA polymerases, which read the template DNA from 3' to 5' and generate an exact RNA copy of the DNA coding strand from 5' to 3', except that uracils will replace thymines. RNA polymerases will get recruited to a start region of a gene, which is called promoter. In prokaryotes, only one version of RNA polymerase exist, which contains an exchangeable subunit, the σ factor, which ensures the sequence specific binding.

Unlike to prokaryotes three different eukaryotic RNA polymerases exist, which all generate different types of RNAs. RNA Pol I transcribes genes, encoding large ribosomal RNAs (rRNA) whereas RNA Pol III transcribes tRNAs, 5S RNAs, SINEs and small RNAs (for example U6 spliceosomal RNA, some snoRNAs, or micro RNAs which are upstream of Alu sequences or tRNAs). RNA polymerase II generates mRNAs, micro RNAs and most of the small nuclear RNAs (spliceosomal RNAs for the snRNPs U1, U2, U4, and U5) and snoRNAs (which facilitate tRNA processing). Protein encoding genes will be transcribed by RNA Pol II into a pre-messenger RNA (pre-mRNA or hnRNA), which is processed (addition of 5' cap, 3' polyadenylation and spliced) and exported from the nucleus in order to get translated. The recruitment of RNA Pol II is highly complex and relies heavily on auxiliary factors, called general transcription factors (GTF) and associated factors (TAFs). These transcription factors are called general because they are part of the assembly of the transcription preinitiation complex (PIC) at eukaryotic core promoters [5, 6]. These core promoters can contain different variations of a set of characteristic recognition elements (Figure 2). The most prominent sequence motif in humans is an A/T-rich sequence (TATA-Box) located 25-30 bp upstream of the transcriptional start site (TSS), which is targeted by the TATA-binding protein (TBP). The TBP is part of the large GTF TFIID. Once believed to be a prerequisite of all core promoters, the TATA-box contributes to approximately 35 % of all human genes [7]. The initiator element (Inr) is a sequence from -2 to +4 nucleotides relative to the TSS. It can initiate transcription even in the absence of a conserved TATA-Box, but generally works synergistically with the TATA-Box and is bound by the TBP associated factors

TAF1 and TAF2. Promoters which lack a TATA-Box but contain an initiator element are associated with housekeeping genes. Similar to the TATA-Box, the Downstream Promoter Element (DPE) functions in combination with an initiator element to direct the PIC to the transcriptional start site. The only well characterized element which is not bound by TFIID are the TFIIB recognition elements (BREs) which can be upstream or downstream of the TATA-Box. There is also a second class of promoters, which are characterized by the high presence of CpG dinucleotides. Promoter within this class do not possess a defined single TSS but rather have several within a certain area. Mostly these promoters are associated with housekeeping genes. The general transcription factors are historically called TFIIA, TFIIB, TFIID, TFIIE, TFIIIF, TFIIH, according to their presence in different parts in an sub-cellular fractionation. PIC assembly can occur in a sequential recruitment of the general transcription machinery, mostly starting with the binding of TBP to the TATA-Box, or as a so called “two component” recruitment of a preassembled RNA pol II holoenzyme and TFIID to the core promoter [5]. Once this open complex is established, transcriptional initiation starts by the addition of two initiating NTPs complementing the DNA sequence and formation of the first phosphodiester bond. After initiation, RNA pol II has to pass a stage called “promoter clearance”, where the PIC is partially disassembled, while a subset of GTFs remains bound to the promoter and serves as a scaffold for the next transcription initiation complex.

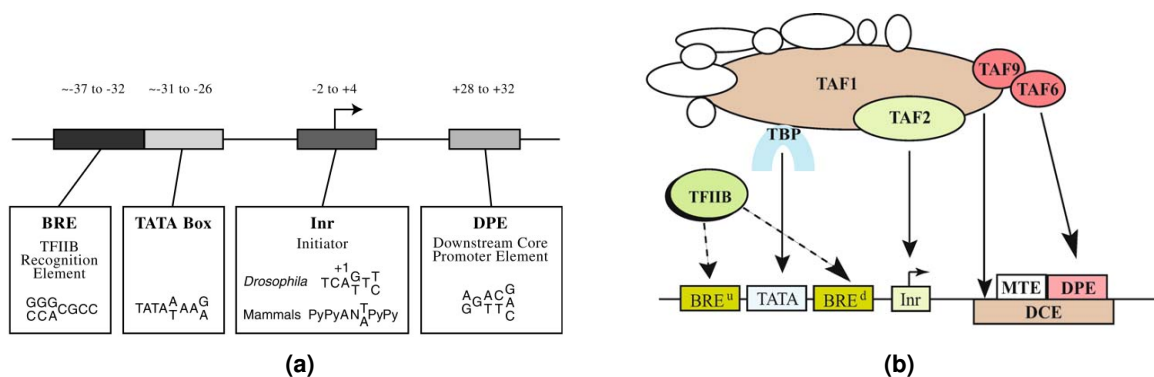


Figure 2: Eukaryotic core promoter motifs. **a:** These motifs have been found to contribute to transcription from a core promoter. They can occur at promoters in different combinations, or can be absent at all. (Figure from Smale *et al.*, 2003 [5]) **b:** Transcription factors binding to the core promoter elements. MTE (Motif Ten Element), DCE (Downstream Core Element) (Figure from Thomas *et al.*, 2006 [6])

1.3 Transcriptional regulation and chromatin

1.3.1 Epigenetics

The human genome comprises approximately 25.000 genes which represent the blueprint for more than 200 different types of cells in the human body. It is important to be aware that all these cells contain the same set of DNA, but they execute a huge variety of different functions. During development, totipotent stem cells, derived from the fertilized zygote, transform into various pluripotent cell lines of the embryo, which in turn become more and more specialized until they form fully committed cell lines, as diverse as neurons, muscle cells, epithelium, endothelium of blood vessels and many more. The key concept behind this process is the differential

expression of genes, which is fine tuned and maintained by gene regulatory mechanisms. In fact there are several levels of regulation, which are summarized under the term of “epigenetics”. Epigenetics can be defined as a change in gene expression underlying a phenotype that is heritable but does not involve a change in the nucleotide sequence in DNA. The molecular basis of epigenetics is the chemical modification of DNA or histones but also chromatin remodelling, the use of histone variants and post-transcriptional regulation like RNA interference. The combination of these mechanisms, the “epigenome”, defines the identity of a cell and in contrast to the genome differs greatly between cell lines.

1.3.2 The histone code hypothesis

The N-terminal tails of histones but also their globular domains can be targeted by histone modifying enzymes which can catalyze acetylation, methylation, phosphorylation and ADP-ribosylation. These modifications are added by “writer”, removed by “eraser” and recognized by “reader” proteins and can have an impact on chromatin accessibility, transcription, DNA replication and DNA repair. The histone code hypothesis proposes that a certain combinatorial pattern of histone modifications defines the activity state of the corresponding gene. These modifications can either alter the DNA accessibility by changing the DNA-histone interaction, by neutralizing the net charge difference between these molecules (only true for acetylation and phosphorylation) or lead to the recruitment of reader proteins. The combinatorial patterns can span nucleosomes, and therefore a “nucleosome code” has been suggested by the original authors Allis and Jenuwein [8], describing that the collective nucleosomal modifications regulate the underlying gene.

1.3.3 Lysine acetylation

The acetylation at the ϵ -amine group of the side chain of lysine residues is catalyzed by lysine acetyltransferases (KATs) and removed by lysine deacetylases (KDACs). KATs and KDACs were first identified as enzymes acting on histone proteins and for this reason the terms histone acetyl transferases (HATs) and histone deacetylases (HDACs) are often used for many KATs and KDACs. In addition to histone proteins, which present the most abundant substrate, many non-histone targets have been characterized so far: transcription factors (like p53 and Rb proteins), metabolic enzymes (Pyruvate kinase and Acetyl-CoA synthase), structural proteins (α -tubulin), enzymes involved in DNA dynamics (PCNA) as well as exogenous viral proteins (SV40 T antigen or HIV integrase) (reviewed in [9]). For that reason it was proposed to rename them more appropriately lysine acetyltransferases or lysine deacetylases (KAT and KDAC) [10]. Since the terms HAT and HDAC have historically entered into the acetylation field they will be used throughout this thesis.

Histone acetylation during nucleosome assembly and chromatin folding During S phase of the cell cycle, the cell replicates its complete DNA prior to mitosis. This newly synthesized DNA has to be packed into nucleosomes to form chromatin, which is the basis for the tightly packed structure of metaphase chromosomes. During replication the existing histones are ran-

domly distributed onto the two strands of DNA while the remaining nucleosomes consist of *de novo* synthesized histones. During the process of assembly, chaperone molecules facilitate the association of histones with other components and prevent their nonspecific aggregation with DNA. Newly translated histones are acetylated but only transiently; this specific acetylation pattern is recognized by the chaperone proteins and after deposition onto DNA, the acetylation marks are rapidly removed. Acetylated lysines within the tails and globular domains of histones H3 (H3K56) and H4 (K5, K8, K12 and K91) appear to serve important roles in chromatin assembly, although some marks seem to be able to compensate for the loss of others. For example newly synthesized histones could still be incorporated into nucleosomes if H4K8 was left unchanged while the C-terminal tail of H3 was removed and H4K5 and K12 were mutated in yeast ([11] and summarized in [12]).

Hyperacetylation causes little differences in the properties of nucleosomes but prevents chromatin from forming a 30 nm fiber, which leads to the assumption that histone acetylation generates an open chromatin structure. One important histone mark that has been associated with both, chromatin folding and heterochromatin spreading represents the acetylation of H4K16. Acetylation of K16, which is part of a sequence of basic amino acids that tightly bonds with an acidic region of the H2A-H2B dimer, is thought to disrupt this bonding and convey the inability of acetylated histones to form condensed chromatin structures [12]. Removal of H4K16ac by the yeast histone deacetylase Sir2 is also a critical step in heterochromatin formation and spreading. Depletion the H4K16 specific histone acetyltransferase MOF leads to increased nuclear fragmentation, underlining the distinct physiological function of this histone mark (reviewed in [13]).

Histone acetylation and transcription The acetylation of lysines in histones is thought to neutralize the positive charge and weaken the interaction of histones and DNA. This allows a relaxed structure of the chromatin which facilitates the binding of transcription factors and the polymerase complex. Histone acetylation marks can also serve as binding motifs for bromodomain and tandem PHD domain containing proteins. This indicates that histone acetylation, akin to phosphorylation and methylation events, creates a binding surface where, in contrast to the charge neutralization model, the acetylation marks of different lysine positions have non-redundant roles. Since the characterization of the transcriptional coactivator Gcn5 as a histone acetyltransferase, histone acetylation has been linked to gene activation, and deacetylation with transcriptional repression. The connection between histone acetylation and transcriptional activation in the context of increased binding of transcription factor and RNA polymerase molecules has been known for some time. Additionally, studies in yeast have recently revealed that histone acetylation is also involved in the process of transcriptional elongation. Promoters of active genes are highly acetylated, nucleosomes within the coding regions of genes, however, need to be hypoacetylated to prevent an aberrant assembly of the preinitiation complex at cryptic initiation sites within the gene body. The histone methyltransferase Set2 colocalizes with the elongating form of RNA polymerase II and deposits a unique modification (H3K36me3) inside the coding sequence. The histone deacetylase complex Rpd3S is recruited to and specifically deacetylates coding region chromatin through the recognition of H3K36me3 by the combined

action of a PHD and chromodomain of the Eaf3 and Rco1 subunits of Rpd3S [14, 15]. Another interesting aspect is that the acetylation of histones has been proven to precede the eviction of nucleosomes during the process of gene activation thereby suggesting a possible contribution to the establishment of a nucleosome free region (NFR) [16]. The most intensively studied histone acetylations are those of H3 and H4. On histone H3, the main acetylation sites are lysines 4, 9, 14, 18, 23 and 27 while lysines 5, 8, 12 and 16 are the main targets for acetylation on histone H4 [17]. In contrast to histone methylation, where the modification of different lysine residues can have opposing effects (e.g. H3K4 methylation is associated with activation whereas H3K9 methylation is a known repressive mark), the acetylation of lysine residues is generally linked to transcriptional active loci (Figure 3). Concerning acetylation marks the model that the decrease in charge differences by lysine acetylation is the reason for transcriptional activation has been challenged since there is a rapid turnover and cyclic acetylation and deacetylation at actively transcribed genes. Therefore the high turnover of acetyl moieties was proposed as the activating process, not their mere presence [18]. However, the acetylation equilibrium established by HATs and HDACs is of crucial importance for several biological functions and perturbances in this balance are observed under pathological conditions [19].

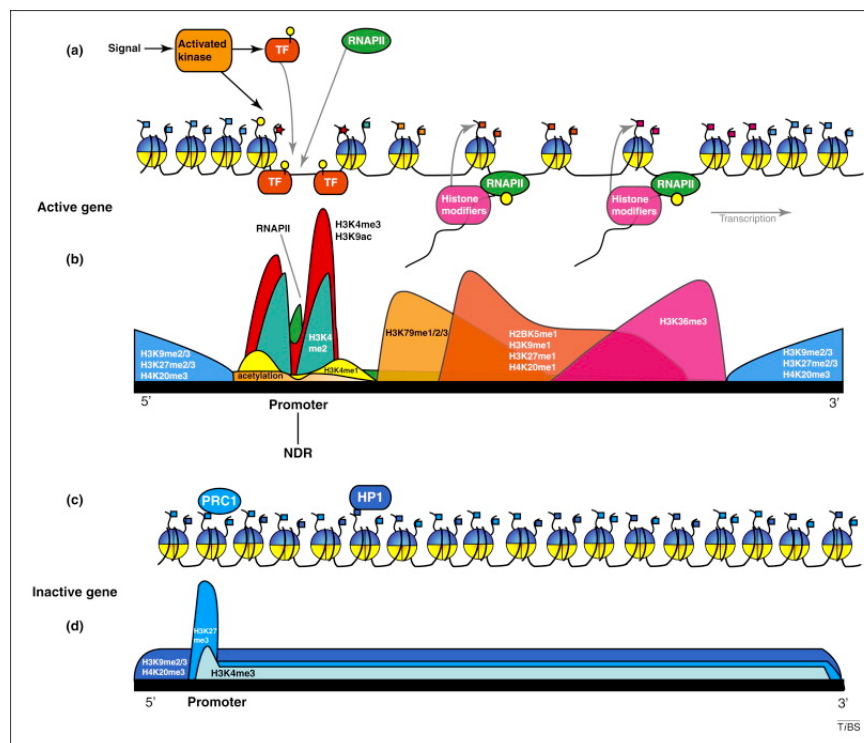


Figure 3: Active (a, b) and inactive (c, d) genes show different distributions of histone modifications and nucleosomal positioning. A nucleosome depleted region (NDR) is found at the TSS of actively transcribed genes, flanked by activating chromatin marks. At inactive genes there is an even distribution of silencing marks like H3K9 methylation and promoter enriched H3K27 methylation marks. Figure from Barth and Imhof, 2010 [13]

1.3.4 Histone acetyltransferases

HATs are the enzymes which are responsible for the transfer of the acetyl group from acetyl coenzyme A onto the ϵ -amine group of lysines. The cloning of a histone acetyltransferase in

Tetrahymena, which was highly homologous to the transcriptional adaptor Gcn5 in yeast, lead to the linking of histone acetylation to gene activation [20]. This concept was further supported through the identification of several other adaptor/coactivator proteins with intrinsic HAT activity including mammalian GCN5 and its ortholog, PCAF, CREB-binding protein (CBP), p300, and TAF_{II}250, which is the largest subunit of the general transcription initiation factor TFIID [21, 22]. The discovery that general transcription factors have HAT activity demonstrates a direct connection between acetylation and activated transcription. As mentioned above, TFIID is one of the first general transcription factors that binds via TBP and allows subsequent formation of the PIC. TAF_{II}250 (also known as TAF1) is thought to directly acetylate histones at the TATA box, thereby facilitating the binding of TBP and consequently TFIID [23]. HATs can be divided upon the suspected cellular origin and function into two major groups: The A-type HATs, which are generally localized in the nucleus and are associated with transcription related histone acetylation, and the cytoplasmic class of B-type HATs which are thought to play a role in the acetylation of newly synthesized histones, serving the transport from the cytoplasm to the nucleus (reviewed in [24]). HATs can also be grouped according to their sequence homology of their catalytic domains and upon shared substrates. The two predominant families are the GNAT (Gcn5-related N-Acetyl Transferases) and MYST (Moz, Ybf2/Sas3, Sas2 and Tip60) HATs. There are also other proteins including the p300/CBP family, Taf1 and nuclear receptor co-activators, which possess HAT activity but do not contain a true consensus HAT domain [17]. Most HATs are incorporated into multisubunit containing complexes and parts of various HAT complexes have been identified and revealed to play critical roles in regulating HAT activity, for example by targeting activity to specific chromosomal regions, or by ensuring lysine specificity [25]. For example the recombinant protein version of Gcn5 can acetylate free histones but is only able to acetylate nucleosomes if it is part of the SAGA, ADA or HAT-A2 complex [26]. Additionally, Gcn5 acetylates free histones mainly at H3K14, SAGA however acetylates lysines 9, 14, 18 and 23 [27]. Both, GNAT and MYST containing complexes (like SAGA and NuA4) are specifically recruited to activator-bound nucleosomes resulting in transcriptional activation [25].

1.3.5 Histone deacetylases (HDACs)

Histone deacetylases represent a group of proteins which is conserved from yeast to humans, and apart from regulating the acetylation levels of histones, they have a variety of non-histone targets, including transcription factors like p53 and E2F. So far 18 mammalian histone deacetylases are known, and based on sequence phylogeny, sub-cellular localization and enzymatic function they are clustered into four distinct classes (Class I, II, IV, and III). The first three classes (I, II and IV) represent Zn²⁺ dependent aminohydrolases, while Class III HDACs are NAD⁺ dependent deacetylases (as reviewed in [28]):

Class I (HDAC 1, 2, 3 and 8) share sequence similarity with the yeast deacetylase RPD3 and are ubiquitously expressed in various tissue and cell types. All class I HDACs share a similar structural organization, with a conserved N-terminal, and variable C-terminal domain. HDAC1 and HDAC2 are highly similar enzymes that are exclusively localized in the nucleus, since they lack any nuclear export signal (NES). HDAC3 contains a NES, and is therefore able to get exported into the cytosol, but it is mostly found in the nucleus. HDAC8 is lowly abundant, but it has

been demonstrated to be localized in the nucleus, after over-expression. This zinc dependent class of HDACs remove acetyl groups from lysines via a conserved catalytic domain which uses a charge relay system consisting of two adjacent histidines, two aspartic acid residues and one tyrosine while the Zn^{2+} atom is bound to the bottom of the pocket.

Class II HDACs are sub-grouped into IIa (HDAC 4, 5, 7 and 9) and IIb (HDAC 6 and 10). Both class II subgroups share sequence homology with the yeast lysine deacetylase HDA1. In contrast to class I HDACs, class II members are large proteins with a catalytic site at their C-terminus and exhibit a more tissue-specific expression. Furthermore, the knockout of class II HDACs generally does not lead to embryonic lethality, with the exception of HDAC7. [29]. Class IIa HDACs are able to shuttle in and out of the nucleus in response to certain cellular signals. This shuttling is regulated by intrinsic nuclear import and export signals. Additionally HDAC4, 5, 7 and 9 contain conserved 14-3-3 binding sites, and interaction of the protein 14-3-3 with the phosphorylated binding sites leads to nuclear export or cytoplasmic retention of the HDAC protein [30]. HDAC6 is a special member of the class II HDACs and controls cytoskeletal dynamics and chaperon function by acetylation of α -tubulin and HSP90 [31, 32].

Class IV consists of only one mammalian deacetylase (HDAC11), of which no direct yeast homolog is known, but which contains features of class I and II HDACs.

Class III HDACs are NAD^+ dependent deacetylases and are also known as sirtuins since they are related to the yeast deacetylase Sir2, which is one of the crucial players in heterochromatin spreading in *Saccharomyces cerevisiae*. This class contains seven members (Sirt1-7) and are often referred as “anti-aging” proteins, as the life-extending effects of caloric restriction are dependent on sirtuins in yeast [33].

HDAC1 and HDAC2 are two highly related proteins with a total amino acid identity of 86 % and are thought to be the result of a gene duplication, and most vertebrates contain one copy of each gene, with the exception of fish. For example in zebrafish (*Danio rerio*) only one HDAC1/HDAC2 like gene exists [34]. The high sequence identity is not equally distributed, as their N-termini (amino acids 1-325), which contain the dimerization and catalytic domains, are almost identical (92 % amino acid sequence identity), while the C-terminal domains are less conserved (72 %). It is noteworthy that deletion of the C-terminal domain, while keeping the catalytic activity functional, still greatly reduces the enzymatic activity of HDAC1 [35]. Although the two proteins are conserved and tissue expression patterns are highly similar, mouse knock-out studies suggest non-redundant functions during embryogenesis. HDAC1 deficient embryos are severely growth retarded and die during embryogenesis before E10.5 [36, 37]. ESCs which lack HDAC1 show significantly reduced proliferation rates, while regulators of cell cycle progression, like p21 and p27 are upregulated. An additional knockout of p21 could rescue the decreased proliferation in ESCs but not the embryonic lethality of HDAC1 deficient mice [38]. In contrast to the early embryonic lethality of HDAC1 deficient mice, the loss of HDAC2 has less severe consequences during embryonic development. One study reported that HDAC2 deficient mice survive the embryonic development but die perinatally due to a spectrum of cardiac defects [37], while a second study, using a gene-trap embryonic stem cell line, claimed that HDAC2 deficient mice were born and up to 50 % survived the first 25 postnatal days. After

this first month the surviving HDAC2 knockouts were indistinguishable to wild type mice [39]. Interestingly, the deletion of both HDAC1 and HDAC2 *in vitro* causes nuclear bridging, nuclear fragmentation, and finally mitotic catastrophe [40].

In vivo HDAC1 and HDAC2 rely heavily on cofactors to assure activity and localization. They have been found to be in at least three multi-protein complexes: the Sin3, NuRD and CoREST complex [41]. The Node complex, which is found in embryonic stem cells, is a specialized NuRD version containing Nanog or Oct4, and is thought to be involved in silencing of developmentally regulated genes. An additional distinct complex has been reported recently, which has an increased complex formation and increased deacetylase activity during mitosis [42]. Some subunits within these complexes are necessary for histone binding, like the RbAp48 protein in the Sin3 and NuRD complex. Others modulate the HDAC activity, like the MTA proteins in the NuRD complex. Another common feature of these complexes is that repressive methylases or demethylases are part of them. For example the H3K9 methylase G9a is part of the CoREST complex. The H3K4 demethylases LSD1 and RBP2 are part of the NuRD and Sin3 complex respectively. In addition to acting as transcriptional modulators through these complexes, HDAC1 and HDAC2 can occur as a homo- or heterodimer, which can interact directly with DNA binding proteins. The activity of HDACs cannot only be regulated by members of the complexes, but also by posttranslationally modifying the deacetylases. These modifications include chemical moieties (for example: acetylations, phosphorylations, methylations or nitrosylations) or proteins (e.g. ubiquitin or SUMO), and can change their catalytic activity or binding affinities to other members of the complexes. For example phosphorylation of the C-terminal portion of HDAC1 and HDAC2 has been shown to enhance the activity and regulates their nuclear import, whereas acetylation of HDAC1 reduces the catalytic activity ([43], and reviewed in [44]).

1.3.6 HDAC inhibitors

In many cancer types HDACs have been shown to be either overexpressed or aberrantly recruited by DNA-binding proteins. Since HDACs facilitate reversible epigenetic changes, they are an attractive target in cancer therapy and with the emergence of specific HDAC inhibitors (HDIs), these small molecules have been shown to possess potent anticancer activities [45]. A large number of these molecules have been purified from natural sources or were produced synthetically, however since recombinantly produced HDACs are enzymatically not active, a profiling of each HDI was challenging, and only recently accomplished by the combination of affinity capture and quantitative mass spectrometry [42]. HDIs can be sub-grouped into six classes upon their chemical structure. These molecules differ in their inhibition efficiencies against the different classes of HDACs, and can therefore be divided into general HDIs (for example TSA and SAHA) or more specific inhibitors like MS275 which showed the highest inhibition activity against HDAC1 and 2 and only marginally inhibits HDAC3 and 8. Most HDIs bind into the pocket of the catalytic domain, thereby replacing the Zn^{2+} atom and disturbing the charge relay system. Apart from their use in psychiatry, several HDIs have been FDA approved in cancer therapy (SAHA and Romidepsin for cutaneous T cell lymphoma) or are currently in clinical trials (for example valproic acid for cervical cancer or MS275 for lung and breast cancer). In addition to their clinical importance HDIs represent a convenient, fast and direct method

to study the transcriptional role of HDACs *in vitro*. However one should be aware that general HDIs like TSA target multiple HDAC and indirect effects may contribute to the transcriptional readout. Even with more specific inhibitors like MS275 off-target effects cannot be excluded.

1.4 Chromatin in pluripotency and reprogramming

Stem cells are referred to be pluripotent if they still have the potential to differentiate into any fetal or adult cell type. In contrast to totipotency, they cannot develop into a full organism, as they lack the ability to contribute to extraembryonic tissue. Embryonic stem cells (ESC) can be derived from the inner cell mass of the blastocyst, and represent the prototypical pluripotent stem cell. They are a common tool in biology to study mechanisms of pluripotency and self-renewal but also serve as a model for the study of development and disease *in vitro*. In contrast to multipotent adult stem cells, which can only form specific tissue specific cell lineages, ESCs have a high self-renewing capacity and can differentiate into cells from all three germ lines (endoderm, mesoderm and ectoderm). Several alternatives exist to generate pluripotent cells, like nuclear transplantation, cellular fusion, and reprogramming by a defined set of factors (reviewed in [46]). Nuclear transfer involves the injection of a somatic nucleus into an enucleated oocyte, which, when cultured *in vitro* can give rise to genetically matched embryonic stem (ES) cells. Cellular fusion, of somatic cells with ESCs result in tetraploid cells which show all features of pluripotency. In the last few years, a new possibility of somatic cell reprogramming has been established, by introducing and overexpressing a set of key transcription factors. The first report of a method which generates induced pluripotent stem cells (iPSC) by the transduction of four distinct transcription factors (Oct4, Sox2, Klf4 and c-Myc; often abbreviated as OSM [47]) created a major excitement due to its technical simplicity and broad applicability. This method circumvents the technical and ethical problems of ESC extraction, and offers the possibility of creating cells for applications in regenerative medicine. In fact, the gene defect causing sickle-cell anaemia was reversed in mouse models by this method [48].

1.4.1 The embryonic stem cell state

The term “stem cell state” describes the product of all the regulatory inputs that produce a gene expression program that conveys the key characteristics of ESCs: pluripotency and self-renewing. Interestingly the most important signals that produce and maintain this state come from a small set of transcription factors namely Oct4, Sox2 and Nanog. [49]. These factors are highly expressed in undifferentiated ESCs and physically interact with each other in large protein complexes [50]. They act as transcriptional activators on promoters of their own genes, thereby establishing an interconnected autoregulatory loop, and on promoters of other pluripotency related genes (e.g. Klf4) but they also get recruited to genes associated with lineage commitment, which are silent but poised in ESCs [51]. Oct4, Sox2 and Nanog can positively regulate genes by several mechanisms; firstly, they can incorporate a variety of transcriptional regulators into their protein complexes, including transcription factors like Stat3, Smad1 or c-Myc or chromatin modifying enzymes like the HAT Tip60-p400. This large multi subunit containing complexes cannot only bind to promoters, but are especially often found to coordinately

bind to regions with enhancer activity. Additionally, Oct4, Sox2, and Nanog were reported to interact with the coactivator Mediator which binds to RNA polymerase II, thereby recruiting it; While transcription factors like c-Myc can recruit kinases to phosphorylate the CTD domain of Pol II, thereby releasing it from pausing and driving it into productive elongation ([52, 53] and reviewed in [54]).

The stem cell state, which is under the control of this transcriptional circuitry, is implemented in the context of an **open chromatin** state. Compared to somatic cells, the chromatin structure in ESCs is less condensed and the ratio between euchromatin and heterochromatin is higher than in differentiating cells. The association between DNA and many structural proteins, like HP1 α , H1 and core histones is less rigid in pluripotent cells, while others like H3.3 and H1.5 bind tightly in both pluripotent and differentiated cells (reviewed in [55]). Furthermore, epigenetic marks which are associated with heterochromatin and repressed regions, like H3K9me3 and H3K27me3 are reduced in pluripotent cells. Conversely, active chromatin marks including H3K4me3, H3K36me2, H3K36me3 and histone acetylation, especially H3K9ac and H3K14ac, are more prevalent in ESCs. Additionally, genes which are important for differentiation are not expressed but decorated with active histone marks as well as repressive chromatin modifications. This “bivalent” chromatin state supports a rapid gene activation in response to differentiating signals. Interestingly, bivalent domains have been shown to contain H3K4me3 and H3K27me3 on the same nucleosomes, though in an asymmetric distribution on the two sister histones [56]. The consequence of an open chromatin structure is a global increase in transcription; especially satellite repeat sequences and genes which are expressed in both ESCs and differentiated cells, show a higher basal transcription in ESCs [57]. This global open chromatin structure, established and maintained by active chromatin modifications and a high abundance of chromatin remodeling enzymes, is thought to ensure a stable upkeep of the embryonic stem cell state but also the ability to rapidly respond to differentiating signals.

1.4.2 Reprogramming of somatic cells by defined factors

The transduction of somatic cells with a set of transcription factors is thought to jumpstart the transcriptional circuitry that is defining the ESC state. Generally these reprogramming factors include Oct4, Sox2, c-Myc and Klf4. As mentioned, Oct4 and Sox2 are two factors which are important players in the regulatory network that ensures pluripotency and self-renewal. Since these factors can also positively regulate their own promoter and enhancer sites, the ectopic expression leads to the activation of the endogenous genes. Interestingly, the third partner of the “core” transcriptional network, Nanog, is dispensable as a reprogramming factor in mouse models and its endogenous expression is not always activated, suggesting that Nanog is rather a gatekeeper, preventing differentiation pathways, but makes few contributions to the state of pluripotency. The oncogene c-Myc is not part of the core network of pluripotency, but is thought to promote the transition from a condensed chromatin in differentiated cells into a more open structure, thereby enhancing the establishment of transcriptional networks. The role of Klf4 in reprogramming is not fully understood, and several models exist: Klf4 has been reported to be both, a tumor suppressor and an oncogene, and might counteract the apoptotic effects of c-Myc by repressing p53 [58]. On the other hand it might also act in concert with Oct4 and

Sox2 to activate ESC specific genes.

To date, several different techniques exist to deliver the transgenes (as reviewed in [59]): Viral delivery systems are one of the most widely used methods and include moloney murine leukaemia virus (MMLV) derived retroviruses or HIV derived lentiviruses. The advantages of retroviruses are that high titers of replication deficient viral particles can be produced in packaging cells and that inserted transgenes get easily silenced once the cells are reprogrammed. Although lentiviral transduction is more efficient and can also target non-dividing cells the overall reprogramming yields are similar. Cre excisable transgenes are generally used in combination with lentiviruses, since the silencing of ectopic transgenes is less efficient. Alternative delivery systems include the use of adenoviruses, which generate no genomic integrations but reprogramming is slow and inefficient, direct transfection of linear integrating DNA or the use of piggyBac transposons. Additionally several non-integrative approaches exist, for example the delivery of plasmids for episomal expression, synthetic mRNA or the proteins themselves.

All reprogramming methods have one disadvantage in common; They are highly inefficient; for example standard retroviral OSKM reprogramming yields less than 0.1 % iPSCs, and several molecular mechanisms might contribute to this inefficiency. First, the generation of iPSCs may require specific, narrow-range expression levels of the transduced factors, and even slight variations in protein levels might prevent the cells from becoming reprogrammed. For example, a 50 % change in Oct4 levels causes ES cells to differentiate towards the primitive endoderm lineage [60]. Another theory could be that retroviral insertions into the host genome may trigger the activation of additional unknown reprogramming genes by insertional mutagenesis. As this mutagenesis occurs randomly only few cells would trigger the correct additional genes. However, this theory was disproven by the fact that cells can be reprogrammed by non-integrational methods such as plasmid transfection or the use of adenoviruses. One additional explanation is based on the fact that stress-associated genes are triggered in transfected somatic cells. For example, forced expression of c-Myc triggers the upregulation of cyclin-dependent kinase inhibitors that are involved in various differentiation and anti-proliferative pathways. Finally, the transcriptional networks that are responsible for pluripotency and the ESC state have to be built up from scratch, and this process may be more affected by chance variation than the reprogramming by cellular fusion with ESCs or nuclear transfer, where all these networks are already up and running. This gradual establishment of pluripotency has led to the model of a two-stage switch, in which somatic cells transform into partially reprogrammed cells during the first stage of reprogramming and in the later stage form fully pluripotent iPSCs (Figure 4A, [61]). This first stage is defined by the downregulation of lineage genes, either by direct repression or restoration of bivalent domains, the activation of specific ESC genes (for example alkaline phosphatase or Fbx15) and the chromatin remodeling at pluripotency genes by unfolding condensed chromatin and removal of repressive chromatin marks. This first step leads to cells that exhibit a “quasi-pluripotent” phenotype, where cells display ESC characteristics but still depend on the ectopic expression of reprogramming factors and quickly differentiate once these factors are removed. During the second stage, the transition from a partially reprogrammed cell towards an iPSC is facilitated by the establishment of the endogenous interconnected autoregulatory loop, as exogenous Oct4 and Sox2 are now able to target and activate endogenous

Oct4, *Sox2* and *Nanog* loci, which in turn leads to the gradual revival of the full transcriptional network. Additional characteristics of fully reprogrammed iPSCs are the reactivation of telomerase, reappearance of non-CpG DNA methylation, and the abilities of tissue differentiation, teratoma and embryoid body formation and the feature to form embryos when inserted into a tetraploid blastocyst (tetraploid complementation).

1.4.3 Small molecules in reprogramming

As mentioned above, the overall reprogramming efficiency, measured by iPSC colony formation is particularly low, which lead screens of small molecules that could increase the reprogramming fidelity. Among the most promising inhibitors were drugs targeting epigenetic regulators, such as DNA methyltransferases, histone methyltransferases and histone deacetylases. The DNA methyltransferase (Dnmt) inhibitor 5-aza-cytidine (AZA) has been shown to improve reprogramming, by facilitating demethylation at pluripotency associated genes thereby enabling partially reprogrammed cells to transit the reprogramming path and form iPSCs [62]. Similar effects were obtained by the simultaneous inhibition of the mitogen activated protein kinase/ERK kinase (MEK) and glycogen synthase kinase-3 (GSK3) signaling pathways with a dual inhibitor cocktail (2i) [63]. Treatment with HDAC inhibitors like valproic acid (VPA), trichostatin A (TSA) and suberoylanilide hydroxamic acid (SAHA) enhanced reprogramming efficiencies up to 50 fold in the four-factor (OSKM) reprogramming setup. Additionally, treatment with VPA in combination with AZA could speed up the reprogramming process, and VPA could replace c-Myc as a reprogramming factor. VPA treatment alone could not reprogram cells but ESC-specific genes were already upregulated and MEF-specific ones were downregulated [64] (Figure 4B). Another study reported that the use of sodium butyrate, a general HDAC inhibitor, can enhance human iPSC formation by 100 to 200 fold [65]. In summary, HDIs have been repeatedly shown to enhance the reprogramming fidelity, most likely by generating a hyperacetylated chromatin that resembles the structure found in ESCs, and facilitates the establishment and binding of pluripotency related transcription factor networks.

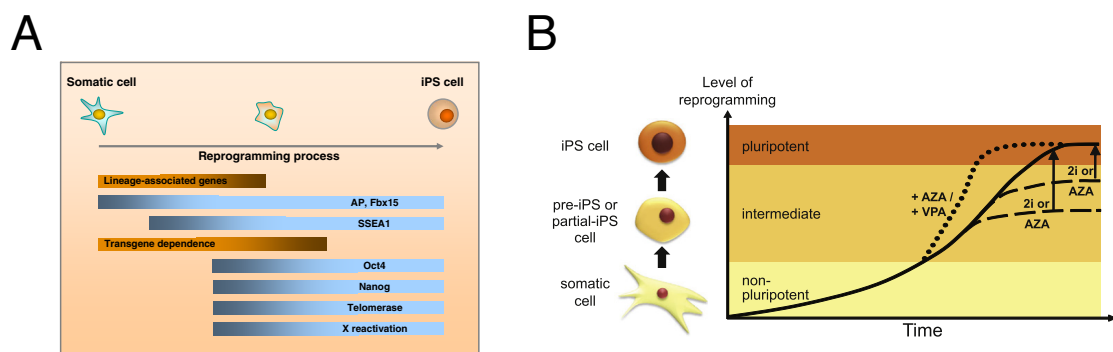


Figure 4: Reprogramming via the transduction of a set of defined factors. **A)** Two-stage switch of reprogramming consists of a series of predictable steps. **B)** Conventional reprogramming of somatic cells without the addition of chemicals, often leads to partially reprogrammed cells (dashed lines). However, with the addition of 2i inhibitors or AZA, these pre-/partial-iPSCs could be further promoted to fully competent iPSCs (black vertical arrows). Addition of chemicals such as VPA or AZA could also accelerate the kinetics of reprogramming by achieving fully competent iPSCs at a faster rate (dotted line). (Figures from Scheper *et al.*, 2009 [61] and Feng *et al.*, 2009 [66] respectively)

1.5 The epidermis

1.5.1 Epidermal structure, self renewal and differentiation

As the largest organ of mammalian integumentary systems, the skin represents a barrier and evolved in order to protect against pathogens, external stimuli, like UV radiation, and excessive water loss. The mammalian skin is mainly composed of two compartments: The Epidermis and the dermis. The epidermal epithelium represents the outmost cell layers of the skin and is a stratified squamous epithelium. It is composed of the proliferating basal and differentiated suprabasal keratinocytes. While keratinocytes are the predominant cell type in the epidermis, constituting 95 % of the cells, several other cell types exist, like Merkel cells (mechanoreceptors), melanocytes (pigment producing cells) and Langerhans cells (epidermal type of dendritic cells). During epidermis development three different lineages, the hair follicle (HF), interfollicular epidermis (IFE) and sebaceous gland (SG) lineage are generated. Hair follicles are appendages of the epidermis and produce and shed hair in a repeating cycle of hair growth (anagen), hair regression (catagen) and a resting phase (telogen) (reviewed in [67]). The sebaceous gland, another appendage of the epidermis, secretes the lipid rich sebum in order to lubricate and waterproof the skin.

The epidermis has high regenerative abilities, which rely on the constant renewal of the cellular layers. The physiological process that maintains a constant number of cells in renewing organs is called tissue homeostasis. Epidermal stem cells (SC) can replenish the pool of keratinocytes that are lost through normal tissue turnover or through cell death due to injury. Cells of the interfollicular epidermis (IFE) have the ability to self-renew and additionally give rise to the progeny of differentiating cells. Stem cells, residing in the IFE, could self-renew and differentiate, either by first dividing asymmetrically into a stem cell and a transit amplifying (TA) cell, which divides symmetrically and gives rise to differentiated cells, or by dividing strictly symmetrically [68]. Although there are several markers for IFE stem cells, their role and importance is still highly debated. One niche, where quiescent stem cells were reported to reside, is the “bulge” area, located at the hair follicle right under the sebaceous gland (Figure 5). In fact, bulge stem cells are able to generate all epidermal lineages and are thought to be the most potent epidermal SC. Bulge SC contribute to the hair cycle and the process of wound repair, but they do not seem to play a major role in the homeostasis of the epidermis, which underscores the existence of a separate SC pool in the IFE [69]. During the process of terminal differentiation, a tightly regulated set of changes in gene expression ensures the proper layering of the IFE. The basal layer cells express specific keratins (K14 and K5) but as cells migrate outwards they lose their mitotic potential and strengthen their cytoskeletal and intercellular connections while the production of keratin markers specific for each layer is triggered. Finally, apoptosis and expression of late differentiation markers, like loricrin, filaggrin and involucrin, as well as SPRR and S100A proteins, lead to terminal differentiation and incorporation of the dead cells into the cornified envelope.

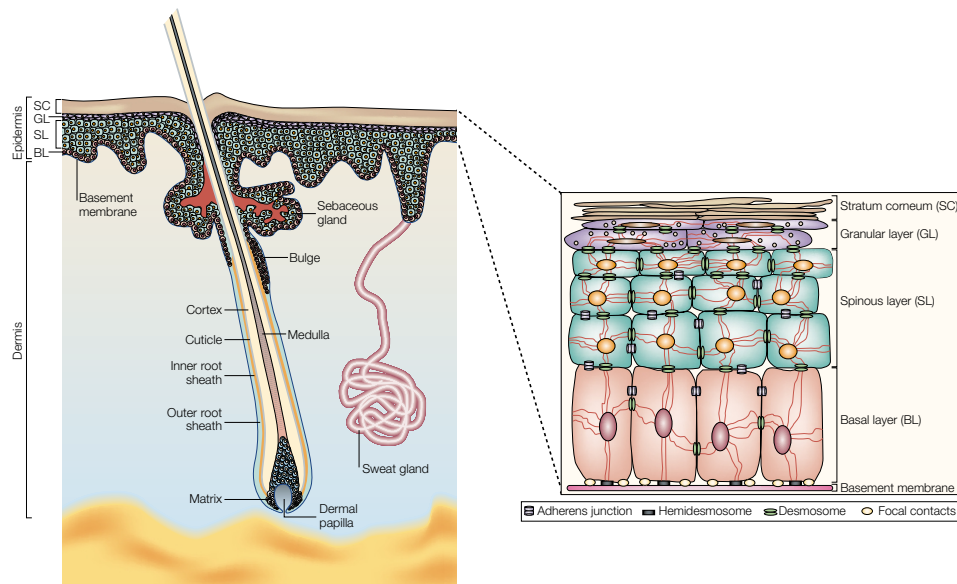


Figure 5: A cross-section of a hair follicle, consisting of an outer root sheath that is adjacent to the basal epidermal layer. The bottom part of the follicle is called the “hair bulb” and is made from a matrix of transit-amplifying cells, which terminally differentiate to generate the different cell types of the follicle. Epidermal stem cells reside in a part of the outer root sheath that is called the “bulge”. The epidermis and dermis are separated by a basement membrane. The basal layer (BL), consists of proliferating, transit-amplifying cells. The basal layer stratifies and differentiates into the spinous layer (SL), granular layer (GL) and the stratum corneum (SC). (Figure and Figure legend adapted from Fuchs *et al.*, 2002 [70])

1.5.2 The epidermal differentiation complex

The EDC is a conserved gene locus harboring four clusters of tandem gene families: Filaggrin (FLG)-like, Late Cornified Envelope (LCE), Small Proline Rich Region (SPRR) and the S100 genes. FLG-like, LCE and SPRRs are structural proteins which are crosslinked to form the essential epidermal barrier, while S100 (especially *S100A8* and *S100A9*) genes encode chemoattractant proteins, that are upregulated upon stress or wounding [71]. Additionally, a network of cis-regulatory elements in the EDC ensures that genes within this cluster are coordinately expressed during epidermal differentiation [72]. A deregulation of these genes has been reported in a variety of skin diseases including psoriasis and atopic dermatitis [71, 73].

1.5.3 The role of HDAC1 and HDAC2 in epidermal development

HDAC1 and HDAC2 have been shown to be crucial for the proper development of the epidermis. The conditional knockout of both HDACs mediated by the expression of a Cre-recombinase under the control of the keratin 14 (K14) promoter, lead to multiple severe ectodermal defects and mice died perinatally [74]. Since similar effects in conditionally p63 deleted mice, were found by the authors, and HDAC1 and HDAC2 double conditional knockout mice lost the suppressive ability of p63, they argued that HDAC1 and HDAC2 directly mediate the repressive function of p63 on its downstream target p53. Thus increased p53 activity induces the expression of p21 thereby promoting apoptosis.

In a recent study Nascimento and co-workers showed in mouse models that the overexpression

of c-Myc leads to the deregulation of proliferation and differentiation specific genes. Especially many of these genes were located in the EDC region and proved to be direct targets of c-Myc. Interestingly Sin3a, one structural component of the class I HDAC containing repressive complex Sin3, can directly repress c-Myc activity, and the absence of the Sin3a protein enhances c-Myc binding. Conversely, the deletion of c-Myc in a Sin3a conditional knockout can rescue the phenotype, thus indicating an important role of class I HDACs in tissue homeostasis [75].

1.6 Histone acetylation in neural cell-type specification

During the early development of the central nervous system (CNS) one specific type of the ectoderm, the neuroectoderm, forms the neuronal plate along the dorsal side of the embryo. The following primary neurulation is similar in all vertebrates. Shortly after the neural plate has formed, the edges thicken and move upwards creating a U-shaped neural groove. By further invagination of the groove and closure of the neural folds, three distinct classes of tissue are generated: the internally positioned neural tube that will form the brain and the spinal cord, the external epidermis of the skin and so-called neural crest cells, which form in the region between the neural tube and the epidermis and will migrate to form the peripheral nervous system, pigment cells (melanocytes) of the skin, facial cartilage, the dentine of teeth and several other cell types. The newly derived neural tube will give rise to the CNS, including numerous types of nerve cells (neurons) and supportive cells (glia) in the brain and spinal cord. The precise progress by which neural progenitor cells differentiate into neurons, oligodendrocytes and astrocytes is controlled by a complex network of transcription factors, epigenetic regulators, and extrinsic developmental stimuli. Transcription factors have been shown to govern an important role during neurogenesis as their expression is highly cell-type specific and their potential to modify transcription of their target genes in a developmental dependent context controlling and maintaining the cell fate identity.

1.6.1 HATs and HDACs in brain development

In addition to transcription factors, epigenetic mechanisms like histone acetylation have been shown to influence cell fate specification, and mouse mutants deficient for several HATs and HDACs exhibit severe neuronal defects (reviewed in [76]). For example, CNS specific deletion of CBP and p300 results in an incomplete closure of the neural tube [77]. In the same study the authors present a mechanism by which an extrinsic signal (retinoid acid) in combination with a transcription factor can alter the chromatin landscape at motor neuron specific genes, which ultimately leads to their expression. The importance of HDACs in the developing murine brain was demonstrated by the addition of the HDI trichostatin A (TSA) to ganglionic eminence-derived neural precursor cells, which lead to a profound reduction in neurogenesis but an increase in immature astrocyte formation, however, other parts of the developing brain showed an increase in neurogenesis [78]. This pleiotropic effect is likely to be caused by the promiscuous inhibition of several different HDACs by TSA, which all may have a distinct function in the developing CNS. Conditional knockout studies, targeting specific HDACs in the CNS, are therefore insightful tools to decipher the individual roles of different HDAC subgroups. For

example, the conditional deletion of either HDAC1 or HDAC2 showed no obvious phenotypes, whereas the combined deletion of both enzymes in developing neurons resulted in severe neurological abnormalities and lethality by postnatal day 7 [79]. These results suggest that HDAC1 and HDAC2 play redundant roles in the progression of neuronal precursors to mature neurons. In stark contrast to the functional redundancy of HDAC1 and HDAC2, which enables them to compensate for each other, are their spatiotemporal dependent expression patterns in wild type murine brains. At all developmental stages, HDAC1 is highly present in proliferative neuro-glial progenitors and is downregulated during their differentiation into postmitotic neurons, while terminal differentiated glia cells (astrocytes) are still HDAC1 expressing. The vice versa situation is true for HDAC2: while lowly expressed in progenitor cells, HDAC2 gets upregulated during differentiation into neurons but is absent in astrocytes [80]. This mutual exclusive expression pattern suggests functional non-redundant roles of HDAC1 and HDAC2 during murine brain development. Additionally, HDAC inhibitors like valproic acid or TSA have been extensively used in neurologic and psychiatric disorders like Rubinstein–Taybi syndrome, Rett syndrome, Friedreich’s ataxia, Huntington’s disease and multiple sclerosis (reviewed in [81]), although the molecular mechanisms which cause beneficial effects by HDI treatment in these diseases is poorly understood.

2 Materials and Methods

2.1 Cell Culture

2.1.1 Media and solutions

All Solutions were prepared in standard tissue-culture glassware and sterilized by filtration. Standard Dulbecco's Modified Eagle Medium (DMEM) was used in aliquots of 450 ml, supplemented with 5 ml AB and 50 ml fetal calf serum (*FCS, Gibco BRL*). TE, β -Mercaptoethanol and AB stock solutions were kept at -20 °C. DMEM medium, 0.1 % (w/v) Gelatin solution and PBS were stored at 4 °C.

10x Phosphate buffered saline (PBS)	0.1 % (w/v) Gelatin Solution
NaCl 80.0 g/l	Gelatin 0.5 g
KCl 2.0 g/l	add water to 500 ml, autoclave
Na ₂ HPO ₄ 16.5 g/l	and add 1x AB after cooling
KH ₂ PO ₄ 2.0 g/l	
adjust pH to 7.4	
	100x β -Mercaptoethanol Stock (0.01 M)
100x Antibiotic stock (AB)	14 M β -Mercaptoethanol 72 μ l
Penicillin G potassium salt 6.0 g/l	to 100 ml with 1x PBS and sterile filter
Streptomycin sulfate 10.0 g/l	
dissolved in 1x PBS	
Trypsin/EDTA (TE)	
Trypsin 2.2 U/mg 700 mg	
10x PBS 25 ml	
1 % Na-EDTA, pH 7.4 5 ml	
add water to 250 ml	

ES Cell Culture Medium (M15)

ES cell qualified high-glucose DMEM containing 4500 mg/l glucose (Sigma) was supplemented with 15 % FCS (*HyClone*), 1x AB, L-Glutamine (584 mg/l final concentration) and 1x β -Mercaptoethanol prior to use.

2.1.2 Culturing teratocarcinoma cells

Two teratocarcinoma cell-lines (F9-NT and F9-HD1-3) were cultured as described in [82]. The plates were coated with 5 ml gelatin (0.1 %) for 30 min before seeding the cells. Normal DMEM-medium with 2 μ g/ml puromycin was used as a selection for shRNA constructs.

Freezing Cells: Cell-pellets were resuspended in ice-cold FCS and dropwise supplemented with FCS containing 20 % DMSO to a final concentration of 10 % DMSO. After resuspension the cells were kept on ice for 30 min, before storing them at -80 °C

Thawing Cells: Frozen cells were quickly thawed in selective medium. After centrifugation at 1000 rcf the supernatant was discarded and the pellet was resuspended in selective medium.

Passaging Cells: Cells were grown to 80 % confluency, washed with 1x PBS and trypsinized with TE solution for 2 min. After resuspending in selection medium 1 million cells were seeded onto one 15 cm dish. Cells were cultured at 37 °C and 5 % CO₂.

2.1.3 Culturing a human osteosarcoma (U2OS) cell line

U2OS cells were cultured in standard DMEM medium, containing 10 % FCS and 1x AB, at 37 °C 7.5 % CO₂. Cells were thawed on 10 cm dishes and 1/2 of it was transferred onto one 15 cm dish when they reached 90 % confluency (= ratio of 1:8). For maintenance, cells were subcultured in 1:5 to 1:8 ratios.

2.1.4 Culturing embryonic stem cells (ESCs) on gelatin

Two ESC-lines were cultured: 66/3 (wt) and 66/4 (HD1-KO). ESCs were grown on gelatin (0.1 %) and cultured in M15 medium supplemented with 10 µl LIF per 100ml medium (10³units/ml medium). Cells were subcultured every second day in a 1:3 to 1:5 ratio, and fed with fresh M15 medium every day. Cells were frozen in FCS (*HyClone*) containing the final concentration of 10 % DMSO. Cells were cultured at 37 °C and 5 % CO₂.

2.1.5 Generation of irradiated feeder cells for ESC culture

Primary mouse embryonic fibroblasts (MEFs), isolated from E13.5 embryos and frozen directly after isolation (P0), were thawed on 10 cm dishes in standard DMEM medium (10 % FCS, 1x AB) and cultured at 37 °C and 5 % CO₂. After transferring them onto 15 cm dishes they were subcultured in a 1:3 ratio until passage 4 (P4). Confluent P4 MEFs were trypsinized pooled and kept on ice in 50ml tubes. Cells were irradiated for 4 min at 1479 cGy by the Gammacell 2000 irradiator. After the treatment the cells were kept on ice and frozen in a ratio that one freezing vial contained the cells of one confluent 15 cm dish.

2.1.6 Culturing ESCs on a layer of irradiated feeder cells

One vial of feeders was thawed onto four gelatinized (0.1 %) 10 cm dishes in standard DMEM medium (10 % FCS, 1x AB). ESCs can be cocultured onto feeder cells one to five days after feeders were put into culture. ESCs were thawed onto feeder layers and cultured in M15 medium supplemented with LIF (10³units/ml medium). Cells were subcultured every second day in a 1:3 to 1:5 ratio, and fed with fresh M15 medium every day. Feeders were removed by trypsinization of all cells and 30 min incubation on gelatinized plates at 37 °C and 5 % CO₂, supernatant was used for RNA or chromatin extraction.

2.1.7 Inhibitor treatment

To specifically inhibit class I HDACs the small molecule inhibitor MS275 was used. Confluent cells were treated with 2 μ M MS275 (dissolved in DMSO) for 6 h. Pure DMSO was used as a mock control. HDAC inhibition by HDIs was verified by the increased bulk histone acetylation detected by Western blot.

2.2 Handling RNA

Prior to all work with RNA, all tools and working surfaces were treated with a mixture of 1 M NaOH and 0.5 M EDTA.

RNA extraction: Cells were harvested by scraping the 15 cm plate in 5 ml PBS. After 5 min centrifugation (at 1200 rpm) the supernatant was discarded and 1 ml of TRIzol[®] Reagent was added. After 10 min centrifugation at 12 000 rpm (4 °C) the supernatant was transferred to a new eppi. 0.2 ml of Chloroform per 1 ml of TRIzol[®] Reagent was added and the tubes were shaken vigorously for 15 sec. The tubes were incubated for 3 min at room temperature and centrifuged at 12 000 rpm (4 °C) for 15 min. The upper, aqueous phase was transferred into a fresh tube and precipitated at room temperature with 0.5 ml of isopropyl alcohol for 10 min. The precipitated RNA was pelleted by centrifuging it at 12 000 rpm (4 °C) for 10 min. The supernatant was discarded and the pellet was washed with 75 % EtOH. The resulting pellet was air-dried and redissolved in 200 μ l sterile dH₂O. The second precipitation was done by adding 20 μ l NaOAc (3M) and 500 μ l EtOH (96 %). After overnight incubation at -20 °C the sample was centrifuged at 12 000 rpm (4 °C) for 30 min, and the resulting pellet was washed with 75 % EtOH. After air-drying, the pellet was dissolved in 30 μ l sterile dH₂O at 55 °C while shaking at 300 rpm. The RNA concentration was measured by spectrophotometric analysis (A260) via NanoDrop.

Analysis of RNA integrity: 1 μ g of RNA was incubated with RNA Sample Buffer at 65 °C for 5 min and loaded onto a MOPS/EDTA gel (1.2 g agarose +90 ml sterile dH₂O + 10 ml 10x MOPS; after heating + 5.2 ml 37 % formaldehyde) and run at 70 V.

10x MOPS/EDTA	
MOPS	0.2 M
Na-Ac	50 mM
EDTA	10 mM
adjust to pH 7.0	

cDNA conversion was performed using the iScript[®] cDNA synthesis kit (BIO-RAD). Prior to cDNA synthesis, the RNA samples were diluted to 0.5 μ g/ μ l.

Reaction Mix/sample	
5x iScript Reaction buffer	4 μ l
iScript Reverse Transcriptase	1 μ l
dH ₂ O	13 μ l
RNA (0.5 μ g/ μ l)	2 μ l

PCR-settings	
5 min	25 °C
30 min	42 °C
5 min	85 °C

2.3 Chromatin Immunoprecipitation

2.3.1 Solutions and Buffers

All Solutions were prepared with dH₂O and sterile filtered after dissolving.

WASH I	400 ml
10 % Triton X-100	10 ml
0.5 M EDTA	8 ml
0.5 M EGTA	0.4 ml
1 M HEPES	4 ml

WASH II	400 ml
4 M NaCl	20 ml
0.5 M EDTA	0.8 ml
0.5 M EGTA	0.4 ml
1 M HEPES pH 7.9	4 ml

Lysis-Buffer	10 ml
20 % SDS	0.5 ml
0.5 M EDTA	0.2 ml
1 M Tris pH 8.1	0.5 ml
50x PI tablet	0.2 ml
1000x PMSF (100 mM in 2-Propanol)	10 μ l
100x Na Butyrate (1 M)	100 μ l

Dilution Buffer	400 ml
4 M NaCl	16.7 ml
1 M Tris pH 8.1	6.69 ml
0.5 M EDTA	0.96 ml
10 % Triton X-100	44 ml
20 % SDS	0.2 ml

RIPA	400 ml
4 M NaCl	15 ml
1 M Tris pH 8.0	20 ml
20 % SDS	2 ml
10 % NaDOC (fresh)	20 ml
10 % NP40	40 ml

High Salt	400 ml
4 M NaCl	50 ml
1 M Tris pH 8.0	20 ml
20 % SDS	2 ml
10 % NP40	40 ml

LiCl Wash	400 ml
4 M NaCl	100 ml
1 M Tris pH 8.0	20 ml
10 % NaDOC (fresh)	20 ml
10 % NP40	40 ml

Elution Buffer	5 ml
20 % SDS	0.5 ml
1 M NaHCO ₃	0.5 ml
DTT	50 µl

TE	400 ml
0.5 M EDTA	0.8 ml
1 M Tris pH 8.0	4 ml

2.3.2 Crosslinking and harvesting of *in vitro* cultured cells

Cells were grown up to 80-90 % confluency in 15 cm dishes. Standard crosslinking with FA for histone modifications was done with 1 % formaldehyde at room temperature for 10 min. Crosslinking was stopped with 125 mM (final concentration) glycine at room temperature for 5 min. After washing twice with ice cold 1x PBS, containing 10 mM Sodium-Butyrate, the cells were harvested in cold PBS.

For the treatment with alternative crosslinkers cells were washed three times with room temperatured PBS containing 1 mM MgCl₂. Alternative crosslinkers (DSG or EGS, *AppliChem*) were dissolved in DMSO to obtain a 0.5 M stock solution. The stock solution was diluted in PBS (containing 1 mM MgCl₂) to get the final concentration of 2 mM. Unless stated otherwise, cells were incubated with this 2 mM crosslinker in PBS at room temperature for 30 min with agitation. After crosslinking and washing the cells twice with room temperatured PBS containing 1 mM MgCl₂, 20 ml of PBS (1 mM MgCl₂) were added to each 15 cm dish, and standard FA crosslinking followed as described above.

Five 15 cm plates were pooled and centrifuged at 1200 rpm at 4 °C for 5 min. The resulting pellet was resuspended in 5 ml Wash I, containing 10 mM Sodium-Butyrate, 1x Complete protease inhibitor (*Roche*) and 0.1 mM PMSF, by pipetting up and down. The cells were incubated on ice for 10 min and centrifuged at 1200 rpm at 4 °C for 5 min. The resulting supernatant was carefully aspirated and the pellet was resuspended in 5 ml Wash II (containing the same inhibitors like Wash I). The sample was again incubated on ice for 10 min and centrifuged at 4 °C at 1200 rpm for 5 min. The resulting pellet was resuspended in freshly prepared Lysis buffer, containing 10 mM Sodium-Butyrate, 1x Complete protease inhibitor (*Roche*) and 0.1 mM PMSF, and rolled at 4 °C for at least 30 min. Chromatin was kept at 4 °C until sonication.

2.3.3 Crosslinking and harvesting of tissue samples

Epidermis Four different methods for epidermis extraction were tested. **A)** Mouse tails and ears were kept in dispase (5 mg/ml) at 4 °C for 2 h, then the epidermis was separated from the dermis and minced with a razor. **B)** Mouse tails and ears were kept in trypsin (0.8 %) at 4 °C for 2 h, the epidermis was separated from the dermis, homogenized with ceramic beads in PBS and poured through a cell strainer. **C)** Mouse tails, ears and back skin were kept in

disperse (5 mg/ml) at 4 °C for 2 h. Then the epidermis was separated, minced, incubated with DNase (0.25 mg/ml) at 37 °C for 30 min and poured through a cell strainer. **D)** Mouse tails and ears were kept in trypsin (0.8 %) at 4 °C for 2 h. Then the epidermis was separated, minced, incubated with DNase at 37 °C for 30 min and poured through a cell strainer. Each of the different methods was followed by washing the epidermis twice with ice cold PBS in 50 ml plastic tubes by centrifugation at 4 °C, 2000 rpm for 5 min. Epidermis samples were crosslinked with 2 mM DSG in PBS at room temperature for 25 min, washed once with PBS (2000 rpm, 4 °C 5 min), crosslinked with 1 % FA in PBS for 10 min and crosslinking was stopped with 125 mM Glycine in PBS for 5 min at room temperature. After washing the epidermis once, the tissue pieces were incubated with 5 ml Wash I containing 10 mM Sodium-Butyrate, 1x Complete protease inhibitor (*Roche*) and 0.1 mM PMSF on ice for 10 min. Then the pieces were spun down, the supernatant was removed and 5 ml of Wash II, containing the same inhibitors, was added and incubated on ice for 10 min. During both incubation steps the tissue pieces were mixed by pipetting with cut tips. After the last incubation step the tissue was resuspended in freshly prepared Lysis buffer, containing inhibitors, and rolled at 4 °C for at least 30 min. Chromatin was kept at 4 °C until tip-sonication.

Brain Brains of P0 mice were dissected and as much fat and blood as possible was removed. Complete brains were homogenized and washed once with cold PBS and transferred into low protein binding tubes (*Eppendorf*). Samples were crosslinked with 2 mM DSG and 1 % FA and chromatin was extracted as described above. After resuspension in lysis buffer, the samples were transferred into 1.5 ml hard plastic tubes and sonicated with the Bioruptor® sonication system 30 - 35 cycles. Hard plastic tubes were changed every 10 cycles to prevent them from breaking.

2.3.4 Chromatin shearing

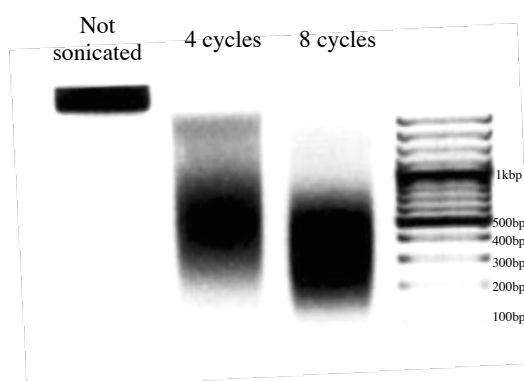
Tip-sonication (BANDELIN sonoplus GM70): 700-1000 µl chromatin in 2 ml eppendorf tubes was sonicated 10x 15 sec (cells) or 12x 15 sec (epidermis) by submerging the tip into the eppi as deep as possible, without touching the wall. (conditions: Power 45 %, Cycle 90) The tip was cleaned with water and samples were kept on ice between sonication cycles.

Bioruptor® sonication system: 700-1000 µl chromatin in 15 ml Polystyrene tubes were sonicated at 4 °C for 8-12 cycles (One cycle = 30 sec on, 30 sec off. High Power). Adaptor rings were used to ensure proper positioning. No tips were submerged, and caps were loosened before sonication. Chromatin concentration did not exceed 1.5 µg/µl. Chromatin samples were incubated at room temperature until all precipitated SDS was dissolved again. Before starting and after 4, 8, 10 and 12 cycles the tubes were vortexed.

Sonication efficiency test: An aliquot of sheared chromatin was spun down at full speed 4 °C 10 min and the supernatant was de-crosslinked with 10 % Chelex 100 at 99 °C while shaking strongly for 10 min. After cooling to room temperature the samples were treated with 2 µl RNase A (10 mg/ml) for 30 min at room temperature. After RNase digestion, the samples were

treated with 4 µl Proteinase K (20 mg/ml) at 55 °C for 1 h. The resulting DNA was mixed with 1/5 orange juice- loading dye and loaded on an agarose gel. For DNA separation 2 % agarose gels were used. The agarose was melted in TAE buffer by boiling, cooled down to 60 °C supplemented with 0,5 mg/ml ethidium bromide and poured into a gel tray. Before loading DNA samples were mixed with 6x DNA loading dye. As a marker, the GeneRuler™ 100 bp Plus or 1 kb Plus (*Fermentas*) were loaded and gels were run at 2 – 8 V/cm. ChIP experiments were carried out using fragmented chromatin with an approximate size of 200-400 bp. If appropriate size was not obtained, chromatin was re-sonicated until reached the desired length distribution. Optimal fragment size for F9 and ES cells was obtained after 8-10 cycles using the Bioruptor sonication system (Figure 6).

Figure 6: Sonication efficiency test of chromatin obtained from F9 cells and sheared using the Bioruptor® sonication system. DNA fragments decrease in size by adding additional cycles.



6x DNA loading dye	
EDTA	1 mM
Urea	4 M
Saccharose	50 %
Bromphenol blue	0.1 %

10 x TAE	
Tris-Acetate	400 mM
EDTA	20 mM
adjust to pH 8.5	

2.3.5 Setting the IP

IP with Dynabeads® Unless stated otherwise, all ChIPs experiments were done with magnetic Dynabeads®. Before setting the IP, the chromatin was measured via NanoDrop. 6.25 - 12.5 µg of chromatin was used as inputs and were kept without Dilution Buffer at 4 °C until the step of Elution. 25-50 µg of chromatin was used for HDAC ChIPs and 25 µg were used for detecting histone marks. The chromatin was diluted at least 10 times with dilution buffer (containing 10mM Sodium-Butyrate, 1x Complete protease inhibitor (*Roche*) and 0.1 mM PMSF) and working amounts (if unknown 4 µg) of the corresponding antibody was added and rolled at 4 °C overnight. In parallel 15 µl of Dynabeads® per IP were washed 3 times with Dilution Buffer, and blocked in Dilution Buffer with 1 µg/µl BSA, rolling at 4 °C overnight. The next day the blocking solution was removed with a magnetic rack and the IPs were added onto the beads and rolled at 4 °C for 3-4 h.

IP with sepharose beads Sepharose beads were either already slurry (Protein G Sepharose 4 Fast Flow, GE Healthcare) or one spoon of beads had to be filled up to 2 ml with TE-buffer

(Protein A Sepharose CL-4B, GE Healthcare). Both were incubated 30 min on ice before washing them three times with TE by inverting and centrifugation (3000 rpm, 4 °C). After the last spin down, the supernatant was discarded and 2 µl salmon sperm DNA, 10 µl BSA (10 mg/ml), 5 µl Na-Azide (2 %) and 85 µl TE were added for each 100 µl beads and blocked by rolling at 4 °C for 30 min. After blocking the beads were centrifuged at 2000 rpm, 4 °C, for 3 min, the supernatant was discarded and the beads were filled up with TE to get 50 % slurry. 25-50 µg of chromatin was used for HDAC ChIPs. Chromatin samples were added up to 1 ml with Dilution buffer (containing 10 mM Sodium-Butyrate, 1x Complete protease inhibitor (Roche) and 0.1 mM PMSF). Due to the higher background signal, chromatin samples had to be precleared with blocked sepharose beads. Therefore 30 µl of blocked beads were added to the chromatin samples and incubated for 2 h while rolling. After preclearing the beads were removed (4000 rpm, 4 °C, 3 min) and the supernatant was used for the IP. Working amounts (if unknown 4 µg) of the corresponding antibody was added to the chromatin samples and incubated overnight while rolling. The next day 30 µl of A or G sepharose beads were added and the IP was incubated at 4 °C for 3 - 5 h while rolling.

2.3.6 Washing the IP

After the incubation with the IP, the beads were washed, by rolling them at 4° for 10 min consecutively with: 1x RIPA, 2x, High Salt, 1x LiCl, 2xTE. Between the wash steps, the beads were separated from the solutions via the magnetic rack, and the wash solutions were discarded. Sepharose beads were separated from the solutions by centrifugation (4 °C, 4000rpm, 3 min). After the last TE -wash the immunoprecipitated chromatin was eluted from the beads by adding 400 µl of Elution Buffer and strongly shaking the samples at room temperature for 30 min. The supernatant was transferred into a new tube and the remaining beads were discarded. The input samples were filled up to 400 µl with Elution Buffer. The chromatin (including inputs) was de-crosslinked with 200 mM NaCl at 65 °C overnight.

2.3.7 DNA Precipitation

Before precipitation, the samples were treated with Proteinase (8 µl 0.5 M EDTA, 16 µl 1M Tris pH 6.5 and 2 µl Proteinase K 20 mg/ml) at 55 °C for 1 h. DNA was separated from proteins by adding 600µl PCI (Phenol-Chloroform-Isoamyl alcohol, *AppliChem*) to the proteinase K digested samples. This mixture was strongly shaken for 20 sec in PhaseTrap tubes (*peqlab*) and centrifuged at 16 000 rcf. The upper DNA-containing aqueous phase, which is separated from the organic phase by the gel barrier, was transferred to a new 1.5 ml tube and supplemented with 3 M NaOAc (1/10 of the volume), ice cold 96 % EtOH (2.5 times the volume) and 1 µl glycogen (20 mg/ml). DNA was precipitated at -20 °C for at least 30 min. After precipitation the samples were spun down at full speed at 4 °C for 30 min. The supernatant was discarded and the DNA-pellet was washed with 1 ml 70 % EtOH and centrifuged again at full speed at 4 °C for 5 min. The resulting pellet was air-dried until it got transparent and redissolved in 100 µl dH₂O.

Table 1: Antibody list used in ChIP experiments

Factor	Antibody (shipped Conc.)	Used per 25 µg Chromatin
HDAC1	Sat13 Abcam ab7028 (12.8 - 15 mg/ml) 10E2	10 µl 0.5 µl 15 µl
HDAC2	Sat33 Abcam ab7029 (12.8 - 15 mg/ml) Abcam ab12169 (2.4 mg/ml) Bethyl A300-705A (0.2 mg/ml) 3F3 3F3 (purified with G-beads)	15 µl 0.5 µl 1 µl 4 µl 15 µl 5 µl
H3K9ac	Millipore 06-942 (1 mg/ml)	4 µl
H3K14ac	Millipore 07-353 (Variable)	4 µl
H4ac	Millipore 06-866 (Variable)	4 µl
H3K4ac	Active Motif 39381 (NA)	4 µl
H4K16ac	Sat53	5 µl
H3 C-terminal	Abcam ab1791 (NA)	2 µl
IgG	Invitrogen 10500C (3 mg/ml)	1 µl
p53	Do7	100 µl
Sin3a	Santa Cruz (K-20X; sc994X) (2 mg /ml)	2 µl
CoREST	Millipore 07-455 (NA)	4 µl
Mta1	Santa Cruz (sc9446) (0.2mg/ml)	20 µl

2.3.8 Quantitative PCR (qPCR)

cDNA was diluted 1:10, ChIP-input was diluted 1:20 and ChIP samples were used undiluted in qPCR measurements. Gene expression values obtained by qPCR analysis of cDNA was normalized to the housekeeping gene GAPDH

One Reaction mix	
2x KAPA SYBR FAST (<i>peqlab</i>)	10 µl
Primer (10 µM) fow/rev	0.4 µl
dH ₂ O	4.6 µl

qPCR Settings		
Temperature	Time	
95 °C	3 min	
95 °C	20 sec	40-50x
Annealing temperature	25 sec	
72 °C	25 sec	
60 °C - 95 °C	Melting curve	

The annealing temperatures were determined by a gradient qPCR with a range from 55-65 °C; Number in brackets indicate the position, calculated relatively to start of first exon (-)upstream, (+)downstream. RT = Primers for reversely transcribed cDNA quantification. All primers are designed for *Mus musculus*; Except last four primers, which are human (h).

Primer name	sequence	annealing temperature	Primer name	sequence	annealing temperature
VSTM2L(-1397)_F	CTGGCTGATGCTGAAGAGGAG	58 °C	Lefty1(RT4)_F	TGTGTGTGCTCTTTGCTTCC	58 °C
VSTM2L(-1397)_R	ACCGTGCTTGCTGTCTTTATTC	58 °C	Lefty1(RT4)_R	GGGGATTCTGTCTTGTTT	58 °C
VSTM2L(24192)_F	AAGGCTCTGTGACCATCTG	58 °C	mGAPDH (RT) F	GTCGTGTGAACGGATTG	58 °C
VSTM2L(24192)_R	GAACGAGGCTCATCCAGTC	58 °C	mGAPDH (RT) R	GACTCCACGACATACTCA	58 °C
nes(7)_F	GTCAGTGTGCGCCGCTACTC	58 °C	m_p21(RT2)F	TCCAGACATTCAGAGCCACAG	58 °C
nes(7)_R	CCTCCATGTGCTGGTCTG	58 °C	m_p21(RT2)R	GAGACAGCCCGCCATGAG	58 °C
nes(4804)_F	CCAGGAAGAAGAAGGGCAAATC	58 °C	m_p21_Aseq (-508)	CGACCTTGATGCCTATTTTC	58 °C
nes(4804)_R	TCAGAGACATCAGTGGCTCATC	58 °C	m_p21_Bseq (-508)	TTGCCTAACTTGCTGGAAG	58 °C
SCRT1(-784)_F	AGCCTCCAGACCTTAAAG	58 °C	m_p21_Cseq (-210)	CTGCGTGACAAGAGAATAGC	58 °C
SCRT1(-784)_R	ATACTTGGTGGCATAATCG	58 °C	m_p21_Dseq (-210)	CCACTCCTTCACCGATCC	58 °C
SCRT1(4088)_F	ATGACGCATATCGGAATC	58 °C	m_p21_Eseq (238)	TGCCCGCCAGAGTCACAG	58 °C
SCRT1(4088)_R	CGCAAAGCAAATACAGAG	58 °C	m_p21_Fseq (238)	CGAAGCCTTCAGCCACCAC	58 °C
Lefty1(-173)_F	AGACAGCGGTGACCAGATG	64 °C	m_p21_Gseq (2832)	TGTTTCGGTTGGTTGGTGTTAGC	58 °C
Lefty1(-173)_R	GGCAGGGAGGAAGAAGAGAG	64 °C	m_p21_Hseq (2832)	ACAGCACTCGGGAGGCAGAG	58 °C
Lefty1(-2310)_F	ATCTGCCTGACGAGGAAACC	58 °C	m_p21/3seq (-2924)	TCGGAGACCAGCAGCAAATCG	58 °C
Lefty1(-2310)_R	TCTGTGGAAGGAAGGAGTGTG	58 °C	m_p21/4seq (-2924)	GCAGCCCCACCTCTTCAATTCC	58 °C
Sap30(113)_F	ACAGTCACAGGACCTGGTAG	58 °C	m_p21/5seq (-2026)	GCCAAGCCCTTCCCAGACTTC	58 °C
Sap30(113)_R	TTCACTCCGCACCCCAAG	58 °C	m_p21/6seq (-2026)	CTAGAGATCGTGCCGACAGATG	58 °C
Sap30(1341)_F	TCTGACTGATGGCAAAGGAAG	58 °C	m_p21/9seq (5606)	GCAAGAGAAAACCTGAAGTG	58 °C
Sap30(1341)_R	ACTGAGCTGATTGACACTCTC	58 °C	m_p21/10seq (5606)	CACACAGAGTGAGGGCTAAG	58 °C
PITPNC1(1584)_F	GCATTCTCCGATTCTTCTC	58 °C	m_p21/11seq (6775)	AACATCCTGGTCTGGAAGTCTAC	58 °C
PITPNC1(1584)_R	ACAGACGCAAAGCACTTATG	58 °C	m_p21/12seq (6775)	GGTGTGTCCCTTCTCGTGAG	58 °C
PITPNC1(-1906)_F	TACAGCCAGCCAGCAGTG	61 °C	Spr2h(-208)F	GGATGGTCTCTGAGTCACTGC	58 °C
PITPNC1(-1906)_R	TCGCATTGTTGAGAGTAAGG	61 °C	Spr2h(-208)R	CCCCCCTGTAGGTTGTAAAG	58 °C
VSTM2L(RT)_F	CGGGACTGGACTGACAAG	58 °C	Epgn(-342)F	ATTATCTGTCTGCTGTTCTG	58 °C
VSTM2L(RT)_R	CTCGTAGGTGCCTTCGTC	58 °C	Epgn(-342)R	TCATCTGGCTGTTCTTACC	58 °C
nes(RT)_F	GAAGCAGGCTCTACAGAGTC	58 °C	Epgn (7510)F	TTTGTGGTTTGGTTCCATTCTC	58 °C
nes(RT)_R	GGGTCAGGAAAGCCAAAGAG	58 °C	Epgn (7510)R	TTCGTGGGTATTTAGGGTTAG	58 °C
SCRT1(RT)_F	CGCAGCGATCTCGGAGTG	64 °C	Edn1(-150)F	TGGGATTCAAGAGCGAAGAG	58 °C
SCRT1(RT)_R	CGCACAGCCGACGATAC	64 °C	Edn1(-150)R	TCTCCAGAAGCAAAGTCACC	58 °C
ODZ4(RT)_F	CAACTCCAACCTCACACTCAC	64 °C	h_p21 (p53bs)_F	GGGTTTAGCCACAATCTCTG	58 °C
ODZ4(RT)_R	GCCTAGCAACCGCCTCTG	64 °C	h_p21 (p53bs)_R	CCAGTCTTCTCTCTAACG	58 °C
Sap30(RT)_F	TTTGCAGGAGGACGGTGAG	58 °C	h_p21 (prox)_F	GGTGTCTAGGTGCTCCAGGT	58 °C
Sap30(RT)_R	CCTTCTGTTCCGAACGCTCTG	58 °C	h_p21 (prox)_R	GCACTCTCCAGGAGGACACA	58 °C

Primer name	sequence	annealing temperature	Primer name	sequence	annealing temperature
PITPNC1(RT)_F	ATATCGCCTGTGATGAAATTCC	58 °C			
PITPNC1(RT)_R	TCCACTCGGGTCTGAAGG	58 °C			

2.3.9 DNA purification and RNase treatment for sequencing

Samples which would get sequenced were dissolved in 50 µl instead of 200 µl dH₂O, and treated with 1 µl RNase A (10 mg/ml) for 30 min at room-temperature. Purification was performed using the MinElute® PCR Purification Kit (50) from *Qiagen*. In the case that several samples had to get pooled, samples were loaded sequentially onto the spin column, and eluted together. Elution was done with 50 µl dH₂O.

2.4 Protein analysis

2.4.1 Whole Cell Protein extraction (Hunt Extraction)

80 - 90 % confluent 15 cm dishes were washed once and harvested in 5 ml ice cold 1x PBS. The cells were spun down (1200 rpm, 4 °C, 5 min) resuspended in 1 ml PBS and transferred into a 1.5 ml tube. This was centrifuged at 1200 rpm, 4 °C for 2 min, and the resulting pellet was dissolved in 200 µl Hunt Buffer (20 mM Tris-HCl pH 8.0, 100 mM NaCl, 1 mM EDTA, 0.5 % NP40). Prior to use, the Hunt Buffer was supplemented with 1x Complete protease inhibitor (*Roche*), 0.1 mM PMSF and 10 mM Sodium Butyrate. After resuspension the solution was snap frozen in liquid nitrogen, thawed at room temperature, snap frozen again, thawed at 37 °C, snap frozen again and then centrifuged at full speed at 4 °C for 30 min. The resulting supernatant was removed into a new 1.5 ml tube. Protein concentrations were determined by adding 1 µl of whole cell lysate to 1 ml of Bradford reagent (*Biorad* Protein Assay Dye reagent, 1:5 diluted in water). After mixing the absorption was measured at 595 nm in a plastic cuvette. Relative protein concentration results from: $A(595\text{nm}) \cdot 10 = c \text{ (}\mu\text{g}/\mu\text{l)}$

2.4.2 Histone isolation

80 - 90 % confluent 15 cm dishes were washed once and harvested in 5 ml ice cold 1x PBS. The cells were spun down (1200 rpm, 4 °C, 5 min) resuspended in 1 ml PBS and transferred into a 1.5 ml tube. This was centrifuged at 2200 rpm, 4 °C for 4 min, and resuspended in 1 ml histone lysis buffer (100 mM Tris, 50 mM Na-bisulfite, 10 mM MgCl₂, 1 % Triton X-100, 8.6 % Sucrose, adjusted to final pH of 6.5) containing the inhibitors 10 mM Sodium-Butyrate, 1x Complete protease inhibitor (*Roche*) and 0.1 mM PMSF. This centrifugation and resuspension step was repeated three times. After the last centrifugation step the supernatant was discarded and the pellet was washed once (1200 rpm) with wash buffer (100 mM Tris, 13 mM Na₃EDTA, adjusted to final pH of 7.4) containing inhibitors. The washed pellet was dissolved in 100 µl

dH₂O and supplemented with 2 µl H₂SO₄ (0.4 N) and incubated on ice for one hour. After incubation, the samples were centrifuged at full speed 4 °C for 20 min and the histone containing supernatant was transferred into a new 1.5 ml tube, in which the histones were precipitated with acetone (10 volumes of acetone per one volume of supernatant) overnight at -20 °C. The precipitate was collected by centrifugation at full speed at 4 °C for 20 min. The supernatant was discarded and the pellets were washed three times (full speed, 4 °C) with acetone to remove any residual acid. After washing the pellets were air dried and dissolved either in dH₂O (if analysis of histones by Western blot followed) or in corresponding buffer (if biochemical assays followed).

2.4.3 SDS-PAGE and Western Blots

Discontinuous Poly-Acrylamide (PA) gels, 0.75 mm thick, were used to separate proteins by size. Histones were analyzed with a 16 % PA separation gel. Proteins of higher molecular weight were analyzed on a 10 % PA separation gel. Proteins were cooked at 95 °C with corresponding amount of SDS-loading dye for 10 min. Gels were submerged into 1x Western Running Buffer, samples were loaded, including one lane of Precision Plus Protein Standard (*Bio-Rad*) for protein weight comparison, and run at 18 mA per gel. Separated Proteins were blotted onto a nitrocellulose membrane via semi-dry blotting or by wet blotting.

During the semi-dry blot, a stack of filter papers keeps the membrane and the SDS-PA-gel in the middle. From bottom to top: two filter-papers in Anode Buffer I, one filter-paper in Anode Buffer II, nitrocellulose membrane in Anode Buffer II, SDS-PA-gel in Cathode Buffer and three filter-papers in Cathode Buffer. After each layer, air bubbles were removed. Blotting was performed at 4 °C, 200 mA, 45 min.

Wet-blotting was performed in a glass bowl and all parts of the blot were nicely soaked in pre-cooled wet-blot transfer buffer. Again a stack of filter-papers keep the membrane and gel in the middle. Additionally this sandwich like structure is kept together by a plastic protective grid. From bottom to top: white plastic grid, sponge, two filter-papers, nitrocellulose membrane, SDS-PA-gel, two filter-papers, sponge and finally the black part of the plastic grid. Air bubbles were removed after each layer, finally the plastic support was closed and put into the tank. The casket was filled with wet-blot transfer buffer, a small magnetic stirrer was added and blotting was performed at 250 mA at 4 °C for 2 h or at 40 mA, 4 °C overnight.

After blotting the membrane was stained with 1x Ponceau S, the lanes were marked and blocked with fresh 2 % non fatty dried milk in PBS-Tween for 30 min - 1 h. Incubation with the primary antibody (diluted in blocking solution) was done 6 h - overnight. After washing the membrane three times 5 min with PBS-tween, the secondary antibody (diluted in PBS-Tween) was added for 1-2 h, and the membrane washed again with PBS-Tween three times 5 min. The blots were developed by incubating them with 2 ml of Enhanced Chemo Luminiscence (ECL) solutions (*Perkin Elmer*) or the ECL Prime solution (*GE Healthcare*) for 1 min and exposed to X-ray film (*Fuji*).

Stacking Buffer	
Tris-HCl pH 6.8	0.125 M
SDS	0.1 %

10x Western Running Buffer	
Tris	250 mM
Glycine	1.9 M
SDS	1 %

Separation Buffer	
Tris-HCl pH 8.8	0.375 M
SDS	0.1 %

10x Ponceau S	
Ponceau S	2 %
Trichloroacetic acid	30 %
Sulfosalicylic acid	30 %

SDS-Loading Buffer	
Glycerol	20 %
SDS	4 %
Bromphenol blue	0.01 %
Tris-HCl pH8.8	100 mM
β -Mercaptoethanol	5 %

PBS - Tween	
NaCl	8 g/l
KCl	0.2 g/l
Na ₂ HPO ₄	1.65 g/l
KH ₂ PO ₄	0.2 g/l
Tween 20	0.1 %
adjust pH to 7.4	

Wet blot transfer buffer	
Tris	25 mM
Glycine	192 mM
Methanol	20 %

2.5 Antibody purification

2.5.1 Heterologous expression and purification of His-tagged HDAC1 and HDAC2

Protein expression Two bacterial clones for HDAC1 (clone RPD3 A6 and clone 13/1) and one bacterial strain for HDAC2 expression (clone HD2-3) were used. These clones contained the *Hdac1* or *Hdac2* gene regulated by the inducible lacZ promoter. Overnight bacterial cultures were prepared from the bacterial glycerol stocks in 5 ml LB-amp (100 μ g/ml) / 0.2 % glucose at 37 °C while shaking at 200 rpm. The next day 5 ml of the overnight culture were added to 300 ml of LB-amp and incubated at 37 °C while shaking at 200 rpm. Bacterial growth was checked by measuring the OD₆₀₀ regularly. When OD₆₀₀ reached 0.6 - 0.8, a 1 ml aliquot was taken for the induction test and the rest of the bacteria was induced with 1 mM IPTG by incubation at 37 °C at 200 rpm for 4 h. After incubation, again an aliquot of 1 ml was taken and the rest of the bacteria was split into two samples of 150 ml and centrifuged at 4 °C, 5000 rpm for 15 min (Sorvall centrifuge, GS3 rotor). The supernatant was discarded and the bacterial pellet was snap frozen in liquid nitrogen and stored at -80 °C.

Lysogeny Broth (LB)	500 ml
Bacto™ Tryptone	5 g
Yeast extract	2.5 g
NaCl	2.5 g
ad 500 ml with d H ₂ O, adjust to pH 7.5	

Induction test To test if the induction by IPTG has worked, the samples from before and after the induction were checked by Western blot. Therefore the samples were put into 1.5 ml tubes and pelleted at 4 °C, 5000 rpm for 5 min. The supernatant was discarded and the bacteria were resuspended in 150 µl SDS loading buffer. The samples were vigorously pipetted up and down, incubated at 95 °C for 5 min and cooled again on ice. This procedure was repeated three more times. After the last cooling step the samples were spun down at full speed for 1 min and 10 µl from the supernatant were loaded onto a 10 % PA gel. HDAC1 and HDAC2 were detected by the monoclonal antibodies 10E2 and 3F3 respectively.

Protein purification (based on Novagen Ni-NTA His-Bind® Resin Manual) Each pellet, resulting from 150 ml bacterial culture, was resuspended in 10 ml of Binding buffer A and transferred to a SS-34 tube. To digest the cells lysozyme was added to a final concentration of 0.2 mg/ml and the samples were incubated on ice for 30 min (all enzymes were pipetted with filtered tips). After incubation the cells were sonicated 4x 15 sec (power MS 720, cycle 80, continuous cycle) and the samples were kept on ice between the intervals. Then 15 µl of DNase I (10 mg/ml) and 40 µl of RNase A (10 mg/ml) were added and incubated at room temperature for 30 min, followed by a centrifugation at 4 °C, 15000 rpm for 20 min. The supernatant was moved to a new falcon tube and the inclusion bodies containing pellet was resuspended in 5 ml Binding buffer B and incubated at ice for 1 h to solubilize the proteins. After the incubation the solubilized recombinant proteins were separated from insoluble cell material by centrifugation at 4 °C, 15000 rpm for 30 min. Prior to purification the supernatant was filtered through a 0.45 µm membrane filter.

2 ml of Novagen Ni-NTA His-Bind® Resin were pipetted into an empty column. The column was washed twice with dH₂O (1x bed-volume), three times with Charging buffer (2x bed-volume) and twice with Binding buffer B (1x bed-volume). For the final purification the filtered supernatant was loaded onto the column so that the liquid could pass through the beads. Since gravity flow was too slow, columns were centrifuged at 300 rpm for 1 min and the flow through was collected and reapplied on the same column at least three times. The final flow through was collected and the column was washed three times with one volume of Wash buffer. Elution was done three times with one volume of Elution buffer collected in 0.5 ml fractions (E1, E2, E3). Finally the column was cleared by washing it three times with one volume of Strip buffer and stored at 4 °C in Strip buffer. Stored columns could be charged again for re-use.

The different fractions were checked on a 10 % PA gel: 10 µl of the IPTG induced samples, 20 µl of the supernatant after the treatment with Buffer A; 20 µl of a 1 : 6 dilution of the supernatant after the treatment with Buffer B, 10 µl of the insoluble cell material, 10 µl of the first flow through fraction, 20 µl of each elution fraction and 20 µl of the strip fraction. These samples were supplemented with 10 µl SDS loading (except the IPTG induced cell lysate, which was already in SDS loading dye, see: Induction test), incubated at 95 °C for 10 min and loaded onto the gel.

Buffers for His-tagged protein purification All buffers were dissolved in dH₂O and all Ni²⁺ containing waste had to be disposed separately.

Charging buffer	
NiSO ₄	50 mM

Binding buffer A	
NaCl	0.5 M
Tris	20 mM
Imidazole	5 mM
adjust to pH 7.9	

Binding buffer B	
NaCl	0.5 M
Tris	20 mM
Imidazole	5 mM
Guanidine hydrochloride	6 M
adjust to pH 7.9	

Wash buffer	
NaCl	0.5 M
Tris	20 mM
Imidazole	20 mM
Urea	8 M
adjust to pH 7.9	

Elution buffer	
NaCl	0.5 M
Tris	20 mM
Imidazole	0.5 M
Urea	8 M
adjust to pH 7.9	

Strip buffer	
NaCl	0.5 M
Tris	20 mM
EDTA	100 mM
adjust to pH 7.9	

2.5.2 Purification of polyclonal antibodies

200 µl of the first elution (E1) from the recombinant protein purification, were cooked at 95 °C with 200 µl SDS loading buffer and loaded onto a 10 % PA gel. A special comb was used with just one marker slot and one big slot which could hold 200 µl, therefore the sample had to be loaded twice, and a bigger stacking gel had to be prepared. The PA gel was run like a standard SDS-PAGE, blotted at a nitrocellulose membrane and stained with 1x Ponceau S. The very prominent band for HDAC1 (55 kD) and HDAC2 (60 kD) were excised from the membrane, cut into small pieces (but still big enough that they cannot get sucked into a blue tip during the later wash steps) and transferred into a 1.5 ml tube. The pieces were blocked with 1 ml of Blocking solution (1 % non fatty milk, 1 % PVP, 0.1 % Tween, 0.02 % NaN₃) for 1-2 hours at room temperature. 1 ml of crude serum was used to incubate the membrane pieces overnight at 4 °C while rolling, also an aliquot of pure serum was retained for the purification check later on. After incubation the supernatant serum was removed and stored at 4 °C. The membrane was washed once with 10 mM Tris pH 8.0 and once with 10 mM Tris / 0.5 M NaCl pH 8.0. Washing was done by inverting and centrifugation at 1000 rpm. The acidic elution was done by the addition of 400 µl of 100 mM glycine pH 2.5. The tubes were vortexed for 1 min and spun down at 1000 rpm for 1 min. The supernatant was transferred into a new Eppi containing 100 µl Tris 1 M pH 7.5, 20µl BSA (10 mg/ml) and 0.5 µl NaN₃ (20 %). This first elution was labeled acidic elution 1 (AE1). The acidic elution step was repeated twice to gain AE2 and AE3. After the last elution the membrane was neutralized by washing once with 100 mM Tris pH 8.8. Basic elution was done by the addition of 400 µl 100 mM Triethylamine, vortexing for 1 min, centrifugation and the transfer of the supernatant into a new Eppi containing 100 µl Tris

1 M pH 8.0, 20 µl BSA (10 mg/ml) and 0.5 µl NaN₃ (20 %). Again this basic elution was done three times in total (BE1, BE2, BE3). After the last elution the membrane was washed once with 10 mM Tris pH 8.0, once with 10 mM Tris / 0.5 M NaCl pH 8.0 and twice with 1 x PBS. The last PBS was discarded and the membrane was frozen at -20 °C for further re-use.

The efficiency of the antibody enrichment was verified on a Western blot for all steps of the purification (Crude serum, serum supernatant, AE1-3, BE1-3)

2.5.3 Enrichment of monoclonal antibodies from hybridoma supernatant

HDAC2 monoclonal antibody (3F3) producing hybridomas were cultured and the supernatant of two 10 cm dishes was pooled (20 ml) and centrifuged at 2000 rpm to remove the cells. The supernatant was removed and roughly 1 ml was retained to avoid cell contamination. NaN₃ was added to a final concentration of 0.02 %. To prepare the column, 1 ml of 50 % slurry sepharose protein G beads were transferred into a 2 ml tube and washed three times with 1x PBS, by centrifugation at 3000 rpm, 2 min and removal of the supernatant. Beads were blocked with 0.5 µl NaN₃(20 %), 10 µl BSA (10 mg/ml) and 89.5 µl PBS per 100 µl beads, at 4 °C for 30 min while rolling. After blocking, the beads were washed once with PBS and loaded onto the column (#89896 *Thermo scientific*, 2 ml centrifuge column). The column was washed 5 times with 2 ml PBS by gravity flow. Then the hybridoma supernatant was loaded onto the column sequentially at room temperature by gravity flow and washed three times with 2 ml PBS. The antibodies were quickly eluted with 1 ml glycine (0.1 M pH 2) into an eppi containing 200 µl 1 M Tris pH 8 and 1.2 µl NaN₃(20 %). Elution was done four times by short centrifugation (few seconds at 200 rpm). All elutions (E1-4) were tested on a Western blot for enrichment and protein concentrations were measured by nano drop (280 nm) against a blank (1 ml glycine 0.1 M pH 2 + 200 µl Tris 1 M pH 8). The bead filled column was washed three times with 1x PBS and was stored in 1x PBS, 0.02 % NaN₃ at 4 °C for further re-use.

2.6 Generation of HDAC1 and HDAC2 deficient Mouse Embryonic Fibroblasts (MEFs)

2.6.1 Plasmid production

In the morning primary cultures were prepared from bacterial glycerol stocks (EGFP and EGFP-Cre) in 5 ml LB-amp (100 µg/ml) / 0.2 % glucose at 37 °C while shaking at 200 rpm. In the afternoon 100 ml of LB-amp (100 µg/ml) / 0.2 % glucose were inoculated with 200 µl of the primary culture and incubated overnight at 37 °C. The next day the overnight culture was split into two batches of 50 ml and both of them were harvested by centrifugation (6000 rcf, 15 min, 4 °C) and plasmids were isolated with the Midi prep kit provided by *Quiagen* [83]. The purified vectors were concentrated with a speed vac to yield a concentration of 0.7 - 0.8 µg/µl. To verify the plasmids, an aliquot of the purified DNA was digested either with *ClaI* (# R0197L, *NEB*) or with *EcoRI/BglII* (# R0101S and R0144S respectively, *NEB*) at 37 °C for 1 h while shaking at 300 rpm. The digest was checked on a 2 % agarose gel.

<i>Clal</i> digest	
Vector DNA	1 µg
BSA (10 µg/µl)	2 µl
NEBuffer 4	2 µl
<i>Clal</i>	0.5 µl
ad 20 µl with dH ₂ O	

<i>EcoRI</i> / <i>BglII</i> digest	
Vector DNA	1 µg
BSA (10 µg/µl)	2 µl
NEBuffer <i>EcoRI</i>	2 µl
<i>EcoRI</i>	0.5 µl
<i>BglII</i>	0.5 µl
ad 20 µl with dH ₂ O	

2.6.2 Extraction and direct transduction of unfrozen Mouse Embryonic Fibroblasts

Pregnant mice of desired genotype (HDAC1 f/f and HDAC2 f/f) were sacrificed at day 13.5 of pregnancy by either neck dislocation or CO₂. The uterus was dissected, the embryos separated and kept on ice in PBS in a 6-well plate. The limbs, head, liver heart and everything containing blood was removed from the embryo with fine forceps in an open tissue culture hood. The tail was also removed for genotyping the embryos (DNA extraction was done with the Wizard® Genomic DNA Purification Kit by *Promega* [84]). The carcass of the embryo was transferred into a new 6-well to wash with PBS. After washing the embryo was transferred into a new 6-well containing 1 ml of Trypsin/EDTA (TE). The body was dissolved with a 1 ml micropipette and filtered tips. After the body was dissolved another 1 ml of TE was added and incubated at 37 °C, 5 % CO₂ for 5 min, pipetted up and down again and incubated again for 3 min. Then 4 ml of standard DMEM medium (10 % FCS, 1 x AB) were added, transferred into a 15 ml tube and the falcon was kept standing at room temperature for a few minutes so that bigger pieces of tissue could sink down. The supernatant was transferred into a new 15 ml tube and about 0.5 ml of liquid was left remaining to avoid contamination with bigger pieces. The supernatant was centrifuged at 1200 rpm for 5 min and the medium was sucked off in a closed tissue culture hood. The remaining cell pellet was resuspended in 1 ml of medium and one additional ml was added after resuspension. 9 ml of fresh medium were put into two 10 cm dishes each and one ml of cell suspension was added to each dish. The cells were incubated at 37 °C, 5 % CO₂. The next day the medium was changed to remove dead cells. Once the genotypes were determined the cells were subcultured in a 1:3 ratio and unnecessary cell lines were frozen on the second day after isolation (see Table 2).

Plat E packaging cells [85] were used for the production of a retroviral titer, containing either an EGFP or an EGFP-Cre vector. Plat E cells had to be thawed in standard DMEM medium (10 % FCS, 1 x AB) onto a 10 cm dish in the afternoon and transferred into selection medium (DMEM, 10 % FCS, 1 x AB, 1µg/ml Puromycin, 10 µg/ml Blasticidine) the next morning by transferring them onto a 15 cm dish. Packaging cells were subcultured every second day (1:4 ratio) in selective medium. Excess cells were frozen in FCS / 10 % DMSO (¼ of 15 cm dish per vial). Before lipofection Plat E cells had to be cultured in selective medium for at least three days (at least two passages).

On the day before lipofection Plat E cells were trypsinized and resuspended in standard DMEM medium (10 % FCS) with no antibiotics. The cells were counted (CASY® Model TTC, 150 capillary, 0-30 µm scale) and 6.25 x 10⁵ cells were seeded per 6-well in 2 ml of medium without

antibiotics. For each 6-well of MEFs that had to be infected afterwards, one 6-well of Plat E cells was plated. 24 hours after the seeding the packaging cells were transfected with lipofectamine and corresponding plasmids. For lipofection two hard plastic 15 ml tubes were prepared. For each 6-well 250 µl Opti-MEM® (Reduced Serum Medium, *Gibco*) and 4 µg plasmid DNA were mixed by vortexing in the first tube. In the second one 250 µl of Opti-MEM® and 10 µl Lipofectamine 2000 (# 11668-019, *Invitrogen*) per 6-well were mixed by vortexing. Both tubes were incubated at room temperature for 5 min. After this first incubation both tubes were added together, mixed by pipetting and incubated at room temperature for 20 min. Then the solution was added onto the cells (ca. 515 µl per 6-well, depending on the plasmid concentration) and cultured at 37 °C, 5 % CO₂ for 48 h. Plat E cells were checked for positive lipofection by immunofluorescence microscopy for GFP expression the day before MEF infection.

24 h before the infection with viral supernatant, MEFs were seeded onto 6-wells, for each embryo and each vector one full 6-well plate was used and 80 000 cell were put into each well (in standard DMEM, 10 % FCS, 1x AB).

During infection, the virus containing supernatants of the corresponding vector were pooled into 50 ml plastic tubes and centrifuged at 1500 rpm room temperature for 5 min, to get rid of contaminating Plat E cells. Additionally the supernatant was filtered with a 0.45 µm acrodisc® syringe filter (Supor membrane, low protein binding, PN4614, *PALL Life Sciences*). Polybrene was added to the filtered supernatant to a final concentration of 5 µg/ml. Then the MEF medium was aspirated and 2 ml of viral supernatant (including Polybrene) were put into each well. The 6-well plates were sealed nicely with parafilm, balanced and put into a centrifuge. Only one plate was put into each tray and the cells were transduced by spin infection at 2500 rpm, 30 °C for 2 h. Then the parafilm was removed, the plates were incubated at 37 °C, 5 % CO₂ and the next morning the medium was changed for fresh standard DMEM, 10 % FCS + 1x AB. Once confluent, three 6-wells were pooled and transferred onto one 10 cm dish, to end up with the final amount of two 10 cm dishes per embryo per vector. After three days these plates were confluent and were sorted for GFP expression by FACS analysis. For sorting, both confluent plates for each embryo/vector were trypsinized, spun down at 1000 rpm and the cell pellet was resuspended in 300 µl of standard DMEM medium and pipetted through a cell strainer into a FACS tube. The cells were kept on ice and sorted into 2 ml of ice cold medium. Everything that was sorted for GFP expression from each plate, was put onto one 10 cm dish and cultured until confluency was reached. Once confluent cells trypsinized small aliquots were used for knockout verification and the rest of the cells were frozen in FCS containing 10 % DMSO in batches of 500.000 cells per vial.

	Day 0	Day 1	Day2	Day3	Day4	Day5	Day6	Day7	Day8	Day9	Day10	Day 11	Day 12
Morning		Put Plat E cells into selection medium		Isolate MEFs	Change MEFs Medium					Change MEF-Medium			Sorting
Afternoon -Evening	Thaw Plat E cells			Split Plat E cells		Split MEFs 1:3 (freeze undesired genotypes) Seed Plat E cells (6,25*10 ⁵ cells 6-well)	Lipofect ion	Seed Mefs 80.000/ 6-well	Infection	Split 3x 6-wells to 1x 10cm dish			
Passage of MEFs				P0		P1		P2		P3			P4

Table 2: General timeplan of the generation of HDAC1 and HDAC2 deficient MEFs. Cell lines were directly infected with retroviral vectors, therefore virus producing Plat E cells had to be cultured prior to MEF isolation.

2.6.3 Genotyping PCR

Genomic DNA was centrifuged at 14000 rpm for 5 min and 0,75 µl were used for the PCR reaction. The PCRs were carried out with the GoTaq® Master Mix (*Promega*). DNA from mice of known genotype as used as positive controls and DNA free PCR master mix was used as negative control .

HDAC1 lox PCR		
Temp.	Time	Cycles
94 °C	3 min	
94 °C	60 sec	40 x
54 °C	60 sec	
72 °C	60 sec	
72 °C	3 min	
4 °C	hold	

HDAC1 Δ		
Temp.	Time	Cycles
93 °C	3 min	
94 °C	60 sec	40 x
54 °C	60 sec	
72 °C	3 min	
72 °C	3 min	
4 °C	hold	

HDAC2 floxed PCR		
Temp.	Time	Cycles
95 °C	5 min	
95 °C	30 sec	40 x
58 °C	30 sec	
72 °C	30 sec	
72 °C	3 min	
4 °C	hold	

HDAC2 KO PCR		
Temp.	Time	Cycles
95 °C	5 min	
95 °C	30 sec	40 x
58 °C	30 sec	
72 °C	90 sec	
72 °C	3 min	
4 °C	hold	

Cre PCR		
Temp.	Time	Cycles
94 °C	3 min	
94 °C	45 sec	40 x
58 °C	45 sec	
72 °C	1 min	
72 °C	3 min	
4 °C	hold	

Sex PCR		
Temp.	Time	Cycles
94 °C	3 min	
96 °C	40 sec	40 x
62 °C	70 sec	
72 °C	100 sec	
72 °C	7 min	
4 °C	hold	

PCR	Primers	Sequence	Product size	AT	Cycles
HDAC1 Lox	Hdac1_lox_F Hdac1_lox_R	GGTAGTTCACAGCATAGTACTT CCTGTGTCATTAGAATCTACTT	Flox 900 bp WT 850 bp	54 °C	40
HDAC1 Δ	Hdac1_lox_F HDAC1floxedRev	GGTAGTTCACAGCATAGTACTT GTTACGTCAATGACATCGTCTT	Flox 900 bp Δ 600 bp	54 °C	40
HDAC2 Floxed	Hdac2FLOX_F Hdac2flox_R	CCCTTTAGGTGTGAGTACAT AACCTGGAGAGGACAGCAAA	Flox 850 bp WT 700 bp	58 °C	40
HDAC2 KO	Hdac2ko_F Hdac2ko_R	CCACAGGGAAAAGGAAACAA AACCTGGAGAGGACAGCAAA	Flox 1400 bp WT 1250 bp Δ 670 bp	58 °C	35
Cre	Cre_F Cre_R	TAATCGCCATCTTCCAGCAG CAATTTACTGACCGTACAC	1000 bp	58 °C	35
Sex	SRY-F SRY-R	GAGAGCATGGAGGGCCAT CCTCCTCTGTGACACT	Male 304 bp	56 °C	35

2.6.4 Detection of HDAC1 and HDAC2 knockouts

Immunofluorescent staining On the day of the freezing process small coverslips were put into a 24 well plate and coated with poly L-lysine (0.01 % in dH₂O) at room temperature for one hour. 40.000 cells of each embryo/vector were put into one 24-well. This was done in duplicates, to have backup slides in case of problems during the staining process. The cells were grown at 37 °C, 5 % CO₂ for one day, washed once with warm PBS and fixed with 4 % PFA in PBS for 15 min. Then the cells were washed once with warm PBS and blocked with 1 % goat serum in PBS / 10 % BSA / 0.25 % Triton X-100. After blocking, 45 μ l of primary antibody solution, diluted in 1 % goat serum, were put onto a parafilm in a wet chamber. Then the coverslips, with the cell containing side facing the parafilm, were put onto the droplet and incubated at 4 °C overnight. The monoclonal antibodies 10E2 (1:100) and 3F3 (1:200) were used for the detection of HDAC1 or HDAC2 respectively. The next day the coverslips were washed three times with PBS and incubated with the secondary antibody (Cy3, Alexa 595, *Molecular Probe*, 1:200 in 1 % goat serum). After incubation the stained cells were washed three times with PBS and mounted onto glass slides with 50 μ l ProLong[®] Gold (*Invitrogen*) containing 1 μ g/ml DAPI. Air bubbles were removed by gently pressing the coverslip with the tip of a micropipette. Stained slides were kept at 4 °C and were protected from light.

Western blot Approximately 50.000 cells of each embryo/vector were put into one 6-well, and cultivated at 37 °C, 5 % CO₂ for two days. For protein extraction, the medium was aspirated and the plates were kept on ice. Each 6-well was scraped in 20 μ l Frackelton lysis buffer (containing 1 x Complete protease inhibitor; *Roche*) and lysates were kept on ice for 20 min. Then the lysates were vortexed three times for 20 sec and spun down at 4 °C 15000 rpm for 20 min. The supernatant was transferred into a new tube, the protein concentration was measured and 5 to 10 μ g protein was used for Western blot detection on 10 % PA-SDS gels. Size-separated proteins were transferred onto nitrocellulose membranes by wet blotting to ensure a high yield of transferred proteins.

Frackelton Lysis buffer	
Tris	10 mM
NaCl	50 mM
Na ₄ O ₇ P ₂	30 mM
adjust to pH 7.05 and add Triton X to 1 %	

3 Results

In the last few years, two factors have greatly boosted the knowledge about histone acetylation and HDACs; firstly, the generation of antibodies that specifically recognize different histone modifications, and secondly, the development of small molecules, differing in their HDAC specificity, that can inhibit deacetylation activity at very low concentrations. These tools have helped to better understand the involvement of histone deacetylation in processes, as diverse as gene expression, cell cycle progression, proliferation, differentiation, tumor formation and development.

In the first part of this study we wanted to investigate the role of HDAC1 and HDAC2 in the process of transcription, by examining their binding patterns and changes in gene expression caused by HDIs or loss of one of the two HDACs. Extending a recent study of our lab, that elucidated the oncogenic function of HDAC1 knockdowns in teratoma formation [82], we chose the murine F9 teratocarcinoma cell line as a model system. Therefore, already generated genome-wide data were verified for specific candidate genes and different technical methods were tested to improve the HDAC1 ChIP-seq procedure for additional biological replicas. In the second part of the project we used this biological and technical insights to understand the molecular functions of HDAC1 and HDAC2 in developmental processes in the murine brain and epidermis. Finally, we looked into the role of HDAC1 and HDAC2 in the process of reprogramming by the generation of knockout fibroblasts for these two proteins.

3.1 Expression and HDAC1 ChIP-seq data can be validated by site-directed ChIP and qPCR in F9 teratocarcinoma

In order to confirm the genome-wide data, recently retrieved from ChIP-seq and Agilent Expression Arrays, candidate genes were chosen for testing in qPCR. ChIP-seq data for HDAC1 was generated by Solexa (*Illumina*) sequencing of an HDAC1 ChIP with a rabbit polyclonal antibody (Sat13) (ChIP-seq and expression arrays were done by Gordin Zupkovitz). Additionally genome-wide binding patterns were generated using the HDAC1 specific antibody ab7028 and the two antibodies targeting HDAC2 (ab7029 and Sat33). While the overlap of genes found to be bound by HDAC1 using the antibodies Sat13 and ab7028 was high (up to 80 %), the overlap between the two HDAC2 specific antibodies was poor (47 %). Furthermore, an additional feature of all ChIP-seq tracks was that the fold enrichment over input was low and less stringent peak detection algorithms were used (Gordin Zupkovitz, data not shown). Candidate genes for validation, were chosen upon the presence of HDAC1 near or at the promoter. Well defined peaks were picked, and primers within this peak and outside in a control region were

designed to test the binding dynamics of HDAC1 at these target genes. HDAC1 knockdown cells served as a negative control in all ChIP experiments. Genes with moderate to high expression were categorized upon their transcriptional behavior upon treatment with HDAC inhibitors (HDIs) trichostatin A and MS275. Three different groups of genes were used: Upregulated upon treatment, Downregulated upon treatment and Non-Responsive to any HDI treatments. For each group two to three candidate genes were selected and in addition to the genomic ChIP-primers, expression primers were designed. To avoid genomic amplification during cDNA measurements, expression primers aligned in different exons flanking at least one intron of a minimum size of 1 kb. Alternatively expression primers were designed to cover an exon-exon junction. Amplicon length was restricted to a maximum of 200 bps. Gene groups are listed in Table 3, up- or downregulated genes were defined to have a fold change of 2 or higher.

Gene-name	Expression in WT	Fc-HD1-KD/WT	Fc-TSA/WT	Fc-MS275/WT	HD1 RPKM minus input-RPKM
<i>Vstm2l</i>	8.7	2.3	4.9	8	1.5
<i>Nestin</i>	10.5	2	4.9	3.2	0.8
<i>Scrt1</i>	7.5	1.5	9.1	2.6	1.8
<i>Cdkn1a</i>	9.6	1.5	8.5	4.5	1.19
<i>Lefty1</i>	12.3	-1.5	-5.2	-5.2	1.2
<i>Odz4</i>	13.4	-1.0	-6.4	-3.0	1.3
<i>Sap30</i>	12.3	1.1	1.1	1.0	2.1
<i>Pitpnc1</i>	10.2	1.0	1.0	1.0	1.8

Table 3: List of target genes - Agilent expression values (5 - 8.5: low; 8.5 - 15.5: medium; 15.5-19: high). RPKM = reads per kilobase per million reads of a window +/- 3 kb of the TSS, Fc=Fold change, TSA=Trichostatin A, HD1=Histone Deacetylase1, KD=Knockdown, WT = Wild Type

Upregulated genes

This group of genes represents the classical view of HDACs as a transcriptional repressor. Upon inhibition of deacetylase activity, which is thought to result in hyperacetylation of the promoter, these genes show an increase in the transcriptional rate. Compared to expression data obtained by microarrays, upregulated target genes showed an even stronger response to inhibitor treatment when measured with qPCR using the same cDNA from the microarray (data not shown) or a biological replica (Figure 7A). Among the genes which were upregulated upon HDI treatment, and HDAC1 knockdown in the microarray, were genes which are known to be directly regulated by HDAC1 like *Cdkn1a*, also known as *p21* [38]. Since *Cdkn1a* served as a positive control for the enrichment of HDAC1 prior to the ChIP-seq experiment, it is not surprising that HDAC1 is enriched at the promoter but not at the 3' end (Figure 8C). The ChIP-seq data suggests that other upregulated genes (including the three additional candidate genes of this validation process) are direct targets of HDAC1 as well. Nestin is an intermediate filament protein which is expressed in neuronal stem cells and during the early stages of development in the CNS. Its expression is driven by a minimal promoter between position -11 and +183 [86],

which is also the location of the most prominent HDAC1 peak in our ChIP-seq data. Teratomas comprise of cells from all three germ layers, therefore ectodermal derived cells could express Nestin in F9 cells. This may also be true for the expression of Scratch1 (*Scrt1*) which is a homolog of the transcription factor Snail and has been reported to be important in neuronal development [87]. Less is known about the third target gene *Vstm2l*, but its human ortholog VSTM2L has been shown to antagonize the neuroprotective function of Humanin (HN) [88]. The presence of HDAC1 was verified via site-directed ChIP using the same antibody, and primers within the potential peak and within a control region. Within the promoter region of the upregulated candidate genes, HDAC1 was significantly enriched over non-specific (IgG) control, and control regions (Figure 8A - H) which validates the ChIP-seq data.

Downregulated genes

Since HDACs were found to remove acetyl residues from lysines at histones, a mark which is correlated with active gene expression, one would suggest, that blocking the catalytic domain by a small molecule inhibitor results in the derepression of those genes. However HDACs are also known to deacetylate lysines of non-histone proteins, which includes transcription factors. It is known that the acetylation of specific transcription factors, like p53 increases its potential as a coactivator. Similarly, acetylation of transcriptional corepressors caused by inhibition of HDACs could indirectly lead to the downregulation of HDAC bound genes. Another way of direct downregulation could be that the dynamic cycle of acetylation and deacetylation gets disturbed, which has been proposed to be the necessary process which is involved in actively transcribed genes [18]. The gene *Odz4* spans a huge locus of roughly 700 kbp that uses five alternative promoters. All of them are actively transcribed in a variety of tissues and cell types but only two contain Open Reading Frames (ORFs) [89]. The first promoter was used for HDAC ChIP validation as it codes for the transcript detected by the Agilent microarray. *Odz4* is a transmembrane protein which is thought to be important for the establishment of the anterior-posterior axis during gastrulation. *Lefty1*, a TGF-beta homolog, was first described to contribute to the left-right axis formation by inhibiting Nodal signaling. However recently *Lefty1* and its homolog *Lefty2* were found to be highly present in ESCs and upregulated upon forced differentiation, which indicates that *Lefty1* can reroute differentiation by making cells nonresponsive to diverse differentiation factors such as Nodal [90]. Downregulation upon inhibitor treatment was confirmed by qPCR, however the expression data for the HDAC1 knockdown (HD1KD) could not be validated by qPCR, since the expression levels were either not changed (*Odz4*) or even upregulated (*Lefty1*) (Figure 7B). The HDAC presence at the promoters of these two target genes was confirmed since it showed enrichment over non-specific antibody control, but in the case of *Odz4* the control region, which should not show HDAC presence, was enriched to the same extent (Figure 8L).

Not deregulated genes

From the microarray and ChIP-seq data it is known that a great proportion of HDAC1 bound genes do not show a change in expression upon HDI treatment, or HDAC1 knock down. This

class of genes represents an interesting group where HDAC1 is recruited to the promoter, but apparently does not influence the rate of transcription by its catalytic deacetylating activity. Another explanations would be that these genes are sheltered from the increased acetylation (as reported for some genes in [91]) or even if the acetylation is increased, this alone is not sufficient to elevate the levels of transcription. Interestingly one of the unresponsive genes is *Sap30*, which itself encodes a component of the HDAC containing repressive complex Sin3. The unresponsiveness to HDIs of two HDAC targets was confirmed, by qPCR (Figure 7C) however one gene, *Pitpnc1* was upregulated in the HDAC1 knock down cells, although it was not upregulated in the microarray. The presence of HDAC1 at the promoter of these genes was confirmed as the promoter region shows significant enrichment compared to the control with unspecific antibodies, and compared to the control regions (Figure 8O and 8P).

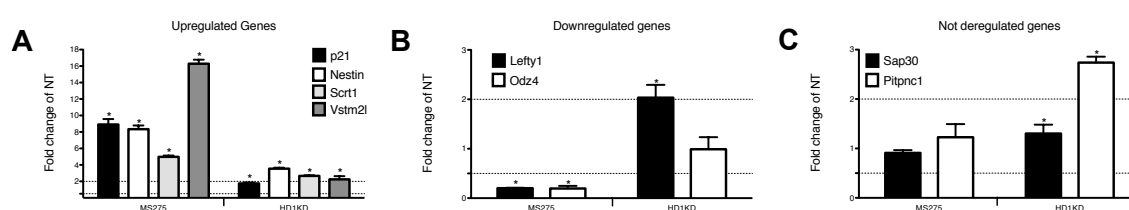
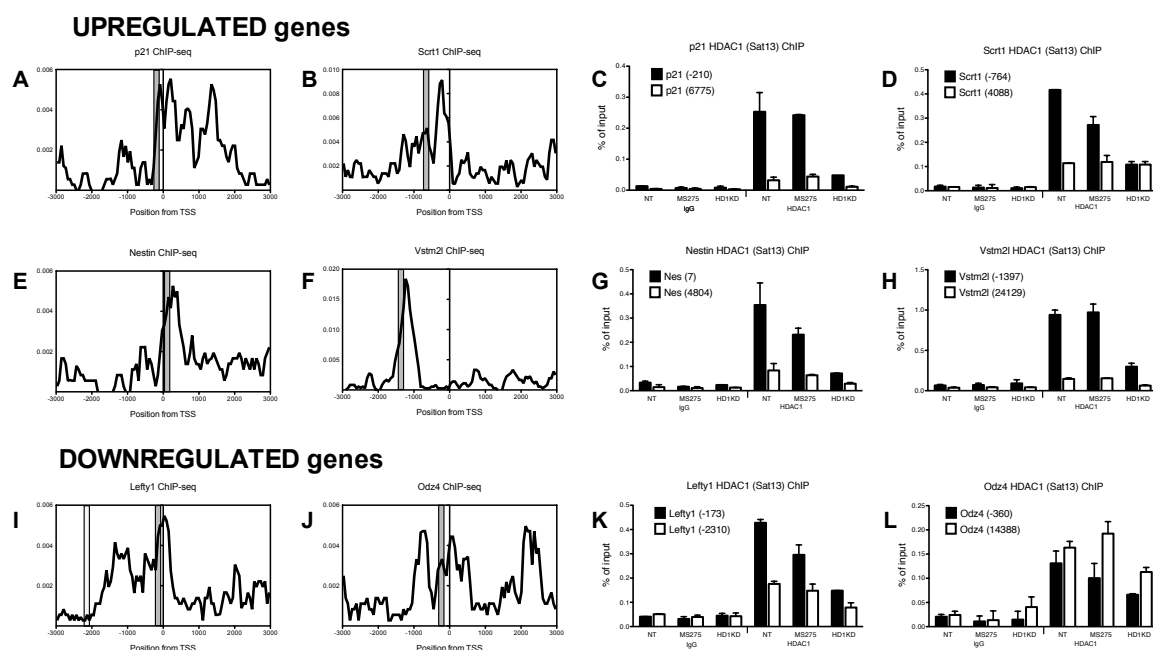


Figure 7: Candidate gene expression, which were either **A)** upregulated, **B)** downregulated or **C)** not found deregulated in the microarray data, tested with qPCR (NT = Not targeted wild type, HD1KD = HDAC1 Knockdown). Expression values were normalized to the housekeeping gene GAPDH. Dotted lines within the graphs represent the fold-change thresholds 0.5 and 2. Genes above or below these thresholds were considered up or downregulated respectively. Fold-Change values between 0.5 and 2 were categorized as not deregulated. (* = p value < 0.05, Error bars represent SD of two technical replicas)



NOT DEREGULATED genes

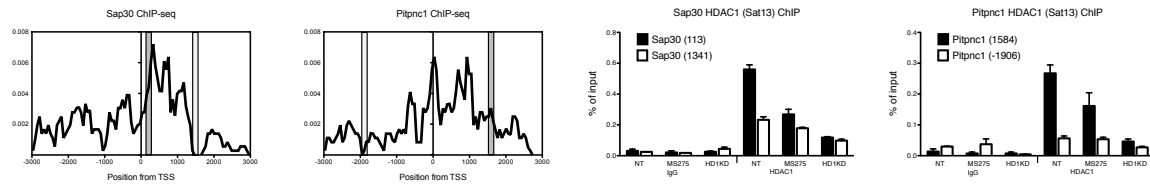


Figure 8: Validation of F9 HDAC1 ChIP-seq and microarray data. HDAC 1 RPKM values of 100bp windows (+/- 3000bp from TSS) obtained by ChIP-seq and checked with ChIP followed by site directed qPCR at promoters (black bars) or at control regions (white bars). Numbers in brackets indicate position from TSS = Transcriptional Start Site. (IgG = nonspecific control, NT = not targeted wild type, MS275 = HDAC inhibitor treated cells, HD1KD = HDAC1 Knockdown, Error bars represent SD of two technical replicas)

3.2 The HDAC1 ChIP in ESCs does not show reproducible results

One part of the project was to generate a genome-wide map of HDAC1 occupancy in mouse ESCs by ChIP-seq. The advantage of generating these binding data in ESCs is that mouse embryonic stem cells are one of the most extensively studied cell line. A vast amount of ChIP-seq tracks for a variety of chromatin modifying enzymes, transcription factors and chromatin marks does already exist and is available online for comparison studies. Additionally, ChIP-seq data for acetylation (H3 pan-acetyl) and methylation (H3K4me3) marks were already generated in our lab, therefore ESC chromatin was harvested and used for HDAC1 ChIPs. For ChIP-seq preparation, the same antibody was used at least 3 times in parallel IPs and the resulting DNA was treated with RNase A and purified with the MinElute® PCR Purification Kit (50) from Qiagen. Within this purification steps these three replicas were pooled to ensure sufficient DNA yield for sequencing. Before submission to the sequencing facility the purified samples were checked by site directed qPCR. However the results differed from each ChIP (Figure 9A - E). Furthermore, the enrichment of the promoter signal versus the 3' end of the positive control Cdkn1a was always too low for sequencing, where a 10x enrichment of a target region over the control region is desired. However histone-acetylation-ChIPs always worked reproducibly (Figure 9F - H) and showed an increase in H3K9ac marks upon treatment with HDAC inhibitors which is in line with the upregulation of the target gene Cdkn1a (p21). This suggests that either the HDAC1 antibody was not specific enough or the ChIP procedure for HDAC1 had to be optimized.

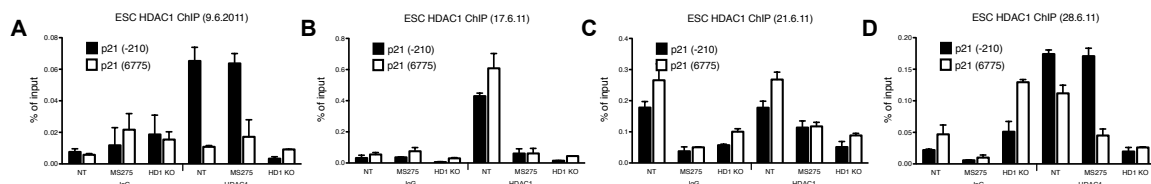
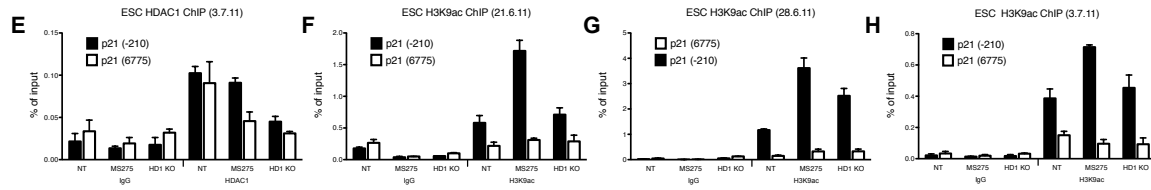


Figure 9: HDAC1 and H3K9ac ChIPs in mouse ESCs. (continues on next page)



continued Figure 9: HDAC1 and H3K9ac ChIPs in mouse ESCs. Number in brackets represent the position of primers relative to the transcriptional start site. (IgG = nonspecific control, NT = not targeted wild type, MS275 = HDAC inhibitor treated cells, HD1KO = HDAC1 Knockout; Error bars represent SD of two technical replicas)

3.3 Antibody purification

Recombinant HDAC proteins accumulate in bacterial inclusion bodies and can be purified using Ni-NTA-columns

Since the antibody quality was questioned by the ChIP results in ESCs, new antibody purifications had to be done. Sat13 is a polyclonal antibody, produced in rabbits against a recombinant HDAC1 protein, which was truncated for the first 52 amino acids and modified with a N-terminal His-tag. However in the past this antibody was purified with a N-terminal Myc-tagged recombinant HDAC1 protein. This could weaken the purified antibody, because the Myc-tag could mask epitopes and thereby lead to a negative selection of potential HDAC1 binding antibodies. The polyclonal antibody Sat33 was generated against an peptide containing the last 16 amino acids of the murine HDAC2 protein (EKTDPKGAKSEQLSNP). For its use in Western blot or ChIP, a purification of the serum was also necessary. Therefore His-tagged recombinant protein was produced in *E.coli* and used for the purification of crude rabbit serum. These bacterial strains contain the mouse *Hdac1* or *Hdac2* cDNAs, under an inducible lacZ promoter. The production of recombinant protein gets induced by IPTG in all three clones tested (Figure 10 A). However, for HDAC1 only clone 13.1 was used as it showed better growth rates and faster induction. The recombinant protein was extracted as described in the Material and Methods section. During this extraction, the treatment with guanidine hydrochloride (6M) containing Buffer B was especially important as this solubilizes the recombinant protein, which gets packed into bacterial inclusion bodies. Therefore the recombinant protein was enriched in the supernatant of Buffer B relative to the soluble protein fraction in Buffer A, even though 3 x more protein from Buffer A than Buffer B was loaded. (Figure 10B and C). Although the supernatant of Buffer B was diluted 1:6, the high salt concentrations lead to uneven protein migrations. The purification of His-tag containing proteins is based on the molecular interaction between the imidazole of the six histidines and the Ni-nitrilotriacetic-acid (NTA)-agarose, in which the Ni²⁺ ions are integrated into a chelating complex. Once bound to the Ni-NTA-column, the His-tagged proteins can be eluted using high concentrations of imidazole, which competes with the histidines for binding. As this affinity purification is specific for imidazole, proteins which are endogenously rich in histidines can also be captured with this method and may contaminate the elution fractions. The recombinant protein was clearly purified and enriched in the elution fractions, especially in E1 and E2. The first elution fraction was used to produce a membrane containing just the

recombinant protein. Therefore the correct band was excised from a membrane and cut into small pieces (Figure 11).

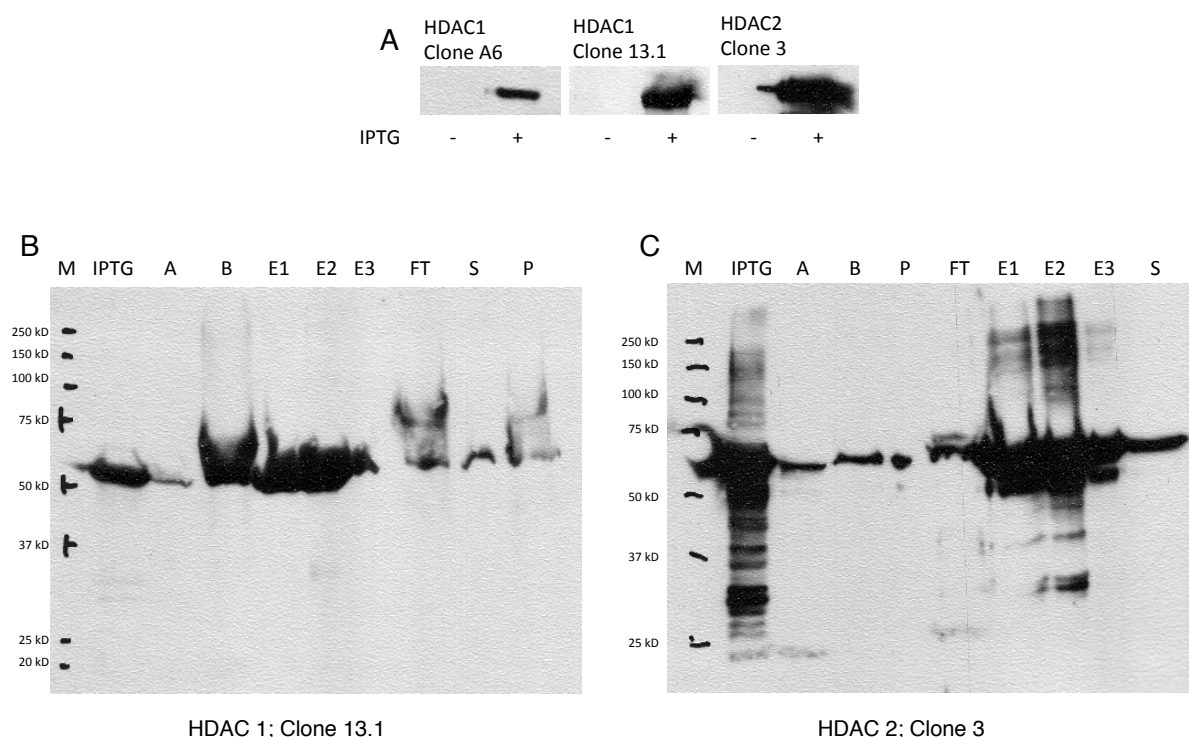


Figure 10: Production of recombinant HDAC proteins. **A)** Induction test of different bacterial clones. **B)** HDAC1 purification of clone 13.1 and **C)** HDAC2 purification of clone 3 using Ni-NTA His-Bind® Resin filled columns. (M = Precision Plus Protein Standard Marker; IPTG = Bacterial lysate after IPTG induction; A = Supernatant after treatment with Buffer A - soluble proteins; B = Supernatant after treatment with Buffer B - proteins solubilized with guanidine-HCl; E1, E2, E3 = Elution fractions from Ni-NTA-column; FT = Flow through / wash fraction from Ni-NTA-column; S = Strip fraction from Ni-NTA-column; P = Pellet of proteins insoluble in guanidine-HCl)

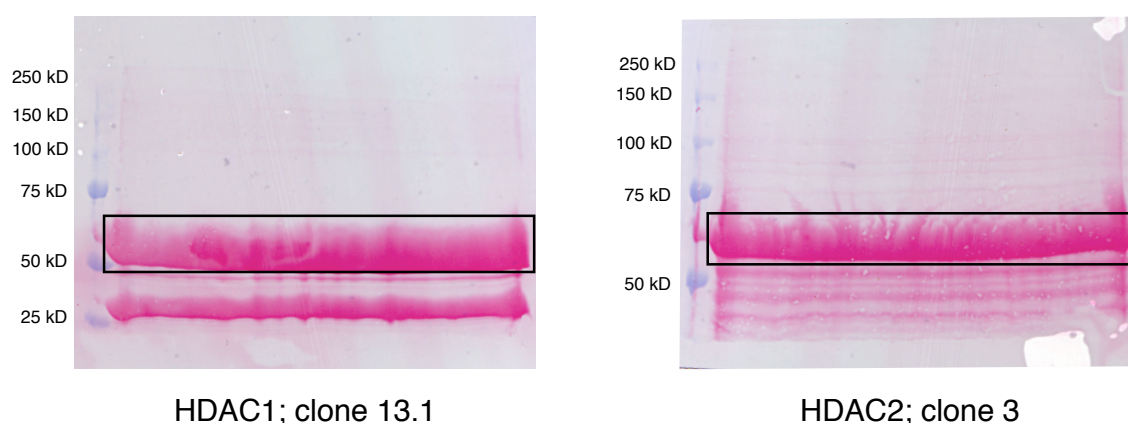


Figure 11: Preparative 10 % PA gel. 200 µl from the first elution, containing the highest recombinant protein enrichment, were loaded and stained with Ponceau S. The black box indicates the band of recombinant protein which was excised and used for purification.

Purification of the polyclonal antibody Sat13 with recombinant HDAC1 protein

The recombinant HDAC1 protein from clone 13.1 was used to purify the crude rabbit serum from the polyclonal antibody Sat13, and the resulting fractions showed that the crude serum recognizes at least one additional prominent band around 80 kD (Figure 12A). Antibodies within the serum, which contribute to this unspecific recognition were removed during the purification process. This subpopulation of antibodies were unable to bind to HDAC1 and therefore were retained in the supernatant but absent in the elution fractions. The crude serum and different elution fractions were re-tested on chromatin samples from either wild type or HDAC1 knock-down F9 cell (Figure 12B). The purified antibody showed a reduced binding in HDAC1 knock-down cells, even though the HDAC1 knockdown in the F9 cell line HD1-3 was not very efficient. The Sat13 elution A1 was used for further ChIP experiments.

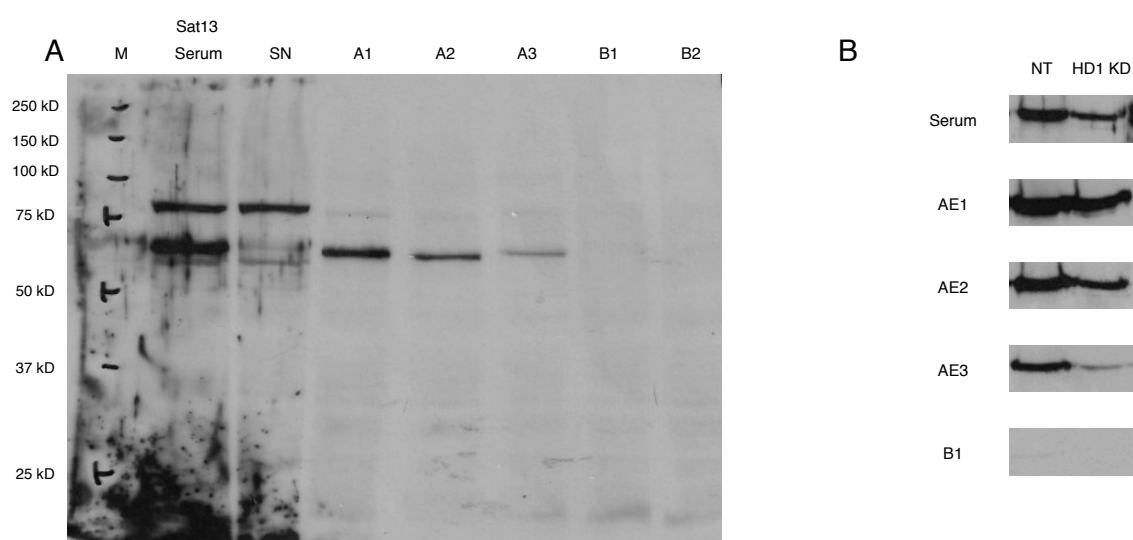


Figure 12: Purification of the polyclonal HDAC1 antibody Sat13. **A)** Purification fractions on tested on a WB with 20 µg F9-NT whole cell extract per lane. **B)** Purification fractions re-tested with chromatin from F9-NT and F9-HD1 KD. Crude serum was used 1:5000, all other fractions were used 1:1000 (M = Precision Plus Protein Standard Marker; Sat 13 Serum = Crude rabbit serum used as input; SN = Supernatant after overnight incubation with recombinant protein; A1, A2, A3 = Acidic elution fractions; B1, B2 = Basic elution fractions; NT = not targeted wild type; HD1KD = HDAC1 Knockdown)

3.4 HDAC1 and HDAC2 ChIPs can be improved with the alternative crosslinker DSG

Another possible way to improve the HDAC1 and HDAC2 ChIPs would be the use of alternative crosslinkers. During the generation of chromatin from cells or tissues, cells are normally treated with formaldehyde, which ensures that proteins which are bound, or in near proximity to the DNA are fixed. Formaldehyde molecules produce 2 Å big spacers and can crosslink DNA-DNA, DNA-protein and protein-protein interactions. As HDACs reside in huge multi subunit containing complexes, it may be that small molecules like formaldehyde cannot crosslink HDACs efficiently enough to produce constant ChIP results. Alternative crosslinkers, which can only link protein-protein interactions, offer a way to span bigger distances.

The molecules DSG (Disuccinimidyl glutarate) and EGS (Ethylene glycol bis [succinimidylsuc-

ciate)] can produce 7.7 Å and 16.1 Å big spacers respectively (Figure 13A). However, subsequent treatment with formaldehyde is necessary to crosslink the protein complexes to the DNA. Since the crosslinking by formaldehyde but not by DSG is reversible, the efficiency of crosslinking can be seen by loading chromatin on a Western blot. The big, still crosslinked complexes have a higher molecular weight and therefore HDAC1 was detected at the very top of an SDS gel after DSG crosslinking (Figure 13B). The same was true for the detection of HDAC2, although in the DSG treated samples, HDAC2 was only visible in the HDAC1 knockdown, in which HDAC2 is generally upregulated (Figure 14A).

For the first test of alternative crosslinking different times of crosslinking were used to establish the optimal balance between capturing bigger complexes while keeping epitopes accessible. This first ChIP was done in MEFs and showed that the dual crosslinking of DSG for 30 min and followed by formaldehyde for 10 min, lead to an increased pulldown efficiency of the promoter region of the HDAC1 target gene *Cdkn1a* (p21) while the overall background (unspecific IgG or 3' end of the gene) was not increased to the same extent. This resulted in an increased signal/background ration. Based on this observations, the method of dual crosslinking with DSG was tested in F9 teratoma cells, and again DSG crosslinking resulted in the specific enrichment at the promoter while background signal of control regions remained low (Figure 13C, D and E). To test if different antibodies, targeting HDAC1, would benefit from DSG treatment several antibodies were tested in F9 cells, including: two different Sat13 purifications (old, new) using either 5 or 10 µl; one commercially available antibody (ab7028) and two different amounts of a monoclonal antibody (10E2). The “old” Sat13 purification was done using the Myc-tagged HDAC1 protein, while the “new” Sat13 was purified with His-tagged recombinant protein. The His-tagged purified Sat13 antibody showed no increased pulldown efficiency compared to the “old” purification, however, using 10 instead of 5 µl improved the ChIP results slightly. The commercially available antibody ab7028 showed no significant increase. As did the monoclonal antibody 10E2, which failed to show any enrichment in both experiments.

In wild type F9 cells a total of 14 ChIPs were performed, using DSG and the antibody Sat13, and a total of 11 ChIPs were done with single (only formaldehyde) crosslinking while using the same antibody Sat13. Each of these ChIPs was analyzed by qPCR in two technical replicas. An estimated signal to background ration was calculated by comparing the promoter region of the gene *Cdkn1a* (p21) to the 3' end of the gene. In average formaldehyde crosslinking gave a signal to background ration of 4.05 while DSG crosslinking gave a mean ratio of 7.99 (p value = 5.17×10^{-9} , Figure 13G).

The dual crosslinking with DSG also improved the HDAC1 ChIP in mouse ESCs, by reproducibly increasing both pulldown efficiencies and signal to background ratios (Figure 13H). Therefore a preparative ChIP of two technical ChIP replicas was done, which both showed a comparable HDAC1 enrichment (promoter over 3' end) of more than six times. However, as later ESC passages tended to differentiate when cultured on gelatin, these chromatin samples were retrieved from ESCs grown on a layer of irradiated “feeder” MEFs. These MEFs were removed by incubating the trypsinized cells for 30 min on gelatinized plates, but feeder contamination could not be excluded. Additionally the yield of the preparative ChIP was too little (4 ng of total DNA), therefore the sample was not submitted for sequencing.

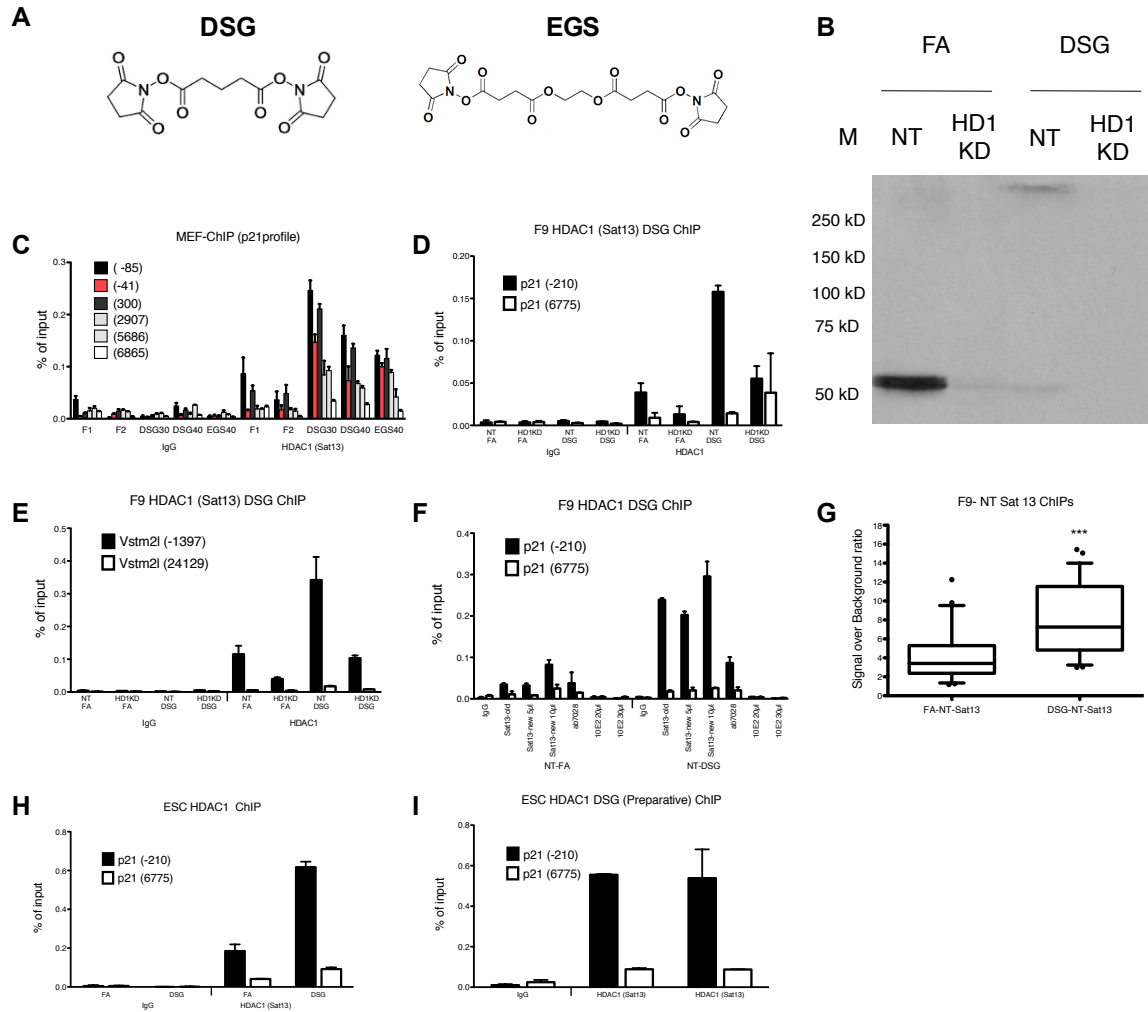


Figure 13: Effects of alternative crosslinkers on HDAC1 ChIPs. **A)** Chemical structures of the two alternative crosslinkers (DSG and EGS) used in this test. **B)** Formaldehyde (FA) and DSG (30 min) crosslinked chromatin checked on a Western blot by the detection of HDAC1. **C)** First ChIP with crosslinking test in MEFs. Formaldehyde only crosslinked samples was done in duplicates (F1 and F2). The alternative crosslinker DSG was used for either 30 min (DSG30) or 40 min (DSG40). EGS was only tested for 40 min. **D)** HDAC1 ChIP with formaldehyde only (FA) or DSG crosslinked F9 chromatin at the gene *Cdkn1a* (p21) or **E)** *Vstm2l*. **F)** Different HDAC1 antibodies tested for DSG crosslinking. **G)** Box-Whisker-Plot of signal/background ratios of HDAC1 ChIPs with the antibody Sat13 in F9 cells (Whiskers show 5 and 95 percentiles; n = 22 and 28 for FA and DSG respectively; *** = p value < 0.0001). Numbers in brackets indicate position from TSS = Transcriptional Start Site. **H)** DSG crosslinking test in wild type ESCs. **I)** Preparative HDAC1 ChIP for sequencing in ESCs (IgG = nonspecific control, NT = not targeted wild type, HD1KD = HDAC1 Knockdown, Error bars represent SD of two technical replicas).

To test if DSG can also improve ChIP experiments other than those carried out with Sat13, antibodies for three additional parts of HDAC1 containing complexes were tested in F9 teratocarcinoma cells: One commercially available antibody and one polyclonal antibody for HDAC2, ab7029 and Sat33 respectively. Two antibodies for the structural components of two major HDAC1 and HDAC2 containing complexes, Sin3 and CoREST, were also used. DSG also increased the pulldown efficiency of the HDAC2 specific antibody ab7029 and gave reproducible results, especially in the case of an HDAC1 knockdown (Figure 14 B and C). However the enrichment of signal versus background was in the wild type situation for both FA and DSG

crosslinking rather low (between two and three times enrichment). The antibodies for Sin3a (K20 -X) and CoREST (07-455) generally showed small increases in pulldown efficiencies in F9 cells (Figure 14 D-F), but the results of the Sin3a and CoREST ChIPs in HDAC1 knockdown cells were not conclusive, as in FA treated samples Sin3a and CoREST were increased in the knockdown but not in the DSG treated samples.

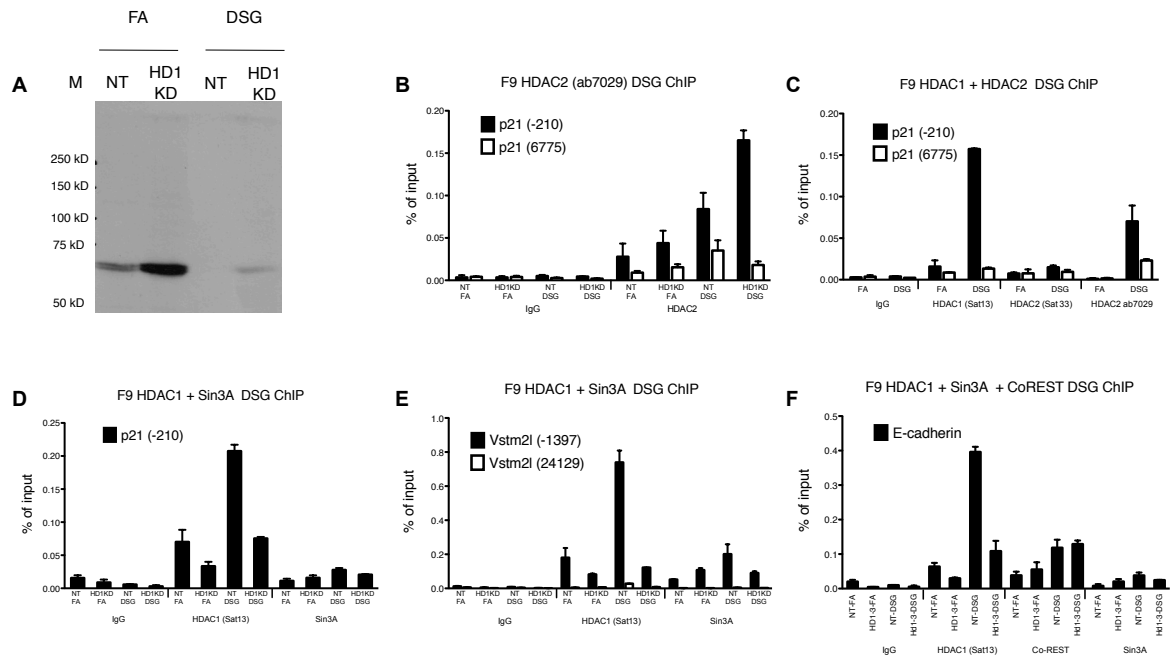


Figure 14: Effects of alternative crosslinkers on HDAC2, Sin3a and CoREST ChIPs. **A)** Formaldehyde (FA) and DSG (30 min) crosslinked chromatin checked on a Western blot by the detection of HDAC2. **B)** HDAC2 (ab7029) ChIP with formaldehyde only (FA) or DSG crosslinked F9 chromatin at the gene Cdkn1a (p21). **C)** Comparison of HDAC1 (Sat13) ChIPs with two different HDAC2 antibodies: Sat33 and ab7029. **D)** HDAC1 and Sin3 ChIPs with formaldehyde only (FA) or DSG crosslinked F9 chromatin at the gene Cdkn1a (p21) or **E)** Vstm2l. **F)** Comparison of FA and DSG crosslinking on HDAC1 (Sat13), Sin3a (sc994-X) and CoREST (07-455) ChIPs at the CoREST target gene E-cadherin. Numbers in brackets indicate position from TSS = Transcriptional Start Site. (IgG = nonspecific control, NT = not targeted wild type, HD1KD = HDAC1 Knockdown, Error bars represent SD of two technical replicas)

3.5 The alternative crosslinker DSG improves the results in HDAC1 ChIP-seq experiments

Since the HDAC1 ChIP data from DSG crosslinked chromatin looked promising, the biological replica, which should complement the existing HDAC1 ChIP-seq tracks, was done using DSG crosslinked chromatin (Figure 15A). Therefore a preparative ChIP was done with four technical ChIP replicas, which were treated with RNase, pooled and purified using the MinElute® PCR Purification Kit. An aliquot of the pooled and purified sample was used for a test-qPCR to check the enrichment. The enrichment of HDAC1 at the p21 promoter over its 3' end (6.7 times) was considered sufficient for genome-wide detection of binding patterns by sequencing (Figure 15C). The sample was measured (13.59 ng total DNA) and submitted for sequencing with the Genome Analyzer IIx by *Illumina*. Library preparation, sequencing and raw data analysis was performed at the Campus Science Support Facilities (CSF). Roughly 28 million reads

passed the basic quality filters and 22 million reads could be mapped uniquely to the mouse reference genome mm9, using the software package bowtie (version 0.12.2) [92] (Figure 15E). The amount of reads was comparable to the previous HDAC1 (Sat13) - ChIP-seq experiment using formaldehyde crosslinked chromatin which gave a yield of 29,004,353 (total) reads and 18,039,162 (uniquely mapped) reads. Only uniquely mapped reads were used in further steps of analysis.

Additionally, a preparative ChIP for HDAC2, using the polyclonal antibody ab7029, was done with DSG crosslinked chromatin. Similarly, the fragmentation was checked, four ChIPs were pooled, purified, and checked by qPCR (15B and D). The pooled and purified sample was measured (7.6 ng total DNA) and submitted for sequencing with the HiSeq 2000/1000 sequencing system by *Illumina*. Again, library preparation, sequencing and raw data analysis was performed at the CSF. Sequencing with Illumina's HiSeq technique proved to yield greatly increased amounts of reads (ca. 130 million) of which roughly 103 million could be mapped uniquely (Figure 15F). Interestingly the ratio between uniquely matched reads with no errors (U0) to uniquely matched reads containing one or two errors (U1 and U2 respectively) was increased in this sequencing run compared to the (Sat13) - ChIP-seq experiment (Figure 15E), which could indicate an inferior sequencing quality.

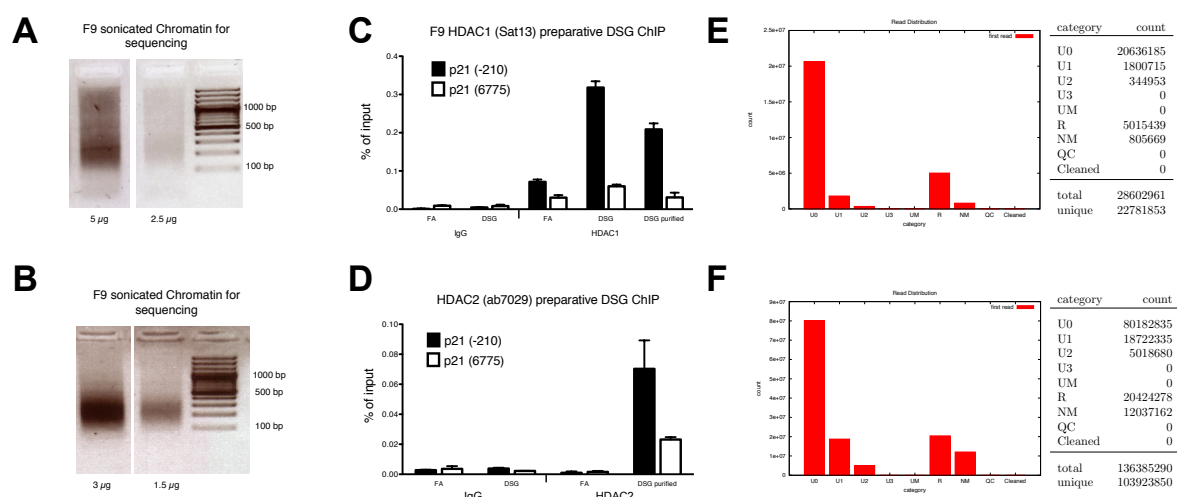


Figure 15: Quality control of HDAC1 and HDAC2 ChIP-seq samples. **A)** Chromatin sample used for HDAC1 and **B)** HDAC2 ChIPs respectively, submitted for Solexa sequencing. **C)** ChIP with the HDAC1 specific antibody Sat13 using formaldehyde or DSG crosslinked chromatin. **D)** ChIP with the HDAC2 specific antibody ab7029 using formaldehyde or DSG crosslinked chromatin. The results labeled “DSG purified” represent the test qPCR of the sample submitted for sequencing (IgG = nonspecific control, NT = not targeted wild type, Error bars represent SD of two technical replicas). **E, F)** Read alignment results HDAC1 and HDAC2 ChIP-seq data respectively. (U0, U1, U2, U3, UM = Uniquely mapped reads with zero to three or more mismatches; R = Reads matching to multiple sites therefore considered as repetitive; NM = reads that could not be matched to the reference genome; QC = reads that failed quality control during mapping)

The visualization of ChIP-seq data generated from DSG or formaldehyde crosslinked chromatin with the Integrated Genome Browser (IGB, [93]) showed that HDAC1 is generally enriched near genes and that the specific signals could be enhanced by dual crosslinking with DSG. For example, all target genes which were validated in section 3.1 showed a specific increase of

the HDAC1 signal at the promoter site, while background signals were not increased (Figure 16). Unfortunately, visualization of the HDAC2 (ab7029) DSG-ChIP-seq showed no enrichment (peaks) within the track, although a significant enrichment was given compared to the input sample. This could have been because the antibody specificity was too little or the sequencing quality was too low for a conclusive mapping. Interestingly, ChIP-seq tracks using the antibody ab7029 and formaldehyde crosslinking (experiments done by Gordin Zupkovitz), showed low but detectable enrichments of HDAC2. Therefore, we could not exclude the possibility that DSG crosslinking could produce ChIP artifacts with this antibody.

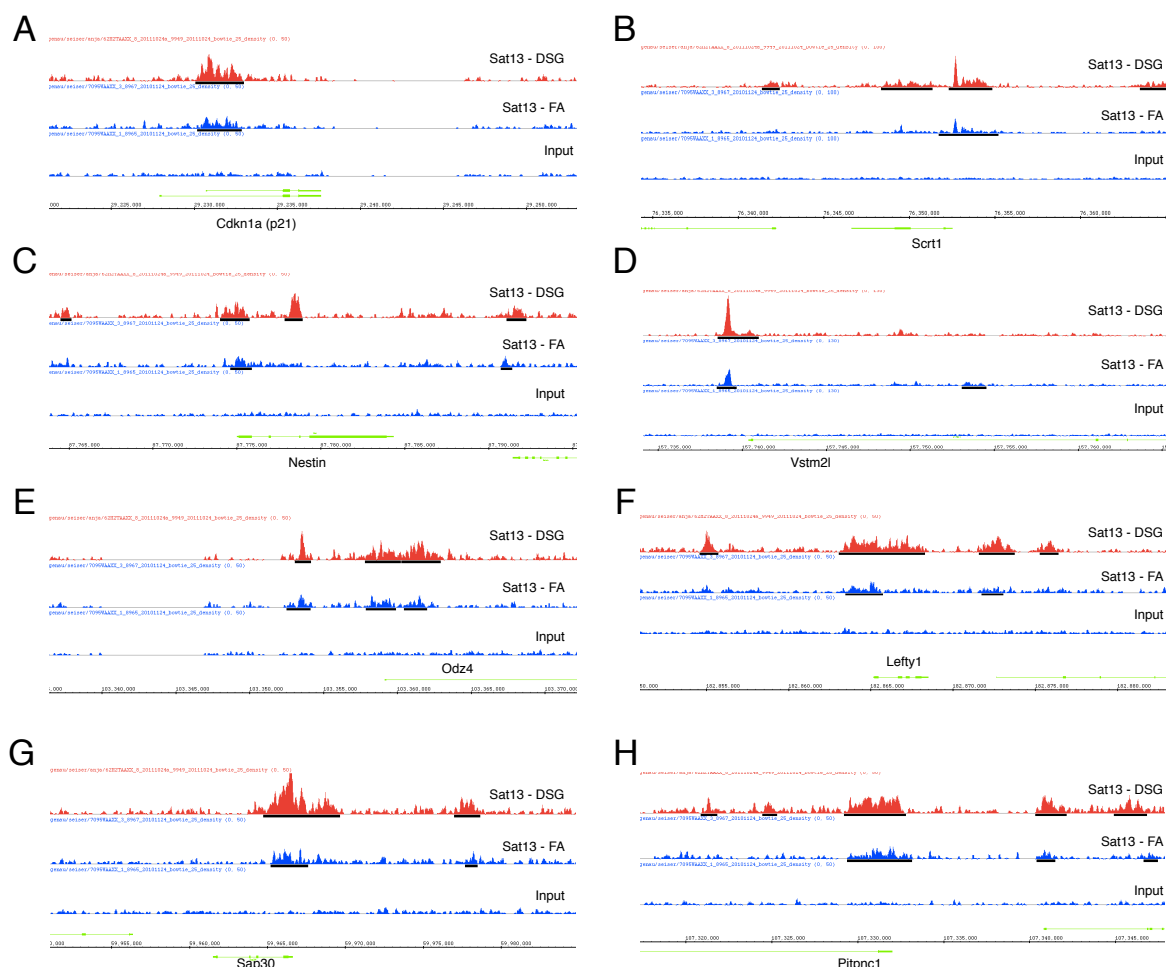


Figure 16: HDAC1 ChIP-seq data visualized with the Integrated Genome Browser (IGB) at eight representative genes. Read density plots of genes which are considered to get transcriptionally activated (**A-D**), transcriptionally downregulated (**E, F**) or do not respond in transcription (**G, H**) upon inhibition of HDAC1. Tracks represent the proportional view of read density plots of ChIP seq data. Each panel shows the density plots of ChIP seq data using the HDAC1 specific antibody Sat13 (on either DSG dual-crosslinked or Formaldehyde crosslinked chromatin) and the “input” reads generated from formaldehyde crosslinked chromatin which was not enriched with any antibody. Green lines above the chromosomal coordinates represent genes in “+” direction, read from left to right, while green lines below the coordinates show genes in “-” direction and code from right to left. Black bars below the tracks indicated the range of enrichments identified by the peak calling software MACS (detection cutoff $p=10^{-10}$ for DSG crosslinked chromatin, and $p=10^{-5}$ for formaldehyde crosslinked chromatin) [94].

Next we asked at which parts of a gene HDAC1 preferably binds and if there is a correlation between HDAC1 binding and general transcription level in wild type cells. Therefore all genes

were sorted according to their transcriptional levels in NT (non targeted) F9 cells. The visualization of read densities in a heat map of a 3 kb window around the transcriptional start site (TSS) showed that HDAC1 preferentially binds to around the near proximity of the TSS of highly active genes. In fact, there was a strong and almost linear correlation between the wild type expression levels and HDAC1 binding. This was true for both sequencing experiments (DSG and formaldehyde), although the DSG crosslinked version showed significantly higher read density plots (Figure 17A). Plotting the read density along a so called “metagene” (proportional representation of all genes within a certain category in one single chart of a gene) verified the heat map results and, additionally, showed that HDAC1 predominantly binds both to a 500 - 1000 bp window up- and downstream of the TSS but peaks directly downstream of the TSS (Figure 17B and C). The observation, that HDAC1 preferentially binds to active genes is counterintuitive considering the historical view of histone deacetylases as transcriptional repressors but is in line with more recent reports on global HDAC1 binding [95, 96].

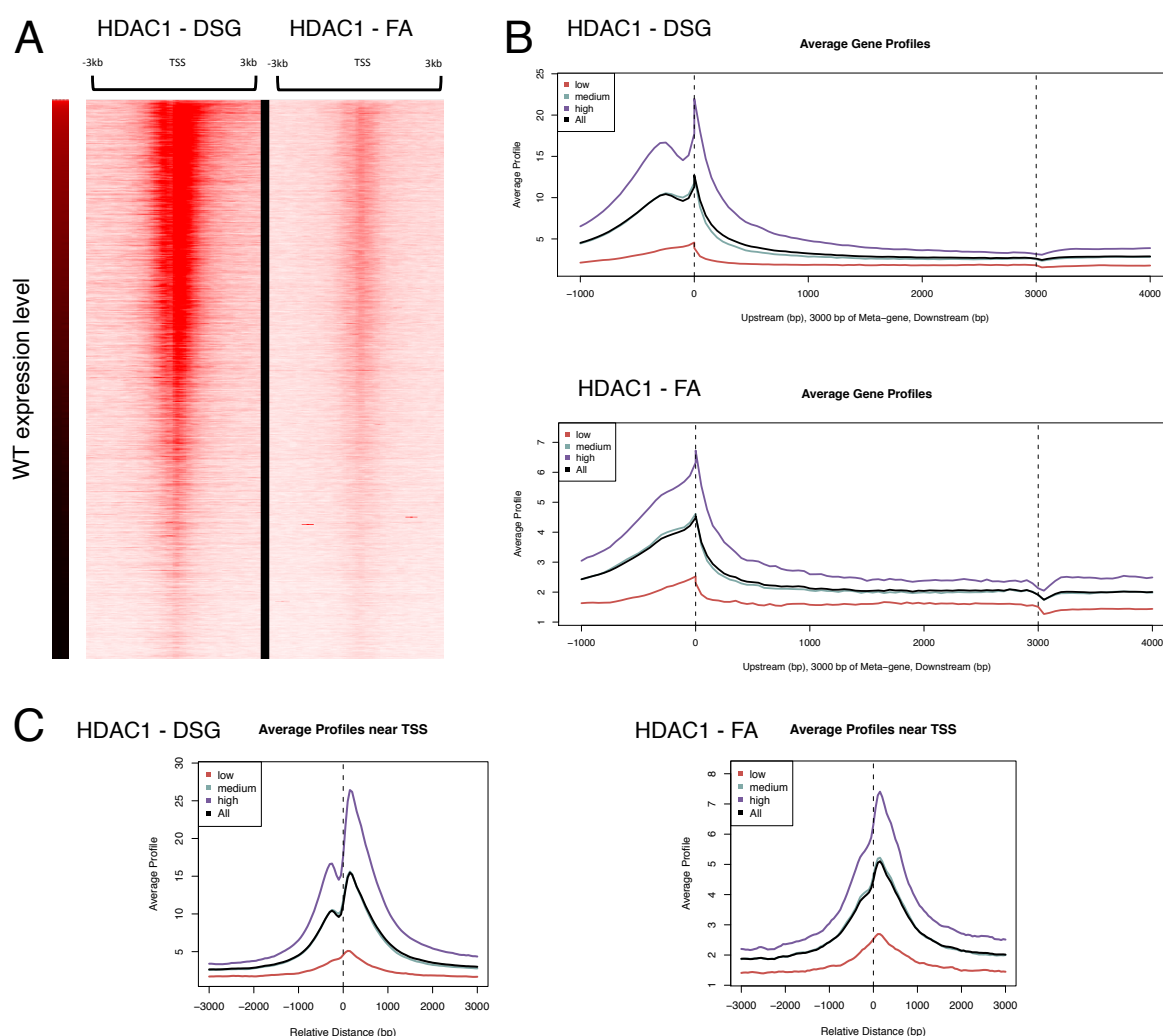


Figure 17: HDAC1 ChIP-seq profiles according to expression data. **A)** Genes were sorted according to their wild type expression levels and the read density of a six kilo base window around the transcriptional start site (TSS) was generated, using SeqMINER [97]. **B)** Read density along a metagene and **C)** near the TSS generated with the bioinformatic tool CEAS [98] (High = Top 25 % of genes with highest wild type expression; Low = Last 25 % of genes with lowest wild type expression; Medium = Genes between 25 and 75 %; All = Metagene of all genes regardless of expression levels).

The next step was to identify HDAC1 ChIP-seq enrichments by the peak calling software MACS (Model-based Analysis of ChIP-Seq) [94]. Peak calling was done in parallel for both ChIP-seq experiments, using two different stringency settings, which resulted in numerous enrichments along the genome (Formaldehyde: 12 569 and 2 453; DSG: 35 233 and 21 992 for a $p < 10^{-5}$ and $p < 10^{-10}$ detection cutoff respectively). Overlaps between the two ChIP-seq experiments showed that peaks that were called from the formaldehyde crosslinked version, formed indeed an almost perfect subset within the peaks from the DSG crosslinked ChIP-seq (Figure 18A). Saturation curves were plotted in order to determine the quality of the peak calling process. Expectedly, peaks with a high enrichment compared to input were easily detected with low sampling coverage. However, the majority of peaks called from the formaldehyde ChIP-seq sample did not show the typical saturation curve, indicating that if sequencing had been deeper, i.e. had generated more reads, that would have increased the amount of detected peaks (Figure 18B and C). On the other hand, the DSG crosslinked ChIP-seq sample showed a saturating curve of peak detection by increasing amounts of sampling (Figure 18D and E). Additionally, it can easily be seen that lowering the stringency of detection increases the rate of detection even at low coverage, though increasing the risk false positives. Therefore, peaks were considered to be solid hits if they were called by MACS both in the formaldehyde ChIP-seq data (p-value detection threshold smaller than 10^{-5}) as well as in the DSG ChIP-seq data (p-value $< 10^{-10}$).

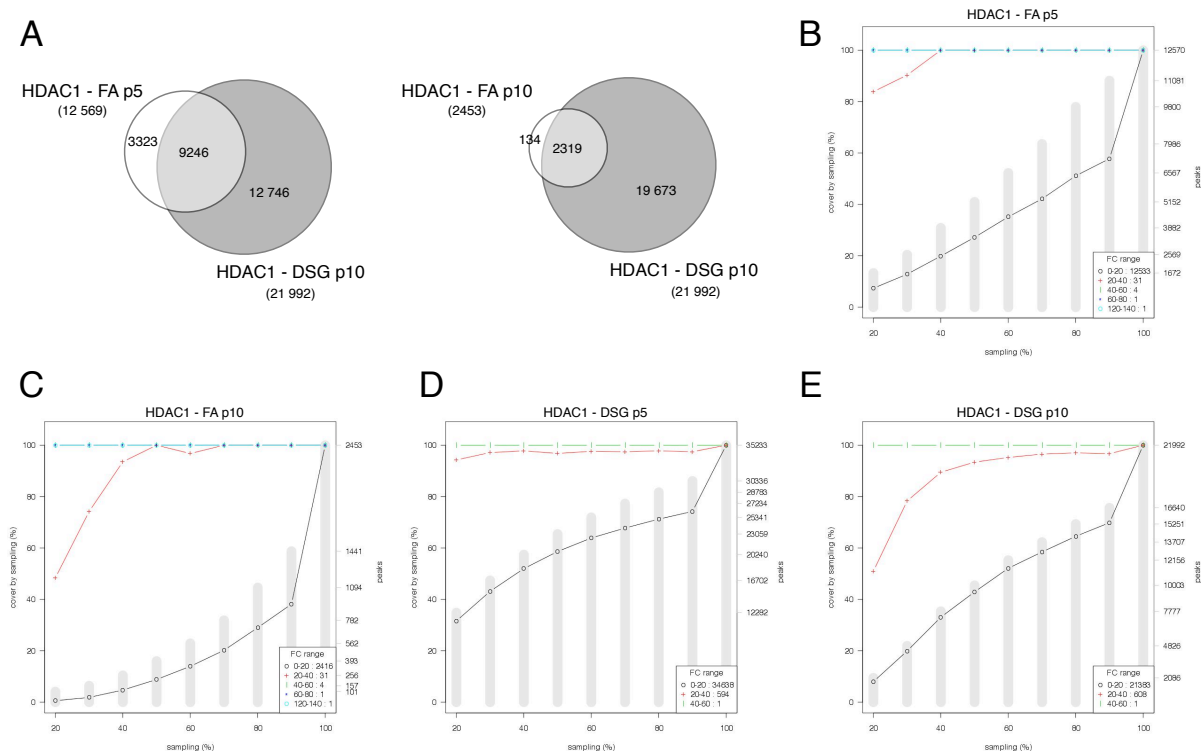


Figure 18: Peak calling by the program “Model-based Analysis of ChIP-Seq” (MACS). **A)** Overlaps of HDAC1 peaks, called by MACS using a stringent cutoff (p10) for the DSG version, and either a lower (p5) or the same stringency for the formaldehyde crosslinked ChIP-seq data. **B-D)** Saturation plots for each peak calling setting. The amount of reads, which was used for peak calling (= sampling), is plotted against the amount of detected peaks. (FC= Fold enrichment change of peaks, compared to input; p5, p10 = p value $< 10^{-5}$ and $< 10^{-10}$ respectively)

In order to investigate putative direct target genes of HDAC1 in F9 teratocarcinoma cells, transcriptional changes were measured by Agilent expression arrays, in wild type, different knockout and HDI treated cells. The expression profiles of NT (wild type) cells were compared to those of HDAC1 knockdown (HD1-3), HDAC2 knockdown (HD2-1), TSA and MS275 treated cells (Inhibitor treatments (MS275: 2 μ M for 6 h; TSA: 66.1nM for 6 h) and expression arrays were prepared by Gordin Zupkovitz). Upon these comparisons genes were defined as deregulated if they are at least 2-fold up- or downregulated while showing a p-value of 0.05 or less. This analysis showed that the most deregulated genes were observed in those cells, which were treated with HDIs like MS275 and especially many were found deregulated in TSA treated cells (Figure 19A). Only a small amount of genes showed deregulation upon knockdown of either HDAC1 or HDAC2. Additionally, the overlap between the two sets of deregulated genes was comparatively low. This might be due to the fact that other HDACs could compensate for the loss of one HDAC, or that remaining molecules, which could be still present after an incomplete knockdown, were sufficient to repress the transcriptional response. In contrast to that, major overlaps between deregulated genes upon treatment with HDIs exist. In fact, deregulated transcripts after treatment with MS275 (especially upregulated genes) showed a high overlap with genes deregulated upon TSA treatment, which supports the view of MS275 representing a more specific inhibitor of HDAC1, HDAC2 and HDAC3 compared to TSA, which inhibits the catalytic activity of a broad spectrum of HDACs (Figure 19B).

To compare HDAC1 presence and the transcriptional response to a knockdown or HDI treatment, the two datasets were linked. The majority of HDAC1 peaks that were considered solid hits (9246 peaks) were found at genes of which gene expression data existed, resulting in 6606 unique refseq entries, corresponding to 6193 genes. However this combined view of expression data and HDAC1 presence shows yet another picture. When only genes were taken in consideration, which show HDAC1 presence, only a minor fraction of genes respond transcriptionally to HDIs or knockdown of either HDAC1 or HDAC2 (Figure 19C). This would mean that HDAC1 binds to a considerably high number of genes, but its knockdown or catalytic inactivation does not influence the majority of its bound genes. It is especially surprising in the case of treatments with HDAC inhibitors, because incomplete shRNA silencing or compensation mechanisms can easily explain the unresponsiveness of the majority of HDAC1 bound genes in knockdown cells, this is not true, however, for treatments with HDIs, because they bind into the catalytic groove, thereby completely blocking the enzymatic ability to deacetylate lysine residues. This blockage is thought to lead to hyperacetylation of histones, or nearby bound transcription factors which should trigger a transcriptional change. On the other hand, when looking at the situation from the other way, considering the percentage of genes that are deregulated and have HDAC1 bound, up to 50 % of deregulated genes could be direct transcriptional targets of HDAC1 (Figure 19D). Curiously, the effect of possible directly regulated genes was found to be especially high in the category of downregulated genes upon HDI treatment.

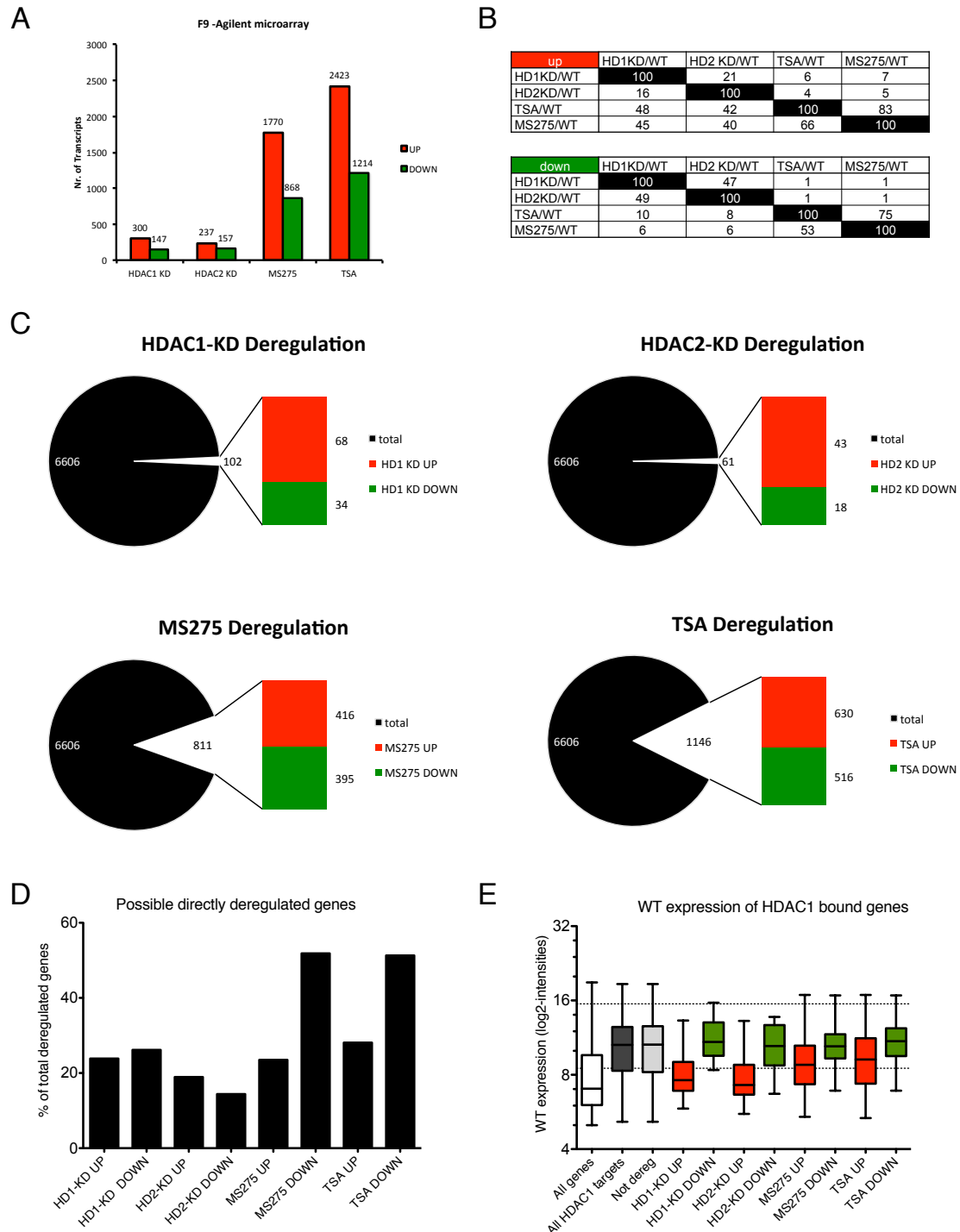


Figure 19: Combined results from expression arrays and HDAC1 ChIP-seq data. **A)** Agilent microarray results, summarized as number of genes (unique refseq entries) which are significantly deregulated (fold change ≥ 2 ; p-value < 0.05). Column bars indicate number of deregulated genes of wild type vs knock-down or HDI treatments. **B)** Percentual overlaps of deregulated genes. **C)** Number of unique refseq entries which are occupied by HDAC1 and deregulated upon HDAC1 knockdown, HDAC2 knockdown, treatment with MS275 or treatment with TSA. **D)** Possible directly regulated target genes are shown as the percentage of deregulated genes bound by HDAC1 to total deregulated genes. **E)** Averaged wild type (WT) expression levels are shown as box-whiskers-plots for all genes, HDAC1 bound genes and the different categories of HDAC1 bound genes according to their response to HDAC1 knockdown or inhibitor treatment. Area between dotted lines represent moderate to high expression. (Whiskers indicate minimum and maximum) (HD1-KD = HDAC1 knockdown, HD2-KD = HDAC2 knockdown)

Next we asked if there is a correlation between the wild type expression level and the change in expression upon knockdown or treatment. As the heat maps in Figure 17A already suggested, HDAC1 bound genes showed increased expression levels compared to the median expression of all genes (Figure 19E). However, there was a strong tendency for genes, which got upregulated by knockdown or HDI treatments, to be expressed to a lower extent in WT cells than non-responsive genes. Conversely, downregulated genes showed a significantly higher wild type expression level. In theory these effects could simply represent technical artifacts of the microarray analysis, whose detection of upregulated genes may be biased for lowly expressed genes, this is, nevertheless, not very likely as the WT expression levels of these genes are located within the detection range of the microarray.

One technical consideration would be that HDAC inhibitor treatments were done for 6 h; a time frame that could allow for secondary effects that compensate for transcriptional deregulations. These effects could include regulation of mRNA stability and processing or the recruitment of HATs and HDACs. For example, looking at genes that are deregulated upon MS275 or TSA treatment showed that among the most prominent downregulated genes were histone acetyltransferases such as *Kat2a* (Gcn5) or *Kat2b* (Pcaf), which were found downregulated in both treatments or *Myst3* and *Myst4*, which were downregulated in TSA and MS275 treated cells respectively. Interestingly, the genes of *Kat2a* and *Kat2b* were also found to be bound by HDAC1 in WT cells, thereby suggesting a direct transcriptional regulation by HDAC1, although the downregulation of these HATs could also be part of an indirect negative feedback loop addressing global acetylation levels.

3.6 HDAC1 may dissociate from the promoter of the *Cdkn1a* (p21) gene during its activation

To investigate the role of HDAC1 as a negative regulator of transcription, a biological system was used where HDAC1 was reported to have clear repressive functions. The genetic regulation of the cyclin dependent kinase inhibitor p21/WAF1/CIP1 gene has been extensively characterized in man and mouse (Reviewed in [99]) and one study, carried out in our lab described HDAC1 and the transcription factor p53 as antagonistic regulators of the p21 gene [100]. In this study the authors have shown that genotoxic stress leads to the activation of the tumor suppressor p53 which subsequently causes the activation of p21, which itself regulates cell cycle progression. They report that p53 directly binds to Sp1 which leads to the activation of p21, while HDAC1 dislocates from the promoter causing a hyperacetylation of histones. This system was now used to test if the dissociation of HDAC1 could also be confirmed by ChIP-qPCR in human and mouse cell lines. The polypeptide antibiotic Actinomycin D is one of the oldest drugs used in chemotherapy. Actinomycin D inhibits RNA synthesis by intercalating into the DNA by binding to guanine residues and inhibiting DNA-dependent RNA polymerases, especially RNA polymerase I because rRNA genes, which RNA Pol I transcribes, are GC-rich [101]. Treatment with high concentrations leads to double strand breaks, which can trigger the activation of p53. At nanomolar concentrations, Actinomycin D can block transcription of RNA polymerase I which leads to perturbations in ribosome biogenesis and the inhibition of Mdm2, which causes the stabilization of p53 [102, 103]. Therefore cells were treated with nanomolar

concentrations (30 ng/ml) of Actinomycin D (*Sigma*) for 6 h or overnight (ON). ON treatment with Actinomycin D caused an increase of p53 levels and lead to the induction of p21 in F9 teratoma cells (Figure 20 A and B). Similarly, p53 got recruited to both of the p53 binding sites upstream to the *p21* gene but not at its promoter. The results for HDAC1 were not consistent between DSG and FA treated samples, as in FA crosslinked samples HDAC1 seemed to get recruited to the promoter upon treatment while in the DSG crosslinked chromatin HDAC1 levels stayed at comparable levels (Figure 20C and D). Based on these results in F9 cells, it could not be deduced if the mechanism reported in [100] holds true in murine F9 cells.

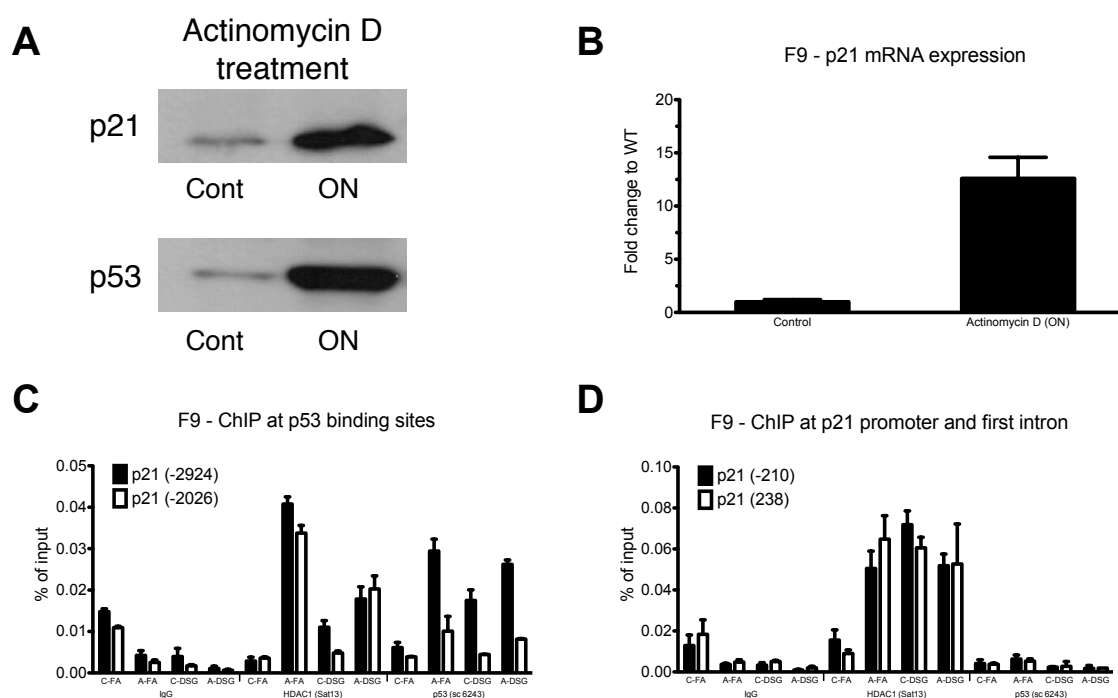


Figure 20: Overnight Actinomycin D treatment in F9 mouse teratoma cells. **A)** Protein levels of p21 and p53 are upregulated upon overnight (ON) treatment with Actinomycin D compared to DMSO- mock control treatments (Cont) **B)** p21 mRNA transcript levels are elevated after the overnight treatment. **C)** ChIP experiments with primers at the two p53 binding sites or **D)** at regions around the TSS at the murine p21 gene. (C = mock control, A = ON treatment with Actinomycin D. Number in brackets indicate position from transcriptional start site TSS, Error bars represent SD of two technical replicas)

To test if the dissociation of HDAC1 could be confirmed by ChIP-qPCR in human cell lines, U2OS cell were cultured and treated with Actinomycin D for either 6 h or overnight. Both treatments lead to the induction of p53 and p21 (Figure 21A). As the ChIP experiments in [100] were done with sepharose beads and with the antibody 10E2 for HDAC1 pulldown, the first experiment in U2OS cells was done in duplicates, once with sepharose beads and once with Dynabeads®. Each set included two antibodies for HDAC1 (Sat13 and 10E2) and the human p53 specific antibody DO7. Upon overnight treatment, p53 got recruited to the p53 binding site in all four settings (using either sepharose beads or Dynabeads® with FA crosslinked or DSG crosslinked chromatin), although sepharose beads showed a significantly lower increase (Figure 21B). Additionally, sepharose beads gave high signals for p53 at the proximal promoter which were inconsistent with the results using magnetic beads (Figure 21 C). The results from

the HDAC1 ChIP using magnetic beads indicated that HDAC1 disassociated from the proximal promoter upon the activation of p21, an effect which was consistent in FA and DSG crosslinked chromatin.

In the second experiment U2OS cells were treated for 6h and overnight. p53 got recruited to the p53 binding site in a time dependent manner, which could be detected in FA and DSG crosslinked chromatin (Figure 21D and E). Unfortunately the ChIP for HDAC1 did not work in this second experiment (Figure 21F), therefore the dislocation of HDAC1 from the promoter of p21 during its activation could not be verified.

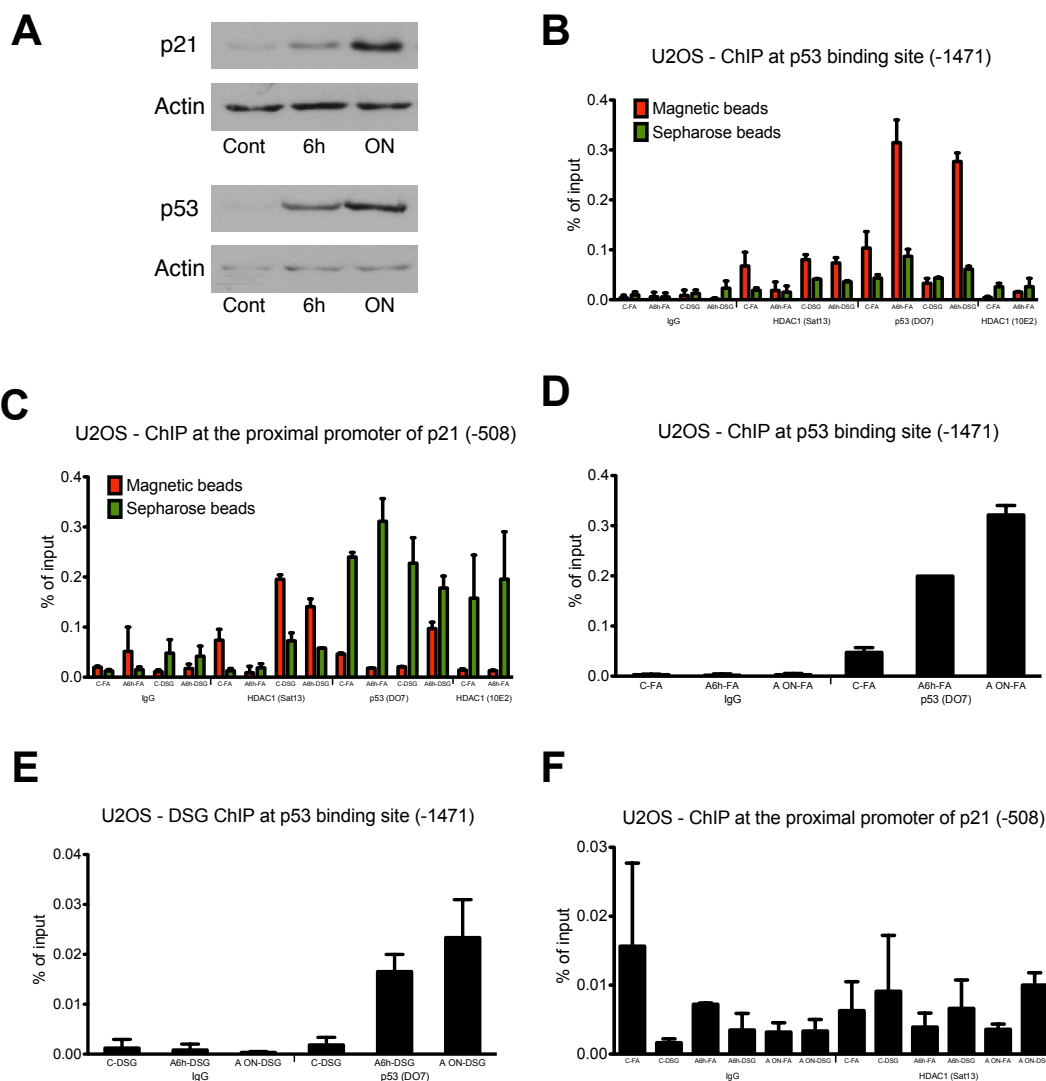


Figure 21: Actinomycin D treatment in U2OS human osteosarcoma cells. **A)** Protein levels of p21 and p53 are upregulated upon 6 h or overnight (ON) treatment with Actinomycin D compared to DMSO- mock control treatments (Cont). **B)** ChIP experiments after 6 h treatment with actinomycin D with primers at the p53 binding site or **C)** at regions around the TSS at the murine p21 gene. ChIP experiments were done with either Dynabeads® (magnetic beads) or sepharose beads. **D, E)** ChIP experiments after 6h and overnight treatment with primers at the p53 binding site or **F)** at regions around the TSS at the human p21 gene. (Number in brackets indicate position from transcriptional start site TSS, Error bars represent SD of two technical replicas)

3.7 Molecular characterization of conditional HDAC1 and HDAC2 knockout models in murine epidermis

Several projects in our lab focus on the characterization of tissue specific roles of HDAC1 and HDAC2, one of them was the description of mice which are conditionally deleted for either HDAC1 or HDAC2 in the epidermis. To achieve that, mice, floxed for the two HDACs (Figure 28A and B), were mated with a deleter strain, containing the Cre recombinase under the promoter-control of the basal epidermal cell specific marker Keratin 5 (K5) [104]. The simultaneous conditional knockout of HDAC1 and HDAC2 caused embryonic lethality due to severe but pleiotropic developmental defects, although the epidermis was fully stratified. This is partly in line with a study, in which the authors used the K14-Cre transgene to delete HDAC1 and HDAC2, causing the death of the mice around embryonic day 18.5. However, the deletion via the K14-Cre transgene caused epidermal malformations and lead to an overall less severe phenotype compared to the ablation via K5-Cre [74].

Since neither HDAC1 knockout mice (*Hdac1* Δ/Δ ep) nor HDAC2 knockout mice (*Hdac2* Δ/Δ ep) showed any obvious phenotype, one additional allele of the corresponding HDAC was deleted. This lead to mice which retain only one single HDAC1 allele (*Hdac1* $\Delta/+ep$ *Hdac2* Δ/Δ ep) or only one single HDAC2 allele (*Hdac1* Δ/Δ ep *Hdac2* $\Delta/+ep$). *Hdac1* single allele mice were viable and fertile and exhibited no obvious phenotype. *Hdac2* single allele mice, on the other hand, showed severely impaired epidermal and hair development (Figure 22A). Additionally, birth rates of *Hdac2* single allele mice were reduced.

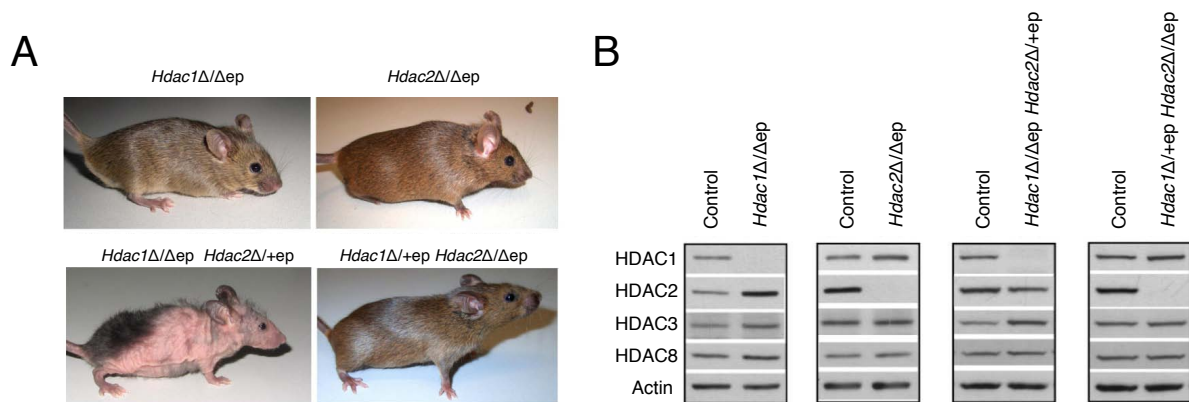


Figure 22: Phenotypic description of conditional knockout mice **A)** Comparison of adult HDAC1 knockout (*Hdac1* Δ/Δ ep), HDAC2 knockout (*Hdac2* Δ/Δ ep), *Hdac2* single allele (*Hdac1* Δ/Δ ep *Hdac2* $\Delta/+ep$) and *Hdac1* single allele (*Hdac1* $\Delta/+ep$ *Hdac2* Δ/Δ ep) mice. **B)** Western blot analysis of tail epidermis from *Hdac1* Δ/Δ ep, *Hdac2* Δ/Δ ep, *Hdac1* Δ/Δ ep *Hdac2* $\Delta/+ep$, *Hdac1* $\Delta/+ep$ *Hdac2* Δ/Δ ep and corresponding control (Cre-) littermate mice with antibodies against HDAC1, HDAC2, HDAC3 and HDAC8. β -actin served as loading control. (Figure adapted from figure 17A and 18A, Dissertation Mircea Winter, p. 58 and 59 [105])

Hdac1 Δ/Δ ep mice showed a 2.5 fold upregulation of HDAC2 and in *Hdac2* Δ/Δ ep mice the HDAC1 protein was found 2 fold upregulated, suggesting a mechanism of compensation. By deleting an additional *Hdac2* allele in *Hdac1* Δ/Δ epidermis or an additional *Hdac1* allele in *Hdac2* Δ/Δ epidermis, the compensatory mechanism was affected causing reduced HDAC1 (110 % of wild type) and HDAC2 (80 % of wild type) levels (Quantification by Mircea Winter [105] p. 59; Figure 22B). Interestingly, the compensatory mechanism was not at the level of

transcription, as *Hdac1* mRNA levels were unchanged once *Hdac2* was conditionally knocked out, and vice versa (Dissertation, Mircea Winter p. 60 [105]). Although the *Hdac1* gene has been shown to feature an autoregulatory feedback loop [106], these data indicate a posttranscriptional regulatory mechanism.

The phenotype of *Hdac2* single allele mice contains hyperkeratosis, hyperproliferation and increased differentiation of the epidermis. In *Hdac2* single allele mice several genes were deregulated both in P5 and P50 mice, including proliferation specific ones, like *Epgn* and *Ada*, or genes like *Sprr2h*, *Lce3b* and *S100a8* which correspond to the Epidermal Differentiation Complex (EDC), a cluster of genes which are often coordinately expressed and regulated [72]. The epithelial mitogen (*Epgn*) is a homolog to the superfamily of epidermal growth factors (EGFs), which stimulates the phosphorylation of the receptor c-erbB-1, triggering the MAP kinase pathway in epithelial cells [107]. The adenosine deaminase (*Ada*) catalyzes the irreversible hydrolytic deamination of adenosine and deoxyadenosine to inosine and deoxyinosine respectively and plays an important role in the degradation of adenine nucleotide. Inhibition or deletion for *Ada* leads to the accumulation of dATP which inhibits ribonucleotide reductase and prevents DNA synthesis and cell division, therefore the deficiency of *Ada1* especially impairs rapidly dividing cells [108]. *Sprr* genes encode a class of polypeptides (Small Proline Rich proteins) that are strongly induced during differentiation of epidermal keratinocytes [109]. The upregulation of these genes in *Hdac2* single allele mice might partly explain the hyperproliferative and hyperkeratotic phenotype. Since mice can tolerate the loss of three of the four *Hdac1* and *Hdac2* alleles only if one allele of *Hdac1* is present but not if one allele of *Hdac2* remains, this indicates that HDAC1 might have a qualitative distinct role during epidermal development. Therefore we tried to see if genes, deregulated in *Hdac2* single allele mice, are directly occupied by HDAC1 and HDAC2 in the wild type and how binding patterns of these transcriptional regulators change, if they get completely knocked out, or if only one allele is left. For this purpose several steps of the ChIP protocol had to be adapted, especially the chromatin extraction efficiency had to be tested. The most efficient technique was to separate the epidermis from the dermis by dispase treatment and mincing the epidermis into small pieces, followed by crosslinking with either DSG and formaldehyde or only formaldehyde. In the first ChIPs, we wanted to test if we could see the specific enrichment of components of the class I HDAC containing complexes in wild type and *Hdac2* single epidermis. However no enrichment over unspecific (IgG) controls could be seen by simple formaldehyde treatment (Figure 23A). Therefore DSG crosslinking was tested in wild type epidermal tissue, which not only gave enrichments for HDAC1, HDAC2 and Sin3a over unspecific controls but also over a 3' end control. However the enrichment over the 3' end, which was our indicator for a successful ChIP experiment, was very low and not significant for the Sin3a antibody K-20X. The same was true for the HDAC2 specific antibody ab7029 (Figure 23B, C and D). Another problem with the antibody ab7029 was, that observations of the binding pattern between the different mouse genotypes was inconsistent, for example in one experiment there was an increase in HDAC2 binding in HDAC2 single mice compared to wild type (Figure 23D) while in the other a decreased binding was observed (Figure 23F). Additionally, this antibody gave unspecific background signals in HDAC1 single allele mice, or, in some cases did not yield any pull down, although the antibody specificity

was clearly given in Western blots (Figure 23G, H and I). On the other hand, the HDAC1 specific antibody Sat13 always showed high specificity, concerning signal to background ratios and Sat13 pulldown was completely abolished in *Hdac2* single allele mice. These features make observations reliable and reproducible. For example, HDAC1 recruitment to the control gene (*p21*) is significantly increased in HDAC2 knockout epidermis, furthermore, HDAC1 recruitment seems to be slightly (but not significantly) increased in HDAC1 single allele mice (Figure 23G and H).

Figure 23: Initial trial ChIP experiments in epidermal tissue. **A)** FA crosslinking in *Hdac1Δ/Δep Hdac2Δ/+ep* (HD2s) and corresponding control littermate mice (WT). **B)** DSG test ChIP for components of class I HDAC containing complexes in wild type (WT) epidermal tissue. **C, D)** HDAC2 ChIPs in WT and HD2 single allele mice, at the genes *p21* and *Epgn* respectively. **E, F)** HDAC1 and HDAC2 ChIPs in control (WT) and *Hdac2* single allele (HD2) mice, at the genes *p21* and *Sprr2h*. **G)** HDAC1 and HDAC2 ChIPs in control (WT) and *Hdac1Δ/+ep Hdac2Δ/Δep* (HD1s) mice. **H)** HDAC1 ChIP and test of two different antibody batches of HDAC2 (ab7029) in *Hdac2Δ/Δep* (HD2KO), *Hdac1Δ/+ep Hdac2Δ/Δep* (HD1S) and corresponding control (WT and WT-HD1S) epidermal chromatin. Western blot of the same chromatin, tested for HDAC2 recognition by the antibody ab7029 is shown in **I)**. (Error bars represent SD of two technical replicas; Adult littermate mice were used for individual experiments)

obtained by the standard ChIP strategy in F9 cells, and no increase of the pulldown efficiency was obtained by the use of more antibody. However the antibody failed to get a specific enrichment in epidermal chromatin and again showed an unspecific signal in HDAC2 conditional knockout samples, which ultimately proved the antibody unsuitable for ChIP experiments in tissue derived chromatin (Figure 24A). Therefore three additional HDAC2 antibodies were tested in F9 cells in various concentrations. The antibody ab12191 showed a high pulldown and a specific enrichment at the promoter compared to the 3' end, if it was used in low concentrations (1 μ l = 2.4 μ g). In addition the antibody A300-705A also gave a specific enrichment when using 4 μ l (= 0.8 μ g) and both antibodies performed significantly better if they were used in combination with DSG treated chromatin (Figure 24B and C). The monoclonal antibody 3F3 did work in ChIP experiments in the past but failed to yield any pulldown efficiency in recent experiments and several reasons could contribute to this inconsistency; for example storage conditions and the variation in antibody concentration between different batches. The monoclonal antibody 3F3 was stored in cell culture medium, which was taken directly from the supernatant of antibody producing hybridoma cells, hence concentrations varied in every batch. For this reason new hybridomas were cultured by Stefan Schüchner, fresh supernatant was retrieved, of which one part was supplemented with NaN₃ and stored at 4 °C, while the other part was purified and concentrated using a column containing sepharose G-beads (see Section 2.5.3). This concentrated version showed no increase in detection signal in Western blots, compared to the crude hybridoma medium, however in ChIP experiments non of the tested amounts of both 3F3 batches stored in medium (existing "old" and freshly retrieved "new" batch) yielded any pulldown, while the concentrated version of the same antibody showed specific enrichments (Figure 24D). Another advantage of the purified sample was that the concentration of the antibody could be measured by nano drop (280 nm), which detects the total protein amount, which should equal approximately the concentration of the antibody, as no carrier protein, like BSA, was added. The first elution fraction, which was used for the assay, had a concentration of 0.7 μ g/ μ l. This enables the reproduction of experiments with the exact same amounts of antibody.

Finally the ChIP settings (antibody concentrations, formaldehyde or DSG crosslinking, and amount of chromatin) which produced high enrichments were used in epidermal chromatin of control, *Hdac1* Δ/Δ ep, *Hdac2* Δ/Δ ep or *Hdac2* single allele mice. Although the purified 3F3 antibody worked in F9 cells, it did not yield any pulldown in the epidermis. On the other hand, all other antibodies gave consistent results, as they showed promoter enrichment over 3' end or a negative control region (*Vstm2l* 24129) and did not detect any background signals in the corresponding knockout samples, especially ab12191 consistently showed high enrichments (Figure 24E and F). Upon these reliable performances, observations of varying HDAC levels could be trusted, if these changes could be seen repeatedly. For example, in *Hdac1* Δ/Δ ep *Hdac2* $\Delta/+$ ep mice, we could detect a slight decrease of HDAC2 recruitment, which was consistent between the two different antibodies used. This pattern was also observed at genes which are associated with epidermal proliferation or differentiation. For example, HDAC1 and HDAC2 are both bound to the promoter region of the epithelial mitogen (*Epgn*) in wild type epidermis. Upon knockout of either of the two deacetylases the corresponding HDAC gets in-

creasingly recruited. In *Hdac2* single allele mice, however, HDAC2 recruitment is decreased, which is also true for the differentiation specific gene *Spr2h* (Figure 25).

Based on these binding dynamics, and the observation that HDAC1 binding does not seem to decrease in HDAC1 single allele epidermis (Figure 23G and H), one could argue that HDAC1, although less of total cellular protein is available, can still bind efficiently enough to ensure suitable gene expression. HDAC2 on the other hand cannot get targeted properly once only one of its alleles is left, which results in a deregulation of the gene. In conclusion, the molecular binding patterns of HDAC1 and HDAC2 nicely reflected observations of the phenotypes and gene expression, and underpin the specific role HDAC1 in the epidermis.

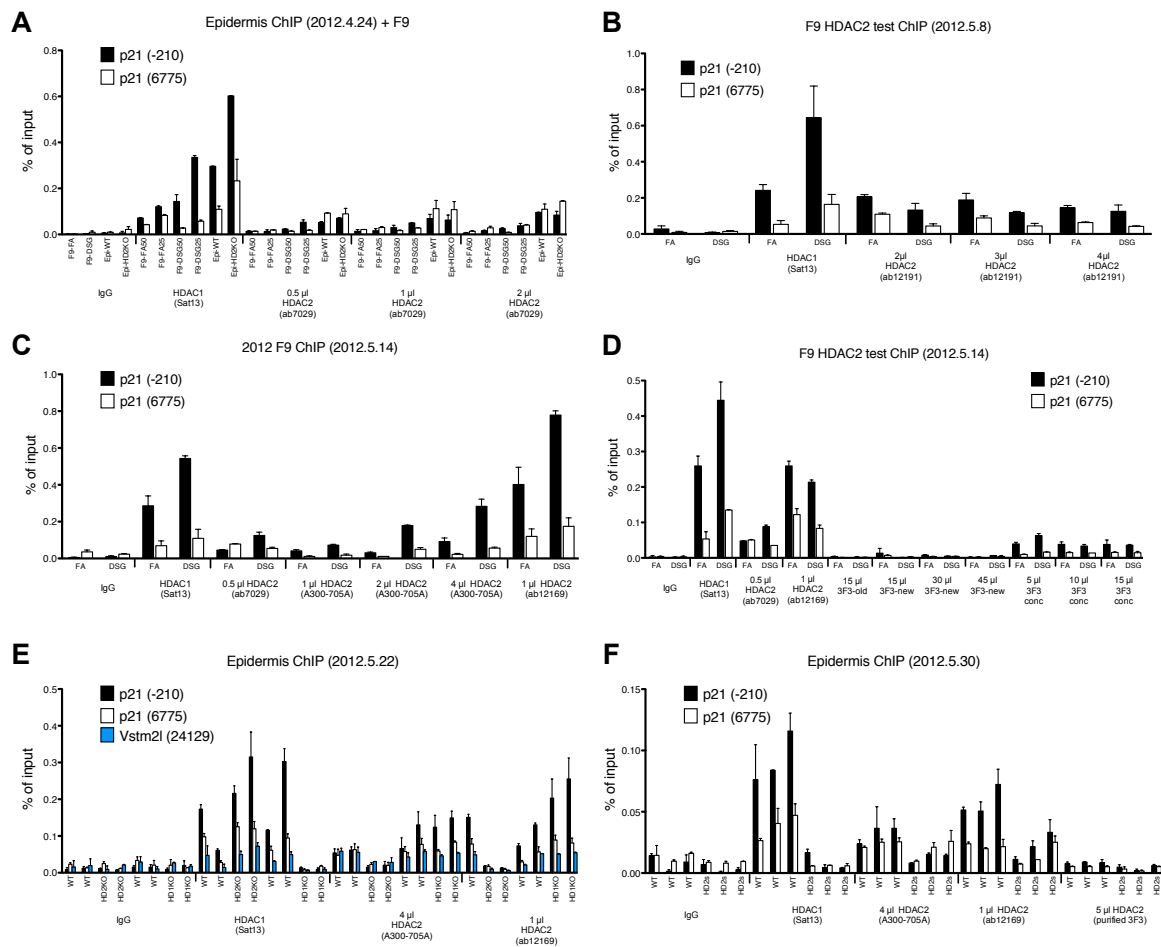


Figure 24: Adjustment of ChIP parameters **A)** Comparison and test of different amounts of chromatin and different HDAC2 (ab7029) antibody concentrations. (F9 = chromatin from F9 teratoma cells; FA25 and FA50 = 25 and 50 μ g respectively of formaldehyde crosslinked chromatin; DSG25 and DSG50 = 25 and 50 μ g respectively of DSG crosslinked chromatin; Epi = 25 μ g of DSG crosslinked chromatin from epidermal tissue. WT = control; HD2KO = *Hdac2* Δ/Δ ep) **B, C, D)** Test of HDAC2 antibodies (ab7029, ab12191, A300-705A, and 3F3) with 25 μ g of differently crosslinked chromatin, in various concentrations or concentrated versions (3F3 conc) in F9 cells. **E)** HDAC1 and HDAC2 ChIPs, with working ChIP settings (DSG crosslinking, 25 μ g chromatin and the amount of antibody indicated below the figure), of epidermal chromatin from *Hdac1* Δ/Δ ep (HD1KO), *Hdac2* Δ/Δ ep (HD2KO) and corresponding control (WT) mice. **F)** HDAC1 and HDAC2 ChIPs, with working ChIP settings (DSG crosslinking, 25 μ g chromatin and the amount of antibody indicated below the figure), of epidermal chromatin from *Hdac1* Δ/Δ ep *Hdac2* $\Delta/+$ ep (HD2s) and corresponding control (WT) mice. (Error bars represent SD of two technical replicas; Adult littermate mice were used for individual experiments)

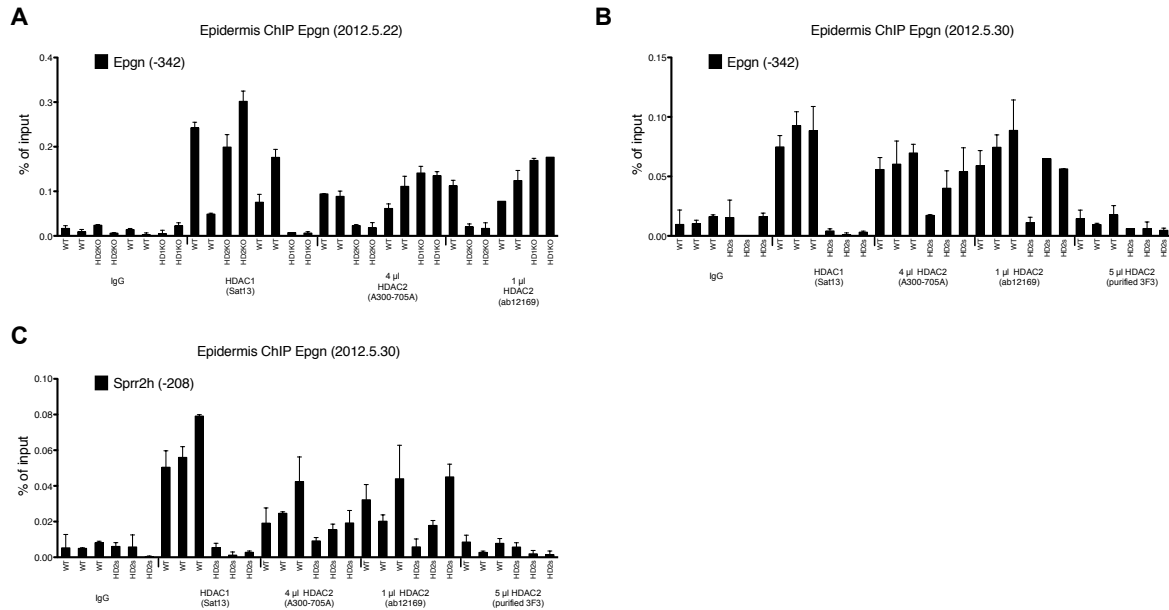


Figure 25: HDAC1 and HDAC2 occupation and binding dynamics at epidermal proliferation and differentiation genes in conditional knockout mice **A**) HDAC1 and HDAC2 ChIPs with primers for the proliferation specific gene *Epgn*, from *Hdac1* Δ/Δ ep (HD1KO), *Hdac2* Δ/Δ ep (HD2KO) epidermal chromatin and from corresponding control (WT) epidermal chromatins. **B**) HDAC1 and HDAC2 ChIPs, with working antibody concentrations, of epidermal chromatin from *Hdac1* Δ/Δ ep *Hdac2* $\Delta/+$ ep (HD2s) and corresponding control (WT) mice. Primers are specific for *Epgn* or **C**) the cornification associated gene *Spr2h*. (Error bars represent SD of two technical replicas; Adult littermate mice were used for individual experiments)

3.8 Molecular characterization of conditional HDAC1 and HDAC2 knockout models in the murine nervous system

The role of histone deacetylases in the nervous system (NS) and particularly in the CNS and brain is especially interesting because small molecule HDAC inhibitors are frequently used for the treatment of a variety of neurologic and psychiatric disorders including Huntington's disease, Parkinson's disease, anxiety and mood disorders, Rubinstein-Taybi syndrome and Rett syndrome (summarized in [81, 110]). Additionally, the two paralogs HDAC1 and HDAC2 seem to play specific roles in development and homeostasis of the brain, since, unlike their general ubiquitous expression, HDAC1 is predominantly found in astrocytes, while HDAC2 is primarily found in postmitotic neurons within the adult brain ([80] and Figure 26A and B). Interestingly, this mutual exclusiveness of HDAC1 and HDAC2 expression in neurons and astrocytes establishes from P0 onwards, while both proteins are expressed in both cell types during embryonic development. Our lab focuses on the role of HDAC1 and HDAC2 in murine NS and brain development, by creating conditional knockout mouse models, which specifically lack HDAC1 or HDAC2 in the NS. Therefore mice, floxed for one of the two HDACs (Figure 28A and B), were mated with a deleter strain, containing the Cre recombinase under the control of the rat promoter of the *Nestin* gene [111], an intermediate filament protein which is expressed in neuronal stem cells and during the early stages of development in the NS. Offspring mice which were deficient for HDAC1 in the NS were viable, fertile and showed no obvious phenotype apart from a general reduction in body mass. In addition to its general upregulation, HDAC2 was also re-

expressed in astrocytes (for example in the corpus callosum, which is rich in astrocytes) thereby efficiently compensating for the loss of HDAC1. In a vice versa manner, the same was true for HDAC2 conditional knockout mice; they were viable, fertile and showed no obvious phenotype apart from a weight reduction. Again the corresponding paralog, HDAC1, was upregulated and expressed in postmitotic neurons (for example in the CA1 region of the hippocampus, a region densely packed with neurons), which are HDAC2 exclusive in the wild type situation (Figure 26A and B). While mice could generally compensate for the loss of one of the two HDACs in the NS, the simultaneous conditional knockout of HDAC1 and HDAC2 caused embryonic lethality. The phenotype of HDAC1 and HDAC2 conditional double knockouts included decreased proliferation, elevated DNA damage, increased apoptosis (starting from E15.5), cerebral hemorrhage, increased H3K56 acetylation and a disturbed cortical layering (Figure 26C and data not shown).

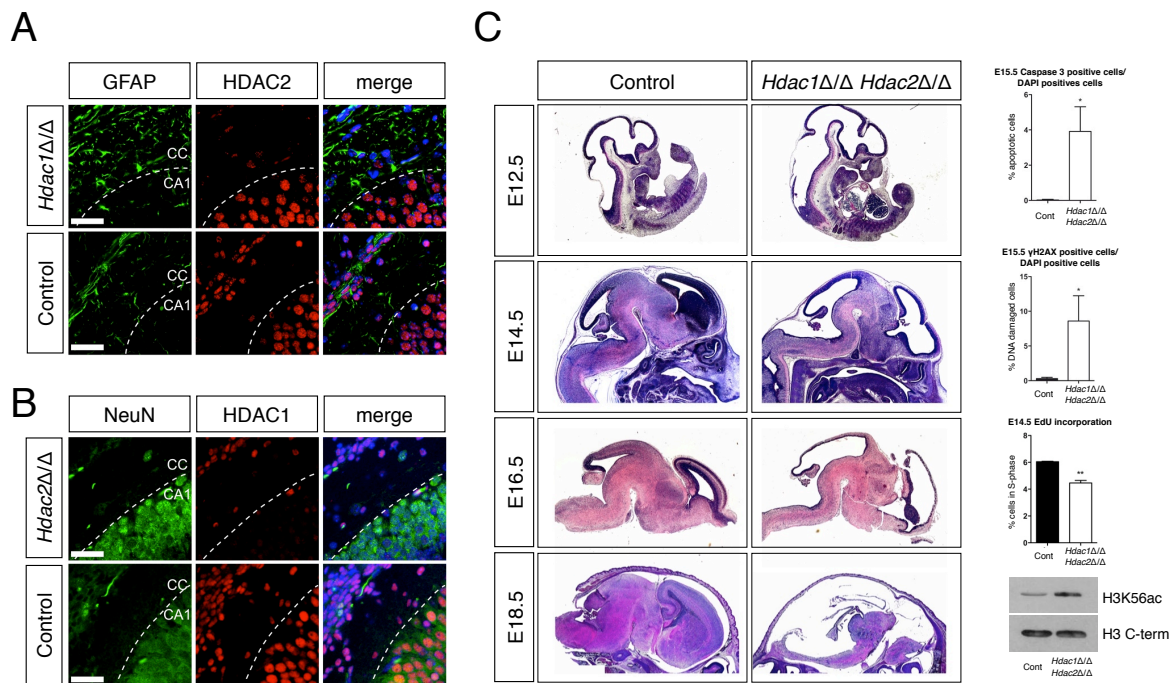


Figure 26: Phenotypic characterization of *Hdac1 Δ/Δ* , *Hdac2 Δ/Δ* and *Hdac1 Δ/Δ Hdac2 Δ/Δ* double conditional knockout brains **A)** Immunofluorescence staining of the CA1 region within the hippocampus, and corpus callosum (CC) of P4 mice with HDAC1 deleted NS or **B)** HDAC2 deleted NS and their corresponding control littermates **C)** Characterization of double knockout (*Hdac1 Δ/Δ Hdac2 Δ/Δ*) and the corresponding control littermates by hematoxylin and eosin staining. Increased apoptosis was measured by quantification of cleaved caspase3 positive cells; DNA damage was quantified by γ H2AX positive cells; Reduced proliferation was measured by EdU incorporation; * = p value < 0.05; ** = p value < 0.01 (Figure: Astrid Hagelkruys)

To test if there is a qualitative difference between the two HDACs, transgenic mice were produced which retain only one single *Hdac1* allele (*Hdac1 $\Delta/+n$ Hdac2 $\Delta/\Delta n$*) or only one single *Hdac2* allele (*Hdac1 $\Delta/\Delta n$ Hdac2 $\Delta/+n$*). Interestingly one single *Hdac2* allele was sufficient to rescue the severe phenotype and embryonic lethality of conditional double knockout mice (*Hdac1 $\Delta/\Delta n$ Hdac2 $\Delta/\Delta n$*). On the other hand, retaining one single *Hdac1* allele only delayed the death until day P0. Several pathologic features including DNA damage, apoptosis, cerebral

hemorrhage and the dramatic drop in total HDAC activity of conditional double knockout mice (*Hdac1* Δ/Δ *Hdac2* Δ/Δ n), were absent in *Hdac1* single allele mice (*Hdac1* $\Delta/+n$ *Hdac2* Δ/Δ n). However some features like the increased H3K56 acetylation, decreased proliferation and a decreased size of the cerebellum and the medulla oblongata were still observed. The fact that one single allele of *Hdac2* can completely rescue the severe phenotype of the double knockout, while one single allele of *Hdac1* cannot, highlights the specific importance of HDAC2 in the developing brain.

Agilent expression arrays showed that only a small proportion, 98 genes, was deregulated in *Hdac1* $\Delta/+n$ *Hdac2* Δ/Δ n mice at the postnatal day P0, and only six of them overlapped with the 140 genes found deregulated in *Hdac1* $\Delta/+n$ *Hdac2* Δ/Δ n mice at E14.5, which made it difficult to choose target genes for ChIP experiments. One gene which was upregulated in P0 *Hdac1* $\Delta/+n$ *Hdac2* Δ/Δ n mice was endothelin 1 (*Edn1*), which is a vasoconstricting peptide produced primarily in the endothelium but can also act as a neuropeptide with neurovascular functions [112]. The upregulation of this gene might cause a reduced blood supply to the brain, and therefore we tested if *Edn1* was directly regulated by HDAC1 and HDAC2.

Since only little amounts of chromatin can be extracted from brains of P0 mice a test ChIP experiment was done, using brain tissue of an adult mouse. Unfortunately, only formaldehyde crosslinked brain tissue could be used, because DSG crosslinking in the adult brain, repeatedly rendered the chromatin resistant to fragmentation by sonication. None of the antibodies used in this first trial ChIP showed any enrichment at the *p21* promoter, which served as a positive control, (Figure 27A). To circumvent the problem of sonication in adult brain tissue, frozen P0 brains were thawed, crosslinked with DSG and the chromatin of three mice was pooled. In order to avoid extensive loss of chromatin during washing steps, the samples were crosslinked and lysed in low protein binding tubes. Bioruptor[®] sonication proved to generate properly fragmented samples, however only after considerable many (ca. 30-35) cycles. Unfortunately, still no enrichment could be detected. One factor that could influence the results was the freezing of the embryo brains, which could damage the tissue and rupture the cellular membranes. Therefore, we chose to freshly isolate brain tissues of *Hdac1* $\Delta/+n$ *Hdac2* Δ/Δ n and corresponding control littermate P0 brains and keep them separated throughout the whole ChIP experiment, which also meant that less antibodies could be tested, using the same chromatin sample. As some HDAC2 specific antibodies turned out to be unreliable in ChIPs using chromatin from primary tissue (see section 3.7), those antibodies which gave the best results in F9 tests, were also used in chromatin from brain tissue, of which one of them (A300-705A) gave promising results as it showed enrichment and signals were almost depleted in HDAC1 single allele tissue (Figure 27C and D). This antibody additionally confirmed the presence of HDAC2 at the *Edn1* gene in wild type brain.

In the recent history of our lab, transgenic mice were generated, which contain a targeting cassette, fused to the 3' end of the *Hdac1* gene. This targeting cassette contains several antibody binding sites, like the FLAG and V5 tag, but also an acceptor site for the BirA ligase (Figure 27F). BirA is an *E. coli* biotin ligase that site-specifically biotinylates a lysine side chain within this acceptor site. Any biotinylated protein can be bound very tightly by the proteins avidin and streptavidin with an extremely low dissociation constant ($K_d=10^{-15}$ M), a binding which is

several orders higher than that of any antibody. Therefore the biotin/avidin affinity system is a commonly used tool for the purification of proteins, including mammalian transcription factor complexes [113]. This high affinity, high comparability of pulldown efficiencies between different biotin-tagged proteins and the low background, due to the possibility of stringent wash steps and the low occurrence of naturally biotinylated proteins, make the use of biotinylated HDAC1 a promising alternative to antibodies in ChIP experiments. Additionally, a different ChIP strategy could verify or disprove binding patterns obtained by specific antibodies. Transgenic mice, which were heterozygous for the HDAC1-biotin acceptor site fusion protein were crossed with mice containing the *BirA* ligase gene within the *Rosa26* locus to generate the biotin-tagged HDAC1 protein. The same mice, but lacking the BirA ligase served as a negative control. A trial ChIP experiment was done, using an HDAC1 specific antibody (Sat13) and streptavidin (SA) coated magnetic beads (M-280 *Invitrogen*). Formaldehyde crosslinked chromatin was used and 50 μ l of SA coated beads were blocked with 1 mg/ml BSA at 4 °C for at least 10 h. Beads and different amounts of chromatin were incubated overnight; Washing, elution and DNA purification was done according to the standard protocol. However, no enrichment was observed at the promoter of the *p21* gene, which served as a positive control. (Figure 27G). This was surprising because the visualization of a ChIP experiment, using 150 μ g chromatin and SA beads, clearly showed that the biotin-tagged protein was present in the elution fraction, although it was underrepresented compared to the wild type version in the input sample (Figure 27H). Together, these results suggest that more extensive test ChIPs would be necessary in order to optimize additional parameters, including crosslinking, amount of beads, incubation time or washing steps.

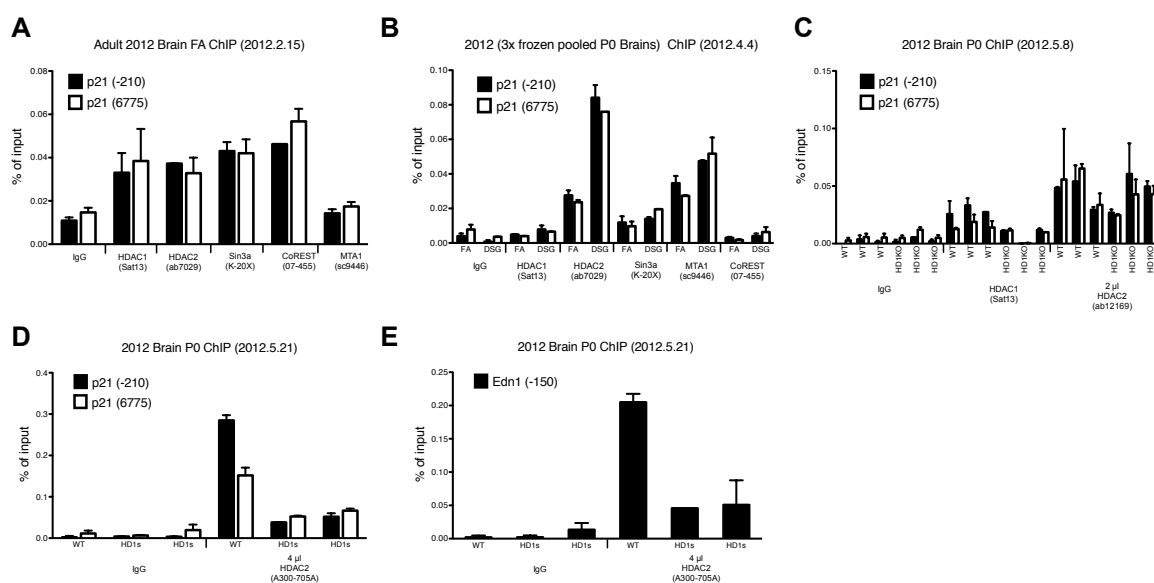
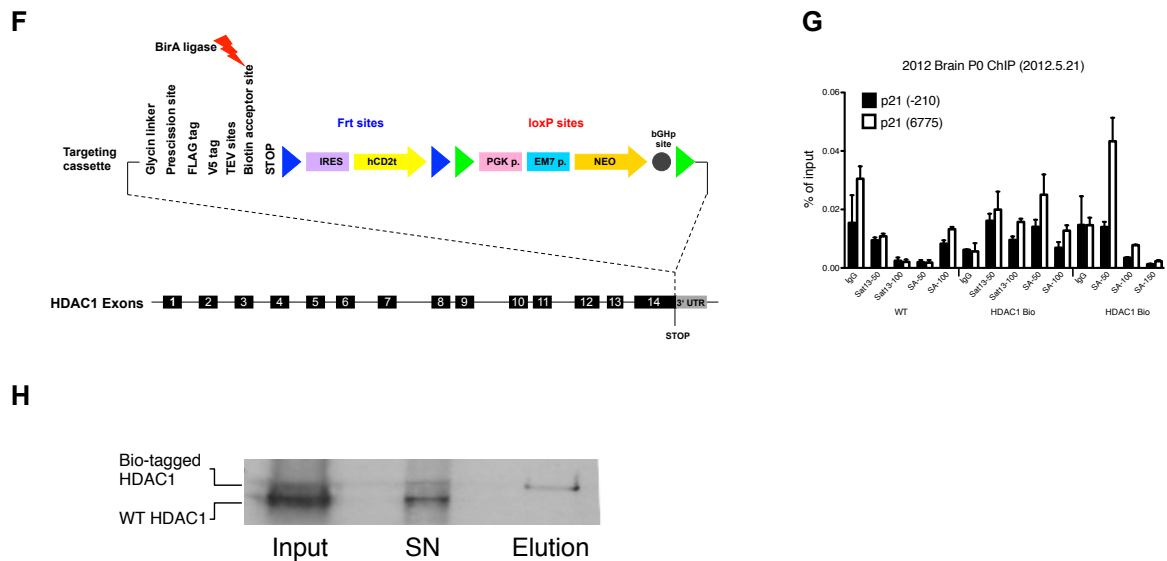


Figure 27: Trial ChIPs in murine brain tissue (continues on next page)



continued Figure 27: Trial ChIPs in murine brain tissue **A**) ChIPs for parts of HDAC1 and HDAC2 containing complexes with formaldehyde (FA) crosslinked chromatin from adult wild type brain tissue. **B**) ChIPs for parts of HDAC1 and HDAC2 containing complexes with formaldehyde (FA) or DSG crosslinked chromatin from P0 wild type brain tissue (Three frozen P0 brains were pooled for each crosslinking method). **C, D**) Antibody test for HDAC1 (Sat13) and HDAC2 (ab12169, A300-705A) with DSG crosslinked chromatin from P0 brain tissue of *Hdac1* Δ/Δ n, *Hdac1* $\Delta/+$ n *Hdac2* Δ/Δ n and corresponding control mice **E**) HDAC2 occupancy at the promoter of *Edn1* in P0 brain tissue of *Hdac1* $\Delta/+$ n *Hdac2* Δ/Δ n or control mice. **F**) Schematic representation of the HDAC1 gene, cloned with the biotin acceptor site containing targeting vector (Figure: Astrid Hagelkruys). **G**) Trial ChIP using either an HDAC1 antibody (Sat13) or streptavidin-coated beads (SA). 50 or 100 µg of FA crosslinked chromatin were used (WT = *Hdac1*bio/+ *RosaBirA*-/-; HDAC1-Bio = *Hdac1*bio/+ *RosaBirA*+/-). **H**) HDAC1-bio ChIP experiment using 150 µg of chromatin and SA beads, visualized by the monoclonal antibody 10E2 (1:1000) on a Western blot. Input = 25 µg chromatin; SN = 1/50 of supernatant of ChIP (ca. 3 µg chromatin); Elution = SDS elution of beads used in ChIP experiment. (Error bars represent SD of two technical replicas; Littermate mice were used for individual experiments)

3.9 Generation of HDAC1 and HDAC2 deficient Mouse Embryonic Fibroblasts

The goal of this particular project was to generate knockout cells, which lack either HDAC1 or HDAC2, in order to investigate if the absence of one of the major deacetylases can improve reprogramming or if the beneficial effects of HDIs are not mirrored by the knockout of one single HDAC. This was done by the introduction of a Cre recombinase into fibroblasts, which were isolated from conditional knockout mice used in our Lab. Mice carrying *Hdac1* floxed alleles were produced in our Lab in collaboration with the Lab of Patrick Matthias (Friedrich Miescher Institute, Basel, Switzerland). The *Hdac2* conditional knockout mouse was generated and provided by the Lab of Patrick Matthias. These mice contain two loxP sites flanking exon 6 of the corresponding HDAC (Figure 28A and B). The deletion of this exon, which also contains the catalytic domain, leads to a frame shift and a premature transcriptional termination. The resulting truncated mRNA version gets degraded which ends in a complete deletion of the protein in homozygous floxed cells. The use of a viral vector is a common tool to deliver genetic material into cells and several viral transportation tools exist, including retroviral, lentiviral and adenoviral strategies. In our experiment, the Cre recombinase was introduced into the MEFs by

a replication-deficient retroviral vector, which means that the viral vector genome did not contain the genes for the three classes of virion proteins gag, pol and enf. Two viral vector constructs were used, one contained the Cre recombinase and the reporter gene EGFP, the other vector was used as a negative control and contained only the EGFP gene (Figure 28C). Both of the vectors harbored long terminal repeats, which are crucial for the integration into the host genome, the Ψ + packaging signal, which facilitates the incorporation into the viral capsid and *E.coli* specific elements like the origin for plasmid replication or an ampicillin resistance gene for bacterial selection. These vectors were produced in *E.coli*, cultured in ampicillin containing medium, to select for plasmid producing bacteria. The vector DNA was extracted using the midi plasmid preparation kit from *Quiagen* [83] and checked by restriction digest, if vectors contained the correct inserts (Figure 28D). The restriction enzyme *Clal* cuts the control vector EGFP only at one position, which resulted in one single band of the linearized plasmid of about 6.7 kb in size. Conversely, the EGFP CRE plasmid contains one additional *Clal* restriction site within the Cre transgene, therefore the *Clal* digest fragmented the plasmid into two bands of 6.4 kb and 2.4 kb. The digest with *Bgl*II and *Eco*RI showed similar results; This digest removed the Cre transgene (about 2 kb) from the EGFP CRE plasmid, but no such band was detected in the EGFP control vector. Once the genetic information of the vectors was confirmed, the plasmid samples were concentrated and stored until transfecting the packaging cells.

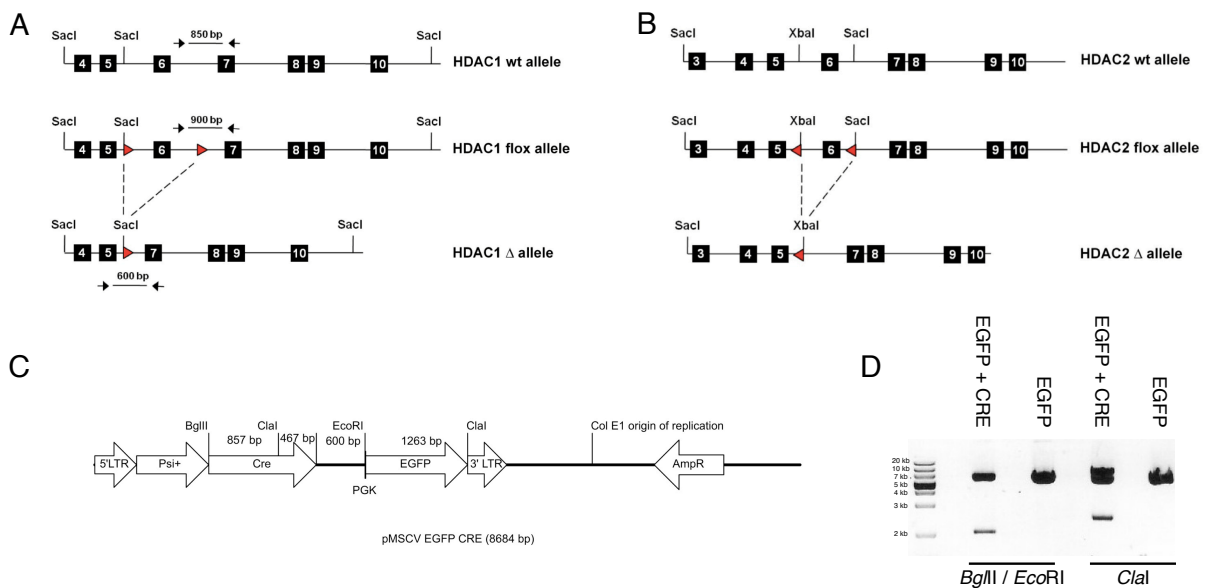


Figure 28: Genetic strategy for the generation of HDAC1 and HDAC2 knockout MEFs. **A)** Two loxP sites (red triangles) were introduced into the wild type *Hdac1* gene by homologous recombination. The loxP sites are flanking exon 6 which gets deleted after transfection with a Cre recombinase containing vector. Arrows indicate genotyping products generated by the HDAC1 lox and HDAC1 Δ PCR respectively. **B)** Two loxP sites were introduced into the wild type *Hdac2* allele. Similar to the HDAC1 knockout strategy, the loxP sites flank exon 6 which gets deleted upon expression of Cre recombinase. **C)** Schematic view of the Cre recombinase containing vector pMSCV EGFP CRE. The corresponding control vector pMSCV EGFP lacks the region between the *Bgl*II and the *Eco*RI restriction site. **D)** Restriction digest of retroviral vectors EGFP CRE and EGFP only. (LTR = Long Terminal Repeat; Psi+ = Packaging signal; PGK (Phosphoglycerate Kinase) Promoter; AmpR = Ampicillin resistance gene (β -lactamase))

The first strategy for the generation of HDAC1 and HDAC2 deficient MEFs was to mate mice, homozygous for the floxed allele of *Hdac1* and *Hdac2* respectively, isolate the MEFs from the embryos at embryonic day 13.5 and freeze the cells at P0 (i.e from the first confluent plate after isolation). Once three embryos of the same sex and of each genotype were isolated, the cells were thawed, seeded and proceeded with the transduction and selection procedure. As this experiment was designed to be performed in triplicates for each HDAC, these three embryos had to be of the same sex. This ensures that any effects which are not knockout specific during the reprogramming experiments can be ruled out at least within each group (triplicate of HDAC1 or HDAC2 knockouts). The first three embryos isolated seemed to be a lucky start as all three of them were females. These embryos (termed 1521 1-3) were supposed to be *Hdac2*^{f/f} as they were the offspring of two mice homozygous for the floxed *Hdac2* allele. However these first isolated embryos turned out to be HDAC2 knockouts, although they were negative for the Cre recombinase (Figure 29), which ruled out the possibility that a wrongly genotyped Cre⁺ deleter strain mouse was used as a parental mouse. Also erroneous PCR reactions of the genetic material isolated from the embryos' tails could be excluded, as PCRs from P1 MEFs gave similar results, and also confirmed the wild type situation for *Hdac1*.

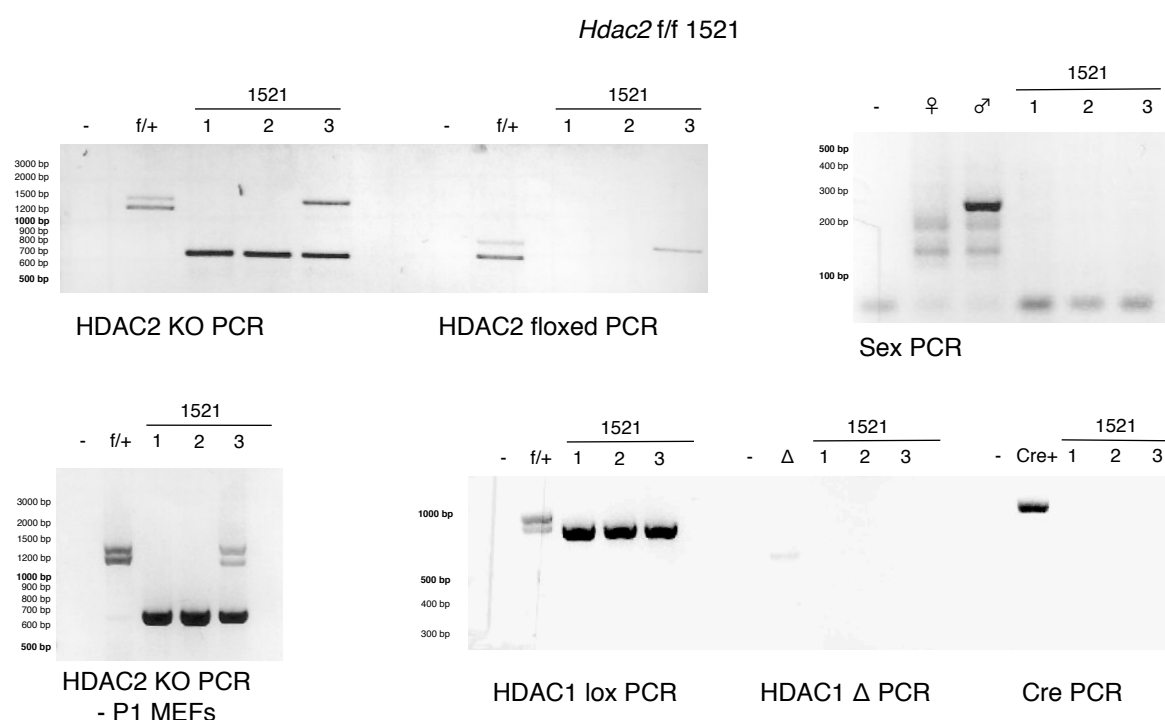


Figure 29: Genotyping of embryos (1521 1-3) from *Hdac2*^{f/f} mice. HDAC2 floxed PCR (850 bp = floxed allele; 700 bp = wild type allele). HDAC2 KO PCR (1400 bp = floxed allele; 1250 bp = wild type allele; 670 bp = KO band), Sex PCR (304 bp = male Y chromosome), Cre PCR (1000 bp = Cre +), HDAC1 Lox PCR (900 bp = floxed allele; 850 bp = wild type allele), HDAC1 Δ PCR (900 bp = floxed allele; 600 bp = Δ band). (f/+ = heterozygous floxed/wild type control; - = Non template control; ♀ = female control PCR; ♂ = male control PCR; Cre + = Control PCR from Cre positive deleter strain)

Viral transduction of MEFs works efficiently but growth rates slow down, especially after FACSing

Therefore, new embryos had to be isolated and this time a different *Hdac2*^{f/f} male mouse was mated. Seven *Hdac1*^{f/f} embryos (1078 1-7) were isolated, which all were confirmed to be homozygous for the floxed *Hdac1* allele, no deletion was detected and three (1078 - 1, 2, 3) of the four obtained female MEFs were frozen for the further transduction. Similarly, five *Hdac2*^{f/f} embryos (1400 1-5) were isolated, all were confirmed to be homozygous for the floxed *Hdac2* allele, no deletion was detected, and three (1400 - 1, 3, 4) of the four female MEFs lines were used for transduction (Figure 30).

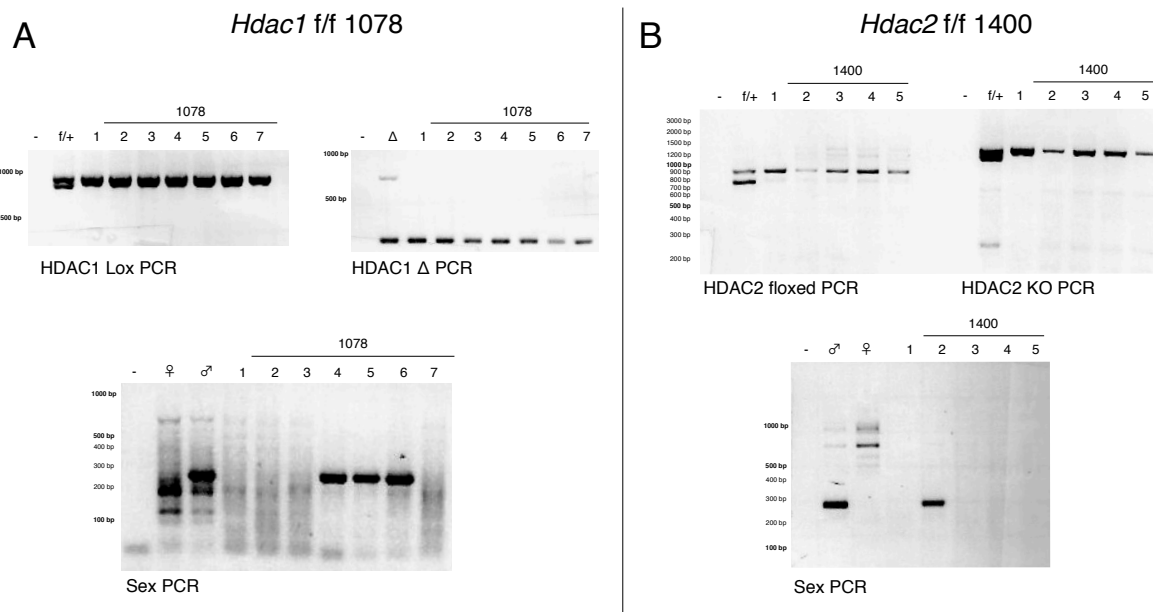


Figure 30: Genotyping of embryos from **A**) *Hdac1* (1078 1-7) f/f and **B**) *Hdac2* (1400 1-5) f/f mice. HDAC2 floxed PCR (850 bp = floxed allele; 700 bp = wild type allele). HDAC2 KO PCR (1400 bp = floxed allele; 1250 bp = wild type allele; 670 bp = KO band), Sex PCR (304 bp = male Y chromosome), HDAC1 Lox PCR (900 bp = floxed allele; 850 bp = wild type allele), HDAC1 Δ PCR (900 bp = floxed allele; 600 bp = Δ band). (f/+ = heterozygous floxed/wild type control; - = Non template control; ♀ = female control PCR; ♂ = male control PCR)

Seven days before the MEFs were thawed again, Plat E cells [85] were taken into culture and put into selection medium the next day. After two days the cells were subcultured in a 1:3 ratio, cultured for two days and seeded into 6-wells one day before the lipofection. For each 6-well of MEFs, one well of Plat E cells with the corresponding vector was prepared. In this first run of transduction, for each of the six MEF lines (3x *Hdac1*^{f/f}; 3x *Hdac2*^{f/f}) two 6-wells were used per vector. Therefore a total of 24 wells of Plat E cells were prepared. Plat E cells contain the genes for the three classes of genes which are important for virion production: gag, pol and env. These gene regions encode for structural capsid proteins, viral protease, integrase and viral reverse transcriptase, and envelope glycoproteins, respectively. The vectors pMSCV EGFP and pMSCV EGFP were packed into liposomes with lipofectamine 2000 (*Invitrogen*) and were introduced into the packaging cells by lipofection. Once introduced into the Plat E cells the plasmids are transcribed into RNA from the promoter region within the LTRs, which

can be monitored by the expression of GFP. This RNA also contains the viral ψ + integration signal, which gets packed into the capsids, together with the viral proteins that are essential for infection: Integrase, reverse transcriptase and proteases. During the budding, the virion gets enclosed into the hosts' membrane, which contains viral glycoproteins that are important for its attachment. The concentration of these replication- deficient viral particles peak at 48 h after lipofection, therefore MEFs were seeded one day after lipofection. The viral supernatant was filtered, supplemented with polybrene to increase the viral transduction rate [114] and added onto the MEF cell lines, which were transduced by "spinfection". After one day GFP expression could be detected by fluorescent microscopy. Two days after spinfection the cells were transferred from two 6- wells onto one 10 cm dish and sorted for EGFP expression after three days. Before cell sorting by FACS, it was already noticeable that cell growth slowed down. Cells were trypsinized and kept at ice before selecting for EGFP expression, which resulted in roughly 80,000 to 370,000 cells for MEF cell lines transduced with the EGFP control vector, and ca. 100,000 to 320,000 cells for MEF cell lines that got transduced with the EGFP-CRE containing retrovirus. For each cell line all GFP positive cells were put onto one 10 cm dish. Unfortunately bacterial infections occurred in two cell lines after the cell sorting, which could have occurred because of non-sterilized conditions during the FACS procedure. Additionally, MEF cell lines were growing very slowly, especially the Cre - transduced cell lines and were only 80 % confluent after six days. Due to concerns that these cell lines may not recover after additional freezing and thawing steps, the cells were frozen (500.000 cells per vial) but not sent to the lab of Eran Meshorer, Hebrew University Jerusalem.

Viral transduction of unfrozen MEFs leads to a high yield of actively dividing transduced cells

To circumvent the problem of cells going into senescence too early, the transduction experiment was repeated without any freezing of obtained MEF cell lines prior to the infection. This also meant that *Hdac1*^{f/f} and *Hdac2*^{f/f} MEFs were not infected in parallel but consecutively. Additionally, once the breedings were successful, and the day for the isolation of the embryos was fixed, Plat E cells had to be thawed three days before the MEF isolation, so that the generated cell lines could be directly transduced (See also Table 2 in the Material and Methods section). Five *Hdac1*^{f/f} embryos were isolated, all were confirmed to be homozygous for the floxed *Hdac1* allele, no deletion was detected and the three male cell lines (2184 - 1, 2, 3) were kept in culture. Eleven *Hdac2*^{f/f} embryos (2456 1-11) were isolated, all were confirmed to be homozygous for the floxed *Hdac2* allele, no deletion was detected, and three (2456 - 8, 10, 11) of the six male MEFs lines were used for transduction (Figure 31).

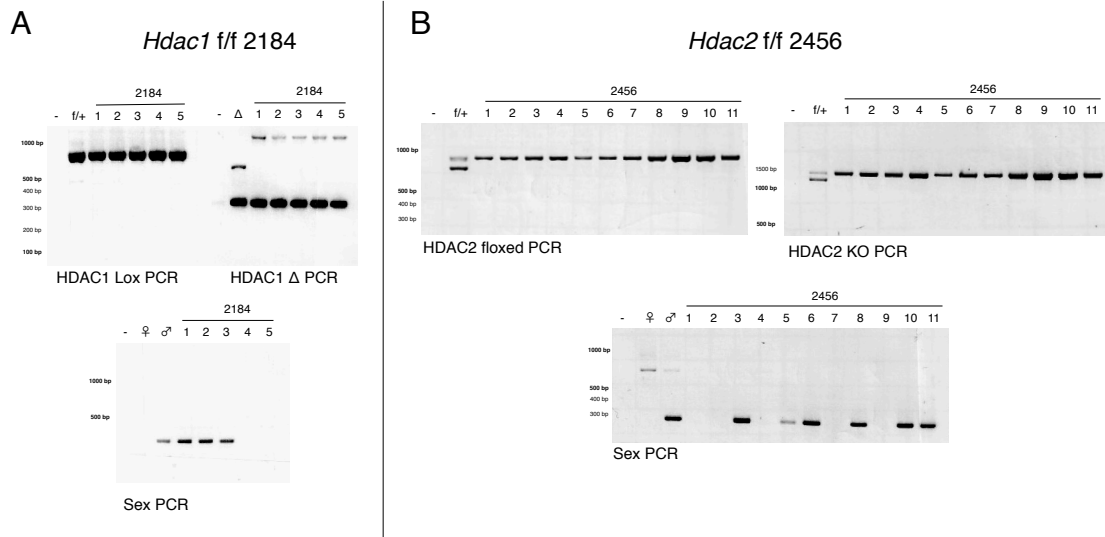


Figure 31: Genotyping of embryos from **AHdac1 (2184 1-5) f/f and **BHdac2 (2456 1-11) f/f mice. HDAC2 Floxed PCR (850 bp = floxed allele; 700 bp = wild type allele). HDAC2 KO PCR (1400 bp = floxed allele; 1250 bp = wild type allele; 670 bp = KO band), Sex PCR (304 bp = male Y chromosome), HDAC1 Lox PCR (900 bp = floxed allele; 850 bp = wild type allele), HDAC1 Δ PCR (900 bp = floxed allele; 600 bp = Δ band). (f/+ = heterozygous floxed/wild type control; - = Non template control; ♀ = female control PCR; ♂ = male control PCR)****

In addition to the omitted freezing step, the experiment was scaled up as a full 6-well plate instead of two wells was used per MEF cell line per vector. By using more cells from the beginning, we ensured that cells had to divide less to yield the required amount of knockout cells for the reprogramming experiment. The protocols for lipofection and spinfection were not changed. After the spinfection the confluent 6-wells were put onto 10 cm dishes (three wells onto one dish) and once these plates reached confluency the two plates for each MEF cell line were not pooled but prepared separately for cell sorting to reduce the risk of an infection during FACSing. The cell lines which were transduced with the EGFP control vector achieved a transduction rate of 70 -90 % which gave 400,000 to 840,000 cells per plate. MEF cell lines that got transduced with the EGFP-CRE containing retrovirus resulted in a transduction rate of 55 - 65 % which yielded ca. 215,000 to 700,000 cells per plate. This time, no infections occurred and more than twice as many cells were available for the reprogramming experiments, as for each cell line two plates were in culture after the cell sorting. Again there was a noticeable decrease of growth rates of HDAC1 knockout compared to control cells. However, cells did not seem to go into senescence as the growth rates did not slow down dramatically and no increased numbers of dead cells were detected. Five days after sorting the plates were more than 90 % confluent, small aliquots (40 - 50,000 cells) were kept in culture for immunofluorescent (IF) stainings and Western blots (WB) and batches of 500.000 cells per vial were frozen for shipment. The aliquots of cells were cultured on coverslips in 24-well plates (IF) and in 6-well plates (WB) for one and two days respectively. The complete knockout of HDAC1 and HDAC2 in MEF cell lines transduced with Cre recombinase was verified in WB (Figure 33). However, it was also visible that in the knockout cells, the corresponding HDAC was upregulated. The knockout was also verified by IF, although the HDAC1 antibody 10E2 was used in a high concentration and gave unspecific cytosolic background signals (Figure 32).

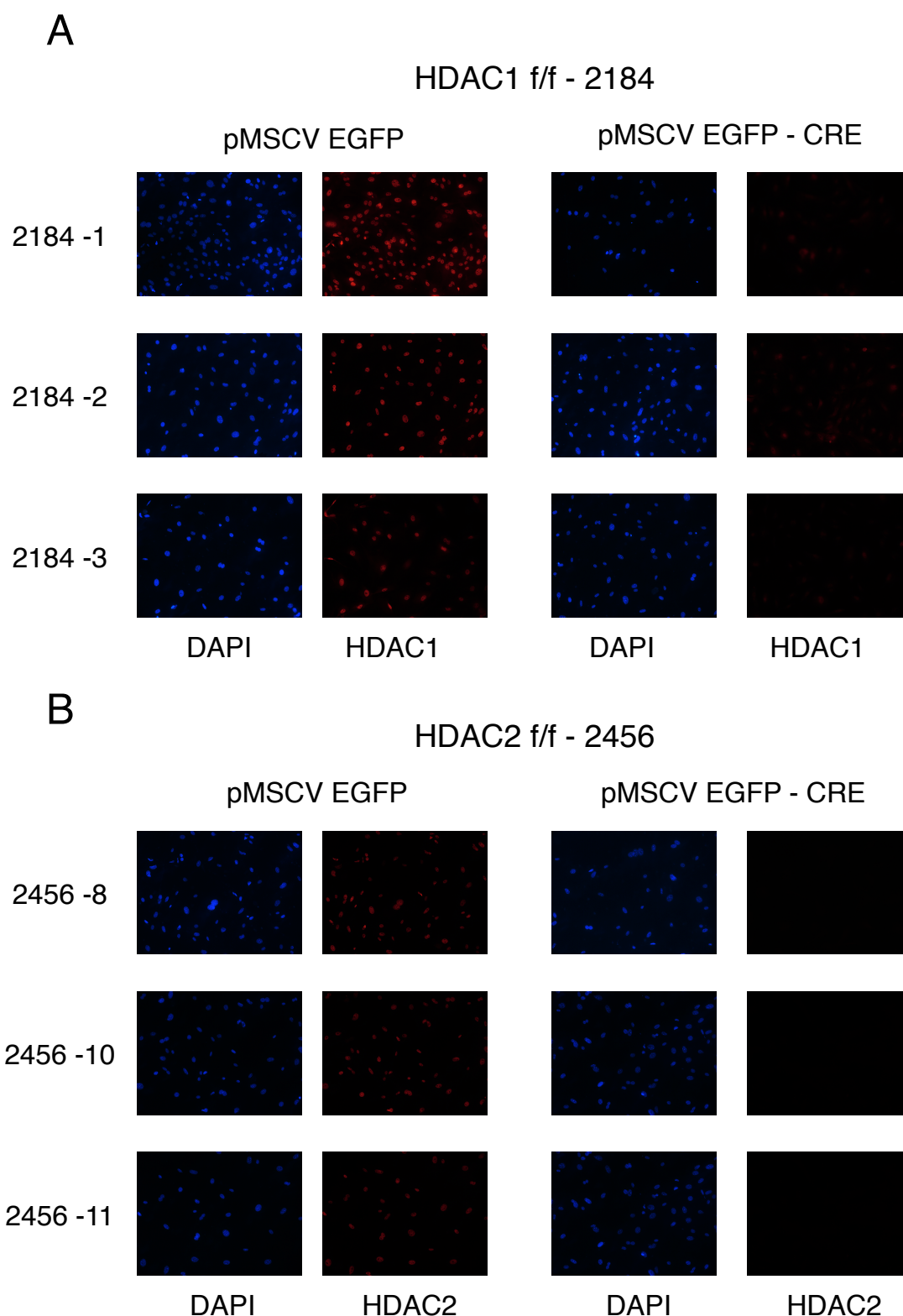


Figure 32: Verification of knockout MEF cell lines by immunofluorescence. **A)** *Hdac1*f/f cell lines (2184 - 1, 2, 3) and **B)** *Hdac2*f/f cell lines (2456 - 8, 10, 11) either transduced with the negative control vector which only contains EGFP or with the Cre recombinase containing EGFP-CRE vector. Cells were stained for HDAC1 and HDAC2 with the monoclonal antibodies 10E2 and 3F3 respectively, and counterstained with DAPI.

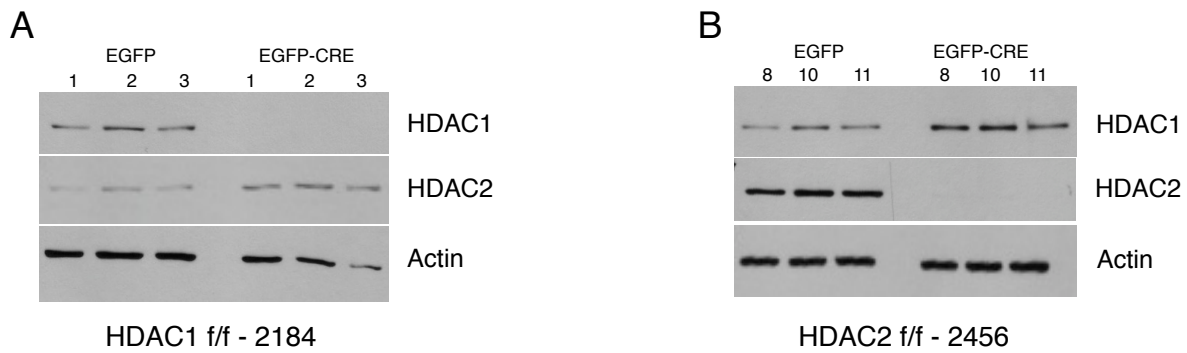


Figure 33: Verification of knockout MEF cell lines by Western blot. **A)** *Hdac1*f/f cell lines (2184 - 1, 2, 3) and **B)** *Hdac2*f/f cell lines (2456 - 8, 10, 11) either transduced with the negative control vector which only contains EGFP or with the Cre recombinase containing EGFP-CRE vector.

The cell lines were kept at -80°C and were sent on dry ice to the Hebrew University in Jerusalem where the cells were thawed and expanded until passage five for reprogramming, which was done with a polycistronic retroviral cassette containing the four stemness factors *Oct4*, *Sox2*, *Klf4* and *c-Myc* (STEMCCA Lentivirus Reprogramming Kit, Millipore) (Figure 34A). The insertion of a polycistronic cassette reduces the viral integration events and improves reprogramming [115]. For each cell line 200,000 cells were plated into 6 x 6-wells, three of which were used for alkaline phosphatase (ALKP) assays to count the number of forming iPSCs after 12 days of reprogramming, and three wells were used to isolate and expand emerging iPS cell lines. ALKP is a stem cell membrane marker and elevated expression of this enzyme is associated with undifferentiated pluripotent stem cells, and the staining of ALKP is used as a marker of pluripotency in human and mouse systems [116, 115]. MEFs which were not transduced with any retroviral vector (neither EGFP-CRE nor EGFP) were used as an additional negative control during the reprogramming experiment. Moreover, MEFs which were not treated with the STEMCCA reprogramming kit formed no alkaline phosphatase positive cells and remained GFP positive, which excluded any effects caused by a contamination with packaging cells. The results of the alkaline phosphatase staining showed that there is no increase in reprogramming efficiency by the knockout of HDAC1 or HDAC2. There was even a slight decrease in iPSC formation in HDAC1 knockout cell lines (Figure 34B - D). Additionally, the cells lost the expression of GFP during the process of reprogramming. The silencing of retroviral promoters in the LTRs is a common feature of the generation of iPSCs, and is actually considered to be a hallmark of class II iPSCs [117]. A similar mechanism could be imagined for the expression of EGFP, although the PGK promoter, which drives EGFP expression, is generally used for long-term persistent expression in cells that are susceptible to promoter silencing from methylation or histone deacetylation, such as undifferentiated embryonic stem (ES) cells [118].

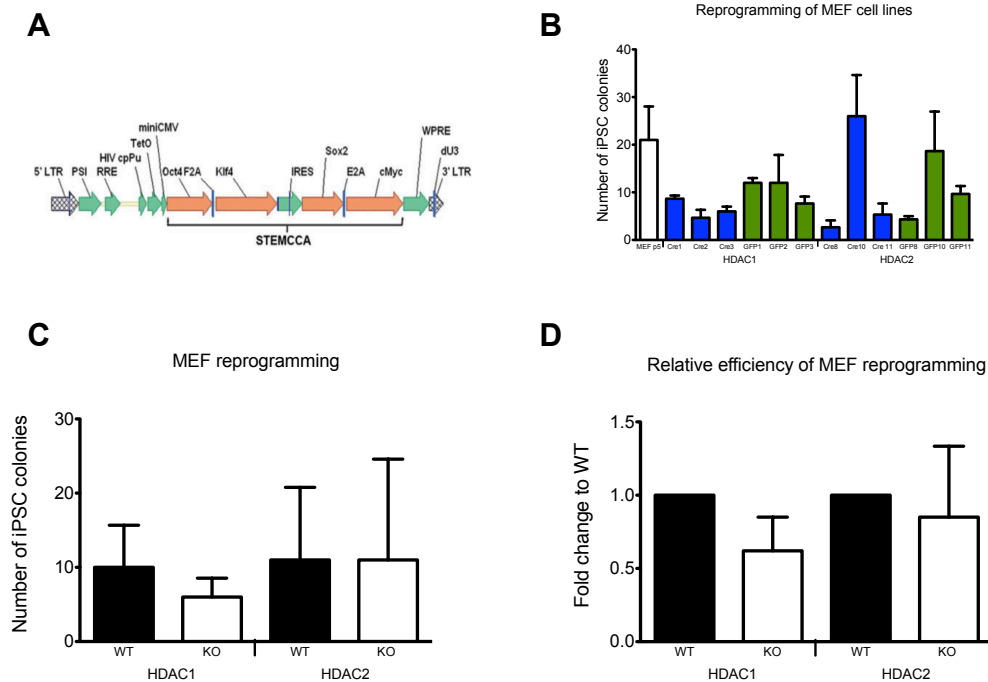


Figure 34: Reprogramming efficiencies measured by the appearance of induced pluripotent stem cells (iPSCs). **A)** Schematic representation of the retroviral vector used for reprogramming (Figure adapted from Sommer, *et al.*, 2009 [115]). **B)** iPSC colonie formation, measured by alkaline phosphatase staining, for each cell line. (MEF P5 = non-infected control; Cre = Knockout line for corresponding HDAC; GFP = negative control vector transduced cell lines) **C)** Average iPSC formation and **D)** relative efficiencies of knockout MEF cell lines compared to “wild type” (= cell lines transduced with the EGFP control vector)

4 Discussion

In the context of transcription, acetylation represents the most extensively studied covalent modification of histones, especially at histone H3 and H4. It is generally believed that histone hyperacetylation is linked to transcriptional activation and gene expression, while hypoacetylation occurs at repressed and transcriptionally inactive genes. The level of histone acetylation is tightly controlled by the two opposing groups of enzymes: the histone acetyltransferases (HATs) and their counterpart the histone deacetylases (HDACs). In this study, we tried to investigate the involvement of the two highly homologous enzymes HDAC1 and HDAC2 in the processes of transcription, murine development and reprogramming.

4.1 Preliminary HDAC1 binding data and response to HDIs suggests three models of action

Our lab generated preliminary HDAC1 binding data and RNA expression studies in F9 teratoma cells, to investigate the role of HDAC1 and HDAC2 during transcription. As a first project we tested if these microarray expression studies and genome-wide HDAC1 binding data can be verified via qPCR and site directed ChIP-qPCR respectively. Therefore several candidate genes were selected upon presence of HDAC1 near the promoter and transcriptional behavior follow-

ing HDAC1 or HDAC2 knockdown or HDI treatment. HDAC1 bound genes were categorized into three classes: Upregulated, downregulated or not deregulated upon depletion of HDAC1 or HDAC2 or treatment with HDIs. We could show that all tested upregulated genes were indeed verified, both their enrichment of HDAC1 at the promoter region compared to control regions and their transcriptional upregulation upon MS275 treatment could be detected by site directed ChIP and qPCR respectively. The transcriptional response of genes, which were categorized as downregulated could only be validated for HDAC inhibitor treatments, as HDAC1 knockdown cells showed no downregulation of these genes. Additionally, the enrichment of HDAC1 could not be detected for one gene (*Odz4*). Similar effects were detected at genes which were categorized as not deregulated. While the presence of HDAC1 was clearly reproduced and transcriptional non-responsiveness was given in MS275 treated cells, a deregulation was observed in HDAC1 knockdown cells. This general discrepancy between microarray and qPCR data of HDAC1 knockdown cells could be caused by the fact that later cell passages were used for the qPCR experiment. Therefore the transcriptional landscape could be different, as cells tend to adapt for a knockdown within a given time. Apart from this discrepancy, these series of validation experiments clearly showed that changes in expression, called by Agilent microarray detection, represent solid data, and especially deregulations after HDI treatments are in good agreement with results obtained by qPCR. The three classes of genes, presented above based on our preliminary binding data, represent three models of HDAC1 can play a role during transcription: HDAC1 acts as a direct repressor and HDI treatment leads to an upregulation of the target gene; HDAC1 activity is required for the transcription of genes and its catalytic inhibition leads to the downregulation of bound genes; and finally, HDAC1 executes a function that is not a main determinant or unrelated to the bound gene's transcriptional fidelity, and a catalytic disruption of HDAC1 does not influence the rate of transcription. Although biological replicas for ChIP-seq experiments were missing at this point, it already seemed that the predominant amount of HDAC1 bound genes fall into the third, and transcriptional unresponsive, class.

4.2 Optimization of HDAC1 and HDAC2 ChIPs

Two factors suggested the optimization of the HDAC1 ChIP technique: the enrichments of HDAC1 and HDAC2 specific antibodies in ChIP-seq were relatively low, and secondly, the reproducibility of HDAC1 ChIPs was challenged in mouse ESCs. One crucial step during each ChIP experiment is the target-recognition and -binding capacity of the antibody. Although class I HDACs can bind to target DNA sequences by homo- and heterodimerization and interaction with DNA binding proteins, like YY1, they generally reside in large multi-subunit containing complexes. In contrast to transcription factors, which directly bind their consensus sequences and are therefore in close proximity to DNA, these large chromatin modifying complexes span a considerable distance and are therefore difficult to target precisely. Therefore, antibody recognition and crosslinking of proteins of interest to DNA are both crucial parameters that determine the pulldown efficiency of ChIP experiments. To this end, we asked if the purification of polyclonal antibodies, using recombinant protein harboring the same molecular purification tag as the initial immunogenic protein, would improve the specificity or pulldown strength. We could show that recombinant protein can be produced and affinity purified in large quantities, using bac-

terial strains containing an IPTG inducible, His-tagged HDAC1 or HDAC2 mouse protein and nickel covered beads. The application of these isolated recombinant proteins in the purification of polyclonal antibodies proved to be highly specific. The use of these purified antibodies in ChIP experiments was reproducible, but did not show any significant increased pulldown performance.

Tackling the second possible parameter for improvement, crosslinking HDAC containing complexes to DNA, turned out to be an efficient way to improve the reproducibility and efficiency for several antibodies, especially the polyclonal HDAC1 specific Sat13. The dual crosslinking with DSG, but not EGS, showed to dramatically increase pulldown at HDAC1 bound sites, while background signals were not increased. This indicates that the extended spacer regions of DSG is long enough to link big complexes prior to crosslinking to DNA, while the use of EGS seemed to increase the risk of over crosslinking, resulting in epitope masking. Interestingly, the use of DSG dual crosslinking did also improve ChIP results of other antibodies, e.g. HDAC2, but showed only minimal effects using antibodies specific for other class I HDAC containing complexes, underlining the importance of optimizing ChIP parameters for each factor. It is also important to mention that, once crosslinking conditions were established for one antibody, results were consistent along different cell lines (F9, MEFs, 3F3, U2OS). Additionally, we could demonstrate that the alternative crosslinker DSG can also specifically improve ChIP-seq results for the HDAC1 antibody Sat13. Peaks, which were detected in formaldehyde crosslinked ChIP-seq data, were almost perfectly covered by the significantly larger amount of peaks found in the DSG crosslinked version, suggesting that dual crosslinking can reveal novel binding events, that are undetectable by standard methods. These newly found peaks may bare additional information, nevertheless, we continued to analyze only peaks that were detected in both experiments, to minimize the risk of false positives. Unfortunately, HDAC2 ChIP-seq data from DSG crosslinked chromatin did not show specific enrichments, although site directed testing did. This artifact could be specific for the combination of antibody and crosslinking, or it may be caused by the inferior sequencing quality. Additionally, DSG crosslinking proved to be necessary and sufficient for ChIP assays in primary tissues, like the epidermis or brain.

4.3 Transcriptional regulation by HDAC1 and HDAC2

The main focus of this project was the investigation of the two class I HDACs and their role in transcription. The two highly homologous enzymes HDAC1 and HDAC2 typically represent transcriptional co-repressors which are attributed with common features of gene silencing: they can promiscuously deacetylate a variety of histone lysine residues whose acetylation have been generally associated with actively transcribed genes. Additionally, HDAC1 and HDAC2 cannot bind to DNA or histones by themselves but are thought to get directly recruited to genes by DNA binding factors or are incorporated into large repressive complexes. Within these complexes different subunits convey necessary functions like histone binding, catalytic regulation of HDACs, methylated DNA binding or histone lysine demethylation. This conventional view has been challenged by several recent studies, which reported that histone deacetylase activity is essential for gene activation. Initial reports were carried out in yeast where the authors describe the histone deacetylase Hos2 as an important factor during the induction of the *GAL1*

gene. The removal of Hos2 leads to H3 and H4 hyperacetylation in the coding region and defective transcriptional activation of *GAL1* [119]. Additionally, treatment with HDIs, even for short periods of time, results in a significant amount of genes that are downregulated, which suggests a direct function in transcriptional activation or maintenance. These effects were not only detected in yeast but also in mammalian systems where a dynamic cycle of acetylation and deacetylation was suggested to be the driving force of transcription and disturbance of this balance, even by hyperacetylation, caused the ablation of transcriptional induction [120].

In this study we complemented microarray expression and HDAC1 ChIP-seq data with a biological replica of genome-wide HDAC1 binding patterns, using the newly established method of dual crosslinking, which greatly enhanced the quality of the data and enabled us to pinpoint a set of high confidence peaks, which were found in both replicas. These ChIP data revealed that HDAC1 binding strongly correlates to promoter regions, showing the most prominent binding in close proximity to the TSS and in a 500 bp window upstream of the first exon. HDAC1 recruitment was also observed downstream of the TSS where the average read intensity peaked in close proximity of the TSS, quickly dropped further downstream and reached a constant low level along the transcribed region of the metagene. Interestingly, we could detect a strong correlation between transcriptional activity and HDAC1 binding. In fact, the higher a gene was expressed the stronger the read density accumulated around its TSS. This was not only true for inducible or lineage specific genes, but also for constitutively active “housekeeping” genes, such as *GAPDH*. Conversely, silenced genes, showed no detectable HDAC1 binding. The view of HDAC1 as a strict transcriptional repressor could not be supported by these data, but requires a differentiated view.

To date, several genome-wide mapping studies for HATs and HDACs exist, which address the question of HDAC recruitment and gene expression. However, it seems that there is a discrepancy between the findings in different model organisms. For example studies in yeast found that the HATs Gcn5 and Esa1 are both bound to the promoters of active protein-coding genes, while HDAC recruitment (Hst1 and Rpd3) does not correlate with active transcription, but is associated with a specific set of genes, coding for regulators of distinct cellular functions, like sporulation or cell cycle progression [121]. In contrast to yeast, global mapping of HATs and HDACs in human CD4⁺ cells report a positive correlation between HDAC binding (HDAC1, 2, 3, and 6), histone acetylation (H3, H4 pan-acetyl) and transcription, which was measured by gene expression and Pol II binding [95]. In this study, HDAC1 showed the strongest connection to active transcription and hyperacetylation and, additionally, was almost exclusively found at the promoter, while HDAC2 and especially HDAC6 were also found in the coding region. Our findings regarding HDAC1 recruitment to promoter regions of actively transcribed genes are in good agreement with this study, which underlines distinct functions of HDACs in yeast and mammalian cells.

Based on these observations Wang *et al.* [95] presented several models for the role of HDAC activity at silenced, primed and active genes; Silent genes are either marked by H3K27me3 and/or completely lack active histone marks. These genes show no HDAC or HAT presence and are not hyperacetylated upon HDI treatment. Primed genes are associated with H3K4 methylation and incorporation of H2A.Z but are transcriptionally inactive. This set of genes

is target of transient acetylation events that are quickly deacetylated, while HDAC inhibition leads to an increase in promoter acetylation and Pol II recruitment but, interestingly, not to an increased transcription, suggesting that HDACs control transcription at the step of initiation. HDACs and HATs are coordinately recruited to actively transcribed genes where they establish a dynamic balance between cyclic acetylation and deacetylation. The reason for this mechanism could be that this cyclic addition and removal of acetyl groups is an important prerequisite for productive transcription [120, 18], or, similar to the action of Rpd3S in yeast prevents cryptic initiation within the gene body [14]. As a matter of fact, several studies, carried out in mammalian model organisms, claim to link different HDACs to deacetylation within gene bodies which prevents spurious transcriptional initiation. Candidates include HDAC6 [95], an HDAC1/Sin3B/Pf1/Mrg15 tetrameric complex [122] or an unphosphorylated version of HDAC2 [123]. These models provide a good framework concerning possible roles of HDACs at different gene classes, but lack a mechanistic insight into the process of transcriptional regulation. Therefore we investigated the binding pattern of HDAC1 and the response of bound genes to HDAC1 or HDAC2 knockdown and HDAC inhibition by the small molecule inhibitors TSA and MS275. Surprisingly, only a minimal proportion of genes that were bound by HDAC1 got deregulated in HDAC1 or HDAC2 ablated cells, of which roughly two thirds were upregulated. As mentioned above in the results section, this could be caused by an incomplete knockdown or a compensation mechanism, which would allow the cells to adapt for the loss of one HDAC enzyme, underlining the importance of redundant pathways in transcriptional regulation by HDACs. In fact, comparison of knockout studies and global mapping of chromatin modifying enzymes in yeast, revealed a great discrepancy between localization, and transcriptional response in knockouts, showing that on average only 2.5 % of chromatin factor occupied genes are transcriptionally affected by its loss [124]. In line with this observations is that a substantial bigger fraction of HDAC1 bound genes turned out to be deregulated upon the treatment with HDAC inhibitors, to the same extend up- and downregulated. The majority (80-90 %), nevertheless, were still not deregulated. The question arises now: What makes a gene responsive to HDAC inhibitor treatment, and what keeps transcription at a constant level even though the catalytic deacetylase ability of promoter bound HDAC1 is blocked? One finding which could address the difference between up- and downregulated genes would be that upregulated genes show a significantly lower initial wild type expression than non-responsive or downregulated ones, which suggests that HDAC1 is recruited to these genes and directly contributes to their repression. Repression could occur by keeping the histone acetylation low, thereby preventing polymerase from binding. Alternative models for gene repression include: Directly counteracting transcription factors by deacetylating them, or by generating deacetylated histone tails which serve as binding sites for SANT-domain containing complexes (reviewed in [12]). The next group of genes, which get downregulated upon knockdown or HDI treatment, were found to have a moderate to high initial wild type expression. HDAC1 recruitment seems to serve a functional different role at this subgroup, whose transcriptional maintenance are dependent on the catalytic function of HDACs.

We also looked into a possible mechanism of HDAC1 as a transcriptional repressor during the activation of a gene. For this end, we used the well characterized transcriptional induction

of p21 caused by genotoxic stress induced p53 upregulation [100]. This model proposes the dissociation of HDAC1 in the process of p21 activation. While we could clearly report the recruitment of p53 to its binding sites at the p21 promoter, both in mouse and human cell lines, we could not reproducibly detect the dissociation of HDAC1 during this process.

Acetylation ChIP-seq data in mouse ESC (H3 and H4 pan-acetyl) generated in our lab and human CD4⁺ cells (H3K9ac and H4K16ac [95]), indicate that genes with the highest expression, and therefore with the most bound HDAC molecules, show the strongest increase in acetylation after HDI treatment. Based on these observations it is therefore surprising that most of the genes do not change in their rate of transcription. This class of genes keep a constant transcriptional level, although hyperacetylation occurs at their promoter. One recent study, investigating the role of H3K9 acetylation in ESCs, reported that treatment with HDAC inhibitor valproic acid (VPA) leads to a moderate, but global increase of H3K9 acetylation [125]. In contrast to this global increase of acetylation, only a minimal proportion of genes were deregulated. Additionally, only 36 % of upregulated genes showed also an increase in acetylation, which suggests that, firstly, histone hyperacetylation does not immediately cause a transcriptional response and secondly a great percentage of deregulated genes may not be linked to histone acetylation. Although these data were generated in a different cell type, they nicely reflect our observation on HDAC1 binding and transcriptional changes.

In conclusion, it seems that the presence of HDAC1 at gene promoters is context dependent; whereas we found a small set of bound genes that was directly repressed by histone deacetylation, we also detected a substantial amount of genes whose expression could be directly activated by histone deacetylases. Curiously, although we found similar numbers of up- and downregulated genes, the proportion of potentially directly regulated genes was increased for downregulated genes. To date our data cannot explain the role of HDAC1 at the predominant number of genes which are non-responsive to HDAC inhibitors. To determine the function of HDAC1 at these genes, future projects could investigate the potential of HDAC1 to serve as a structural component of large complexes, in which the catalytic activity of HDAC1 is not necessary for the bound gene's expression. Therefore it would be interesting to investigate the binding pattern of a catalytic inactive mutant of HDAC1, since transgenic mouse lines are currently generated in our lab. Similar recruitment patterns of inactive HDAC1 or HDAC2 molecules would argue for a structural role. Additionally experiments addressing the capacity of HDAC1 to prevent histone acetylation spreading into the gene body would give insights into a function of HDAC1 that does not directly contribute to the rate of transcription. The high presence of HDAC1 shortly downstream of the TSS already suggests a role that rather prevents the misplacement of transcriptional initiation, than controlling the rate of mRNA production. The use of cryptic initiation sites would lead to the production mRNA molecules containing alternative 5' ends and future projects focusing on this aspect of HDAC1 could include site specific examination by nuclear run-on experiments or global investigation by GRO-seq or short capped RNA sequencing (scRNA-seq).

4.4 HDAC1 and HDAC2 in epidermal knockout mouse models

The conditional ablation of HDAC1 or HDAC2 in the epidermis did not cause any obvious phenotypes, due to a compensating effect which caused the upregulation of the corresponding paralog. In contrast to that, the simultaneous deletion of both enzymes lead to severe developmental abnormalities and embryonic lethality. However, epidermal stratification was still functional. Interestingly, upon deletion of one additional allele of either *Hdac1* or *Hdac2* the phenotypes varied, as retaining a single *Hdac1* allele was able to fully compensate and rescue the severe phenotype of conditional double knockouts, and the mice were undistinguishable from their littermates (Figure 22A). Conversely, a single *Hdac2* allele was insufficient to compensate for the loss of three of the four *Hdac1* and *Hdac2* alleles, and *Hdac1* Δ/Δ ep *Hdac2* $\Delta/+$ ep mice showed a severe epidermal phenotype associated with hyperproliferation, hyperkeratosis and hair follicle degeneration. These data suggest that there is a quantitative redundancy, as two alleles of *Hdac2* can fully compensate for the loss of HDAC1 protein, but also qualitative non-redundant functions of HDAC1 in the epidermal development.

Several genes turned out to be deregulated in *Hdac1* Δ/Δ ep *Hdac2* $\Delta/+$ ep mice: 3749 genes in adult mice (P50) and 834 in pups (P5). A nice subset (386 genes) was deregulated in both arrays, and especially many upregulated genes were found both in the P50 and in the P5 array (Dissertation Mircea Winter). These commonly upregulated targets included a number of genes associated with the epidermal differentiation complex (EDC), for example eight different *Spr* genes, *S100a9* or three different *Lce* genes, and a variety of keratins (*K12*, *K14*, and *K19*). Additionally, proliferative genes, like *Ep*gn and *Ada1* were highly upregulated in both arrays. Since the expression of the K5-Cre transgene starts at E15.5, many of these upregulated genes could be indirect targets, especially in adult (P50) mice. However, a direct regulation by HDAC1 and HDAC2 would link the deregulated genes to the knockout phenotype.

To test if the two HDACs are directly present at the promoters of these deregulated genes ChIP experiments were carried out using chromatin extracted from primary epidermal tissue. Extensive troubleshooting and optimization of the ChIP technique were necessary to establish a working protocol. In general ChIP results from tissue derived chromatin were more ambiguous compared to ChIPs from *in vitro* cultured teratoma cells (in terms of maximal antibody pulldown or signal to background ratios). This might be caused by a less efficient chromatin extraction from epidermal tissue, or by the fact that keratinocytes have approximately two times less cellular HDAC1 or HDAC2 protein molecules compared to F9 cells (Diploma thesis Carina Fischer). The tumor suppressor gene *p21* (*Cdkn1a*) was used as a readout of antibody and ChIP performance, because the binding dynamics of HDACs to its promoter are well established [38]. Once the optimal technical conditions were established we could demonstrate that both HDAC1 and HDAC2 are specifically enriched at the promoter of *p21*, as well as the promoter of *Ep*gn and *Spr*2h. Upon the deletion of HDAC1 or HDAC2, we could see that the recruitment of the corresponding paralog was increased, while antibodies specific for the deleted HDAC, expectedly, gave no signal at all. Interestingly, in the case where only one allele of *Hdac1* was left, the binding of HDAC1 seemed to be similar to the wild type situation, or even increased, although this experiment was only repeated once and additional biological replicas are needed to confirm this effect. On the other hand, if only one *Hdac2* allele was left, HDAC2 binding was reduced

which could lead to hyperacetylation and the upregulation of the target genes. This molecular analysis of HDAC1 and HDAC2 binding dynamics in conditional knockout mice nicely reflects and may even partly explain the phenotype. However, several things have to be kept in mind. First, the binding of HDAC1 or HDAC2 to a promoter does not guarantee for its direct regulation by them. In fact, most of HDAC1 bound genes are not deregulated upon HDAC1 ablation or the complete inhibition by HDIs. One example found in the epidermis is *p21* itself: the promoter shows HDAC1 and HDAC2 presence, but *p21* is not deregulated in any single allele knockout combination. Secondly, gene deregulation may rely on a different mechanism than histone hyperacetylation. For example, transcription factors like c-Myc can be the target of acetylation which stabilizes the protein leading to increased transcription. c-Myc has been reported to be deacetylated by the Sin3 complex, causing the deregulation of EDC genes [75]. In addition, a significant proportion of these genes, regulated by c-Myc, overlap with deregulated genes in our *Hdac2* single allele mice. Unfortunately, we could not detect c-Myc in ChIP experiments at E-box target sequences, neither in epidermal nor in ECS derived chromatin (which should have served as a positive control), which suggests additional optimization for the c-Myc ChIP. Therefore this opposing transcriptional functions of HDAC1, HDAC2 and c-Myc could not be verified on a molecular level.

4.5 HDAC1 and HDAC2 in brain development

HDAC1 and HDAC2 are important regulators during neurogenesis, and their combined deletion has been shown to cause neurological malformations resulting in lethality by postnatal day 7 [79]. The aforementioned study used a GFAP-Cre deleter strain to generate transgenic mice lacking HDAC1 and/or HDAC2 during development of the nervous system, in which they could detect neurological malformations as early as embryonic day 14.5. Our lab uses the Nestin-Cre transgene [111] for deletions of floxed genes in the NS. The conditional deletion of either HDAC1 or HDAC2 by Nestin-Cre expression lead to the complete compensation by the corresponding paralog. The remaining paralog was not only upregulated, but also re-expressed in cell lines which would lack it in the wild type situation. We could detect the re-expression of HDAC1 in HDAC2 deficient neurons, while the vice versa situation was true for HDAC2, which was re-expressed in astrocytes upon loss of HDAC1. The conditional double knockout of HDAC1 and HDAC2 using the Nestin-Cre transgene resulted in an earlier lethality than reported by Montgomery *et al.*, 2009 [79], since mice died already during embryonic development and was accompanied by increased apoptosis, DNA damage, reduced proliferation and increased H3K56 acetylation. Additionally, the retention of one *Hdac2* allele completely reverted the severe phenotype and transgenic mice were viable and fertile, while one remaining *Hdac1* allele only delayed lethality and *Hdac1* Δ / $+$ n *Hdac2* Δ / Δ n mice died shortly after birth, revealing HDAC2 as an important epigenetic regulator of brain development.

Microarray analysis showed that a variety of genes is deregulated in *Hdac1* Δ / Δ n *Hdac2* Δ / Δ n double knockout mice at embryonic day 14.5. The majority (more than 75 %) of the 1546 deregulated genes turned out to be upregulated but most likely represent indirect effects, as most gene ontology classes were associated with mechanisms in immune response, hemopoiesis and vasculature development, suggesting a breakdown of the blood-brain barrier and infiltration

of immune cells already as early as E14.5, which ultimately results in the severe brain hemorrhages that are observed by E18.5. Surprisingly, despite the lethal phenotype of *Hdac1* single allele mice, only limited numbers of genes were deregulated at E14.5 (140 genes) and P0 (98 genes), and only six of these genes were found at both timepoints.

To investigate if genes like *Edn1*, which was found upregulated in P0 *Hdac1* single allele mice, are directly targeted by HDAC1 and HDAC2, the binding dynamics at the promoter of these genes was analyzed by ChIP-qPCR. Similar to results in epidermal tissue, ChIP efficiencies in murine brains were lower compared to *in vitro* cultured cell lines, and several parameters of the ChIP method had to be optimized before enrichments of HDAC1 and HDAC2 could be verified. In addition to the positive control gene (*p21*), we could also show that HDAC2 is bound to the promoter of *Edn1*. Direct regulation of genes, associated with neurogenesis and CNS development is one possible way, how HDACs could influence these processes. Another possibility, would be the deacetylation of non-histone proteins including transcription factors, structural proteins or members of metabolic circuits, like the adenosine monophosphate-activated protein kinase (AMPK), which senses cellular energy deprivation [126]. The small number of deregulated genes in *Hdac1* single allele mice is in stark contrast to their perinatal lethality, which might suggest additional malfunctional pathways which depend on acetylation events.

In summary, the conditional knockout studies in murine brain and epidermal tissue have clearly revealed non-redundant functions of HDAC1 and HDAC2. HDAC1 seems to be especially important in epidermal development, while the same could be true for HDAC2 in brain development. In this project we could show that important players in epidermal and brain development are deregulated in *Hdac2* and *Hdac1* single allele mice respectively, and, additionally, their transcriptional regulation might be directly influenced by HDAC1 and HDAC2.

4.6 HDAC1 and HDAC2 in reprogramming

The generation of HDAC1 and HDAC2 knockout fibroblasts was not a trivial task to do, although transgenic mice that have floxed HDAC1 and HDAC2 alleles are commonly used in our lab. The most straight forward way to obtain knockout fibroblasts would have been to mate these floxed mice with a general Cre⁺ deleter strain and obtain the knockout embryos. Two major obstacles render this strategy impossible: firstly, the complete knockout of HDAC1 leads to severe growth retardation and embryonic lethality before embryonic day 10.5 [36], whereas embryos deficient for HDAC2 would reach embryonic day 13.5, that is necessary for fibroblast extraction. Apart from the embryonic defects, a knockout early in embryogenesis would also allow cells to adapt for the loss of HDAC2, thereby reducing the chance that cells would still be affected by the knockout once they get to the reprogramming step. Therefore a different approach was used, in which MEFs were extracted and transduced with a Cre-recombinase containing, replication-deficient retrovirus. To select for transduced cells the expression of EGFP served as a positive selection marker for fluorescence activated cell sorting (FACS). This approach allowed for the generation of knockout cells *in vitro*, but since MEFs tend to go into senescence after several passages, some optimizations of the knockout procedure were necessary. For example, the initial freezing of the cells, which was done to coordinately perform the knockout experiments in

both cell lines (*Hdac1f/f* and *Hdac2f/f*), had to be omitted, as the cells would stop dividing prematurely. Additionally, the amount of cells that were transduced had to be increased to ensure that cells had to divide less until they yield the required amount of knockout cells for the reprogramming experiment. Using this optimized technique lead to a high knockout efficiency that was confirmed both by Western blot and immunofluorescent staining. However, the reprogramming of these cells, by our collaborators at the Hebrew University in Jerusalem, did not result in any difference in reprogramming efficiencies. This is an indication that the improved iPSC formation, caused by the addition of HDIs during the reprogramming process are not mimicked by a knockout of either HDAC1 or HDAC2. This is partly surprising, since a recent study has reported that the treatment of VPA or a knockout of HDAC2 is necessary and sufficient for the reprogramming of mouse and human fibroblasts using a novel miRNA based approach, that does not require the use of any of the standard OSKM reprogramming factors [127]. The authors also claim that human foreskin fibroblasts do not require an HDAC2 knockout since they show endogenous low levels of the protein. The results from this study, compared with our results lead to the assumption that the effects of an HDAC2 knockout are rather dependent on the reprogramming method than on a general effect of chromatin hyperacetylation.

Several different factors could contribute to the discrepancy between HDI treatments and HDAC1 or HDAC2 knockouts: firstly, the role of HDACs in pluripotency is highly debated, for example the administration of high levels of TSA in mouse ESCs leads to transcriptional and epigenetic changes which mimic those that appear during embryoid body differentiation [128]. In contrast to that, other studies have shown that low levels of HDIs increase self-renewal, interfere with differentiation and can revert mouse embryoid bodies towards an undifferentiated state [129]. Additionally, the amount of HDAC1 is exceptionally high in ESCs and decreases during differentiation [125]. A conclusion of all these studies might be that HDIs exert an anti-differentiation effect when low doses are applied on cells that have already exited from self-renewal e.g. embryoid bodies, whereas higher doses applied on undifferentiated cells provoke differentiation. Applied on the observations during reprogramming experiments, this could lead to the explanation that the treatment with low levels of HDAC inhibitors, targeting a broad variety of HDAC proteins, can shift cells toward pluripotency, but the deletion of one specific HDAC might be insufficient to reproduce this initial shift, or that partially reprogrammed cells are more prone to differentiate and lose pluripotency again because they lack the complete enzyme. The latter would be supported by the fact that class I HDACs are found in ESC specific repressive complexes (NODE-complex), in which they are thought to act as transcriptional cofactors for the silencing of lineage specific genes by stemness factors like Nanog or Oct4 [41].

A second possible explanation for the generally less efficient reprogramming of pMSCV (EGFP and EGFP-Cre) transfected MEFs compared to untransfected control cells could be that the procedure of generating knockouts caused high passage numbers. During the process of viral transduction, the passage number increased to four and after sending and thawing, the cells had to be cultured again until passage five. In theory, a high passage number could already activate cellular pathways that are anti-proliferative and associated with replicative senescence. For that reason, MEFs are generally used for reprogramming experiments within the first three passages [47]. Additionally, the additional retroviral genomic insertion events could stress

MEFs in a way that reprogramming efficiencies are generally decreased. A way to circumvent these problems would be to mate transgenic mice (*Hdac1f/f* or *Hdac2f/f*) with a deleter strain that carries the Cre recombinase and a positive selection marker gene under an inducible promoter. Thereby Cre expression can be triggered at very low passage numbers minimizing the risk of senescence.

Finally, the inability of an HDAC knockout to affect the process of reprogramming could also be caused by the effect that the corresponding HDAC paralog was upregulated upon the depletion of HDAC1 or HDAC2. Therefore a compensation mechanism could prevent any effects caused by the knockout of one HDAC, as it was shown for the developmental roles of HDAC1 and HDAC2 in epidermal and brain tissue by our lab. One option to tackle this problem would be a similar one as the strategies used in tissue development: Single allele cells (*Hdac1f/f Hdac2f/+* and *Hdac1f/+ Hdac2f/f*) could be transduced with the Cre recombinase containing vector thereby reducing the upregulated HDAC paralog to wild type levels again. However, since severe phenotypes in epidermal and brain development were observed if only one of the four *Hdac1* and *Hdac2* alleles was retained, it is questionable if single allele MEFs would be able to grow *in vitro* under tissue culture conditions.

References

- [1] Wong, H., Victor, J.-M., and Mozziconacci, J. *An All-Atom Model of the Chromatin Fiber Containing Linker Histones Reveals a Versatile Structure Tuned by the Nucleosomal Repeat Length*. PLoS ONE (2007). 2(9):e877.
- [2] Valdés-Mora, F., Song, J. Z., Statham, A. L., et al. *Acetylation of H2A.Z is a key epigenetic modification associated with gene deregulation and epigenetic remodeling in cancer*. Genome Research (2012). 22(2):307–321.
- [3] Sullivan, K. E., Hechenberger, M., and Masri, K. *Human CENP-A contains a histone H3 related histone fold domain that is required for targeting to the centromere*. The Journal of cell biology (1994). 127(3):581–592.
- [4] Felsenfeld, G. and Groudine, M. *Controlling the double helix*. Nature (2003). 421:448–453.
- [5] Smale, S. T. and Kadonaga, J. T. *The RNA polymerase II core promoter*. Annual Review of Biochemistry (2003). 72:449–479.
- [6] Thomas, M. C. and Chiang, C.-M. *The general transcription machinery and general cofactors*. Critical Reviews in Biochemistry and Molecular Biology (2006). 41(3):105–178.
- [7] Dikstein, R. *The unexpected traits associated with core promoter elements*. Transcription (2011). 2(5):201–206.
- [8] Jenuwein, T. and Allis, C. D. *Translating the histone code*. Science (2001). 293(5532):1074–1080.
- [9] Yang, X.-J. and Seto, E. *Lysine Acetylation: Codified Crosstalk with Other Posttranslational Modifications*. Molecular Cell (2008). 31(4):449–461.
- [10] Allis, C. D., Berger, S. L., Cote, J., et al. *New Nomenclature for Chromatin-Modifying Enzymes*. Cell (2007). (131):633–636.
- [11] Ma, X.-J., Wu, J., Altheim, B. A., Schultz, M. C., and Grunstein, M. *Deposition-related sites K5/K12 in histone H4 are not required for nucleosome deposition in yeast*. Proceedings of the National Academy of Sciences of the United States of America (1998). 95(12):6693–6698.
- [12] Shahbazian, M. D. and Grunstein, M. *Functions of Site-Specific Histone Acetylation and Deacetylation*. Annual Review of Biochemistry (2007). 76(1):75–100.
- [13] Barth, T. K. and Imhof, A. *Fast signals and slow marks: the dynamics of histone modifications*. Trends in Biochemical Sciences (2010). 35(11):618–626.
- [14] Carrozza, M. J., Li, B., Florens, L., et al. *Histone H3 Methylation by Set2 Directs Deacetylation of Coding Regions by Rpd3S to Suppress Spurious Intragenic Transcription*. Cell (2005). 123(4):581–592.
- [15] Li, B., Gogol, M., Carey, M., et al. *Combined Action of PHD and Chromo Domains Directs the Rpd3S HDAC to Transcribed Chromatin*. Science (2007). 316(5827):1050–1054.

- [16] Reinke, H. and Hörz, W. *Histones are first hyperacetylated and then lose contact with the activated PHO5 promoter.* Molecular Cell (2003). 11(6):1599–1607.
- [17] Kimura, A., Matsubara, K., and y, M. H. *A Decade of Histone Acetylation: Marking Eukaryotic Chromosomes with Specific Codes.* Journal of Biochemistry (2005). 138(6):647–662.
- [18] Clayton, A. L., Hazzalin, C. A., and Mahadevan, L. C. *Enhanced histone acetylation and transcription: a dynamic perspective.* Molecular Cell (2006). 23(3):289–296.
- [19] Peserico, A. and Simone, C. *Physical and functional HAT/HDAC interplay regulates protein acetylation balance* (2011). 2011:371832.
- [20] Brownell, J. E., Zhou, J., Ranalli, T., et al. *Tetrahymena histone acetyltransferase A: a homolog to yeast Gcn5p linking histone acetylation to gene activation.* Cell (1996). 84(6):843–851.
- [21] Yang, X.-J., Ogryzko, V. V., Nishikawa, J.-i., Howard, B. H., and Nakatani, Y. *A p300/CBP-associated factor that competes with the adenoviral oncoprotein E1A.* Nature (1996). 382(6589):319–324.
- [22] Mizzen, C. A., Yang, X.-J., Kokubo, T., et al. *The TAF(II)250 subunit of TFIID has histone acetyltransferase activity.* Cell (1996). 87(7):1261–1270.
- [23] Sterner, D. E. and Berger, S. L. *Acetylation of histones and transcription-related factors.* Microbiology and Molecular Biology Reviews (2000). 64(2):435–459.
- [24] Roth, S. Y., Denu, J. M., and Allis, C. D. *Histone acetyltransferases.* Annual Review of Biochemistry (2001). 70:81–120.
- [25] Carrozza, M. J., Utley, R. T., Workman, J. L., and Côté, J. *The diverse functions of histone acetyltransferase complexes.* Trends in Genetics (2003). 19(6):321–329.
- [26] Grant, P. A., Duggan, L., Côté, J., et al. *Yeast Gcn5 functions in two multisubunit complexes to acetylate nucleosomal histones: characterization of an Ada complex and the SAGA (Spt/Ada) complex.* Genes & Development (1997). 11(13):1640–1650.
- [27] Grant, P. A., Eberharter, A., John, S., et al. *Expanded lysine acetylation specificity of Gcn5 in native complexes.* The Journal of biological chemistry (1999). 274(9):5895–5900.
- [28] de Ruijter, A. J. M., van Gennip, A. H., Caron, H. N., Kemp, S., and van Kuilenburg, A. B. P. *Histone deacetylases (HDACs): characterization of the classical HDAC family.* The Biochemical journal (2003). 370(Pt 3):737–749.
- [29] Witt, O., Deubzer, H. E., Milde, T., and Oehme, I. *HDAC family: What are the cancer relevant targets?* Cancer Letters (2009). 277(1):8–21.
- [30] Grozinger, C. M. and Schreiber, S. L. *Regulation of histone deacetylase 4 and 5 and transcriptional activity by 14-3-3-dependent cellular localization.* Proceedings of the National Academy of Sciences of the United States of America (2000). 97(14):7835–7840.
- [31] Hubbert, C., Guardiola, A., Shao, R., et al. *HDAC6 is a microtubule-associated deacetylase.* Nature (2002). 417(6887):455–458.
- [32] Kovacs, J. J., Murphy, P. J., Gaillard, S., et al. *HDAC6 Regulates Hsp90 Acetylation and Chaperone-Dependent Activation of Glucocorticoid Receptor.* Molecular Cell (2005). 18(5):601–607.
- [33] Lin, S.-J., Defossez, P.-A., and Guarente, L. *Requirement of NAD and SIR2 for Life-Span Extension by Calorie Restriction in Saccharomyces cerevisiae.* Science (2000). 289(5487):2126–2128.
- [34] Brunmeir, R., Lagger, S., and Seiser, C. *Histone deacetylase 1 and 2-controlled embryonic development and cell differentiation.* Int J Dev Biol (2009). 53:275–289.
- [35] Karwowska-Desaulniers, P., Ketko, A., Kamath, N., and Pflum, M. K. H. *Histone deacetylase 1 phosphorylation at S421 and S423 is constitutive in vivo, but dispensable in vitro.* Biochemical and Biophysical Research Communications (2007). 361(2):349–355.
- [36] Lagger, G., O'Carroll, D., Rembold, M., et al. *Essential function of histone deacetylase 1 in proliferation control and CDK inhibitor repression.* The EMBO Journal (2002). 21(11):2672–2681.
- [37] Montgomery, R. L., Davis, C. A., Potthoff, M. J., et al. *Histone deacetylases 1 and 2 redundantly regulate cardiac morphogenesis, growth, and contractility.* Genes & Development (2007). 21(14):1790–1802.
- [38] Zupkovitz, G., Grausenburger, R., Brunmeir, R., et al. *The cyclin-dependent kinase inhibitor p21 is a crucial target for histone deacetylase 1 as a regulator of cellular proliferation.* Molecular and Cellular Biology (2010). 30(5):1171–1181.
- [39] Trivedi, C. M., Luo, Y., Yin, Z., et al. *Hdac2 regulates the cardiac hypertrophic response by modulating Gsk3 β activity.* Nature Medicine (2007). 13(3):324–331.

- [40] Haberland, M., Johnson, A., Mokalled, M. H., Montgomery, R. L., and Olson, E. N. *Genetic dissection of histone deacetylase requirement in tumor cells*. Proceedings of the National Academy of Sciences (2009). 106(19):7751–7755.
- [41] Hayakawa, T. and Nakayama, J.-i. *Physiological Roles of Class I HDAC Complex and Histone Demethylase*. Journal of Biomedicine and Biotechnology (2011). 2011:1–10.
- [42] Bantscheff, M., Hopf, C., Savitski, M. M., et al. *Chemoproteomics profiling of HDAC inhibitors reveals selective targeting of HDAC complexes*. Nature biotechnology (2011). 29(3):255–265.
- [43] Luo, Y., Jian, W., Stavreva, D., et al. *Trans-regulation of Histone Deacetylase Activities through Acetylation*. Journal of Biological Chemistry (2009). 284(50):34901–34910.
- [44] Segré, C. V. and Chiocca, S. *Regulating the regulators: the post-translational code of class I HDAC1 and HDAC2*. Journal of Biomedicine and Biotechnology (2011). 2011:690848.
- [45] Bolden, J. E., Peart, M. J., and Johnstone, R. W. *Anticancer activities of histone deacetylase inhibitors*. Nature Reviews Drug Discovery (2006). 5(9):769–784.
- [46] Jaenisch, R. and Young, R. *Stem cells, the molecular circuitry of pluripotency and nuclear reprogramming*. Cell (2008). 132(4):567–582.
- [47] Takahashi, K. and Yamanaka, S. *Induction of Pluripotent Stem Cells from Mouse Embryonic and Adult Fibroblast Cultures by Defined Factors*. Cell (2006). 126(4):663–676.
- [48] Hanna, J., Wernig, M., Markoulaki, S., et al. *Treatment of Sick Cell Anemia Mouse Model with iPS Cells Generated from Autologous Skin*. Science (2007). 318(5858):1920–1923.
- [49] Niwa, H. *How is pluripotency determined and maintained?* Development (2007). 134(4):635–646.
- [50] Wang, J., Rao, S., Chu, J., et al. *A protein interaction network for pluripotency of embryonic stem cells*. Nature (2006). 444(7117):364–368.
- [51] Boyer, L. A., Lee, T. I., Cole, M. F., et al. *Core Transcriptional Regulatory Circuitry in Human Embryonic Stem Cells*. Cell (2005). 122(6):947–956.
- [52] Kagey, M. H., Newman, J. J., Bilodeau, S., et al. *Mediator and cohesin connect gene expression and chromatin architecture*. Nature (2010). 467(7314):430–435.
- [53] Rahl, P. B., Lin, C. Y., Seila, A. C., et al. *c-Myc Regulates Transcriptional Pause Release*. Cell (2010). 141(3):432–445.
- [54] Young, R. A. *Control of the embryonic stem cell state*. Cell (2011). 144(6):940–954.
- [55] Mattout, A. and Meshorer, E. *Chromatin plasticity and genome organization in pluripotent embryonic stem cells*. Current opinion in cell biology (2010). 22(3):334–341.
- [56] Voigt, P., LeRoy, G., Drury III, W. J., et al. *Asymmetrically Modified Nucleosomes*. Cell (2012). 151(1):181–193.
- [57] Efroni, S., Duttagupta, R., Cheng, J., et al. *Global transcription in pluripotent embryonic stem cells*. Cell Stem Cell (2008). 2(5):437–447.
- [58] Rowland, B. D., Bernards, R., and Peeper, D. S. *The KLF4 tumour suppressor is a transcriptional repressor of p53 that acts as a context-dependent oncogene*. Nature Cell Biology (2005). 7(11):1074–1082.
- [59] González, F., Boué, S., and Belmonte, J. C. I. *Methods for making induced pluripotent stem cells: reprogramming à la carte*. Nature Reviews Genetics (2011). 12(4):231–242.
- [60] Niwa, H., Miyazaki, J.-i., and Smith, A. G. *Quantitative expression of Oct-3/4 defines differentiation, dedifferentiation or self-renewal of ES cells*. Nature genetics (2000). 24(4):372–376.
- [61] Scheper, W. and Copray, S. *The molecular mechanism of induced pluripotency: a two-stage switch*. Stem Cell Reviews and Reports (2009). 5(3):204–223.
- [62] Mikkelsen, T. S., Hanna, J., Zhang, X., et al. *Dissecting direct reprogramming through integrative genomic analysis*. Nature (2008). 454(7200):49–55.
- [63] Silva, J., Barrandon, O., Nichols, J., et al. *Promotion of Reprogramming to Ground State Pluripotency by Signal Inhibition*. PLoS Biology (2008). 6(10):e253.
- [64] Huangfu, D., Maehr, R., Guo, W., et al. *Induction of pluripotent stem cells by defined factors is greatly improved by small-molecule compounds* (2008). 26(7):795–797.
- [65] Mali, P., Chou, B., Yen, J., et al. *Butyrate Greatly Enhances Derivation of Human Induced Pluripotent Stem Cells by Promoting Epigenetic Remodeling and the Expression of Pluripotency Associated Genes*. Stem Cells (2010). 28(4):713–720.

- [66] Feng, B., Ng, J.-H., Heng, J.-C. D., and Ng, H.-H. *Molecules that promote or enhance reprogramming of somatic cells to induced pluripotent stem cells*. Cell Stem Cell (2009). 4(4):301–312.
- [67] Fuchs, E. *Scratching the surface of skin development*. Nature (2007). 445(7130):834–842.
- [68] Blanpain, C. and Fuchs, E. *Epidermal homeostasis: a balancing act of stem cells in the skin*. Nature reviews Molecular cell biology (2009). 10(3):207–217.
- [69] Ito, M., Liu, Y., Yang, Z., et al. *Stem cells in the hair follicle bulge contribute to wound repair but not to homeostasis of the epidermis*. Nature Medicine (2005). 11(12):1351–1354.
- [70] Fuchs, E. and Raghavan, S. *Getting under the skin of epidermal morphogenesis*. Nature Reviews Genetics (2002). 3(3):199–209.
- [71] de Guzman Strong, C., Conlan, S., Deming, C. B., et al. *A milieu of regulatory elements in the epidermal differentiation complex syntenic block: implications for atopic dermatitis and psoriasis*. Human Molecular Genetics (2010). 19(8):1453–1460.
- [72] Patel, S., Kartasova, T., and Segre, J. A. *Mouse Sprr locus: a tandem array of coordinately regulated genes*. Mammalian Genome (2003). 14(2):140–148.
- [73] Wolf, R., Mirmohammadsadeh, A., Walz, M., et al. *Molecular cloning and characterization of alternatively spliced mRNA isoforms from psoriatic skin encoding a novel member of the S100 family*. The FASEB Journal (2003). 17(13):1969–1971.
- [74] LeBoeuf, M., Terrell, A., Trivedi, S., et al. *Hdac1 and Hdac2 Act Redundantly to Control p63 and p53 Functions in Epidermal Progenitor Cells*. Developmental Cell (2010). 19(6):807–818.
- [75] Nascimento, E. M., Cox, C. L., Macarthur, S., et al. *The opposing transcriptional functions of Sin3a and c-Myc are required to maintain tissue homeostasis*. Nature Cell Biology (2011). 13(12):1395–1405.
- [76] Lee, S. and Lee, S.-K. *Crucial roles of histone-modifying enzymes in mediating neural cell-type specification*. Current Opinion in Neurobiology (2010). 20(1):29–36.
- [77] Lee, S., Lee, B., Lee, J. W., and Lee, S.-K. *Retinoid Signaling and Neurogenin2 Function Are Coupled for the Specification of Spinal Motor Neurons through a Chromatin Modifier CBP*. Neuron (2009). 62(5):641–654.
- [78] Shakèd, M., Weissmüller, K., Svoboda, H., et al. *Histone Deacetylases Control Neurogenesis in Embryonic Brain by Inhibition of BMP2/4 Signaling*. PLoS ONE (2008). 3(7):e2668.
- [79] Montgomery, R. L., Hsieh, J., Barbosa, A. C., Richardson, J. A., and Olson, E. N. *Histone deacetylases 1 and 2 control the progression of neural precursors to neurons during brain development*. Proceedings of the National Academy of Sciences (2009). 106(19):7876–7881.
- [80] MacDonald, J. L. and Roskams, A. J. *Histone deacetylases 1 and 2 are expressed at distinct stages of neuro-glial development*. Developmental Dynamics (2008). 237(8):2256–2267.
- [81] Kazantsev, A. G. and Thompson, L. M. *Therapeutic application of histone deacetylase inhibitors for central nervous system disorders*. Nature Reviews Drug Discovery (2008). 7(10):854–868.
- [82] Lager, S., Meunier, D., Mikula, M., et al. *Crucial function of histone deacetylase 1 for differentiation of teratomas in mice and humans*. The EMBO Journal (2010). 29(23):3992–4007.
- [83] QIAGEN. *QIAfilter Plasmid Purification Handbook* (2005). Third Edition:17–22.
- [84] Corporation, P. *Wizard Genomic DNA Purification Kit Technical Manual, TM050* (2010). pages 12–13.
- [85] Morita, S., Kojima, T., and Kitamura, T. *Plat-E: an efficient and stable system for transient packaging of retroviruses*. Gene therapy (2000). 7(12):1063–1066.
- [86] Michalczyk, K. and Ziman, M. *Nestin structure and predicted function in cellular cytoskeletal organisation*. Histology and histopathology (2005). 20(2):665–671.
- [87] Nakakura, E. K., Watkins, D. N., Schübel, K. E., et al. *Mammalian Scratch: a neural-specific Snail family transcriptional repressor*. Proceedings of the National Academy of Sciences of the United States of America (2001). 98(7):4010–4015.
- [88] Rossini, L., Hashimoto, Y., Suzuki, H., et al. *VSTM2L is a novel secreted antagonist of the neuroprotective peptide Humanin*. The FASEB Journal (2011). 25(6):1983–2000.
- [89] Lossie, A. C., Nakamura, H., Thomas, S. E., and Justice, M. J. *Mutation of I7Rn3 shows that Odz4 is required for mouse gastrulation*. Genetics (2005). 169(1):285–299.
- [90] Tabibzadeh, S. and Hemmati-Brivanlou, A. *Lefty at the crossroads of "stemness" and differentiative events*. Stem Cells (2006). 24(9):1998–2006.
- [91] Halsall, J., Gupta, V., O'Neill, L. P., Turner, B. M., and Nightingale, K. P. *Genes Are Often Sheltered from the*

Global Histone Hyperacetylation Induced by HDAC Inhibitors. PLoS ONE (2012). 7(3):e33453.

- [92] Langmead, B., Trapnell, C., Pop, M., and Salzberg, S. L. *Ultrafast and memory-efficient alignment of short DNA sequences to the human genome*. Genome biology (2009). 10(3):R25.
- [93] Nicol, J. W., Helt, G. A., Blanchard, S. G., Raja, A., and Loraine, A. E. *The Integrated Genome Browser: free software for distribution and exploration of genome-scale datasets*. Bioinformatics (2009). 25(20):2730–2731.
- [94] Zhang, Y., Liu, T., Meyer, C. A., et al. *Model-based analysis of ChIP-Seq (MACS)*. Genome biology (2008). 9(9):R137.
- [95] Wang, Z., Zang, C., Cui, K., et al. *Genome-wide Mapping of HATs and HDACs Reveals Distinct Functions in Active and Inactive Genes*. Cell (2009). 138:1–13.
- [96] Kidder, B. L. and Palmer, S. *HDAC1 regulates pluripotency and lineage specific transcriptional networks in embryonic and trophoblast stem cells*. Nucleic Acids Research (2012). 40(7):2925–2939.
- [97] Ye, T., Krebs, A. R., Choukrallah, M.-A., et al. *seqMINER: an integrated ChIP-seq data interpretation platform*. Nucleic Acids Research (2011). 39(6):e35.
- [98] Shin, H., Liu, T., Manrai, A. K., and Liu, X. S. *CEAS: cis-regulatory element annotation system*. Bioinformatics (2009). 25(19):2605–2606.
- [99] Gartel, A. L. and Radhakrishnan, S. K. *Lost in Transcription: p21 Repression, Mechanisms, and Consequences*. Cancer Research (2005). 65(10):3980–3985.
- [100] Lagger, G., Dötzelhofer, A., Schüttengruber, B., et al. *The Tumor Suppressor p53 and Histone Deacetylase 1 Are Antagonistic Regulators of the Cyclin-Dependent Kinase Inhibitor p21/WAF1/CIP1 Gene*. Molecular and Cellular Biology (2003). 23(8):2669–2679.
- [101] Perry, R. P. and Kelley, D. E. *Inhibition of RNA synthesis by actinomycin D: characteristic dose-response of different RNA species*. Journal of cellular physiology (1970). 76(2):127–139.
- [102] Choong, M. L., Yang, H., Lee, M. A., and Lane, D. P. *Specific activation of the p53 pathway by low dose actinomycin D: a new route to p53 based cyclotherapy*. Cell Cycle (2009). 8(17):2810–2818.
- [103] Lohrum, M. A. E., Ludwig, R. L., Kubbutat, M. H. G., Hanlon, M., and Vousden, K. H. *Regulation of HDM2 activity by the ribosomal protein L11*. Cancer cell (2003). 3(6):577–587.
- [104] Ramirez, A., Page, A., Gandarillas, A., et al. *A keratin K5Cre transgenic line appropriate for tissue-specific or generalized Cre-mediated recombination*. Genesis (2004). 39(1):52–57.
- [105] Winter, M. *The Role of the Epigenetic Regulators HDAC1, HDAC2 and DNMT1 in Mouse Epidermis Development and Tumorigenesis*. Dissertation Universität Wien (2012).
- [106] Schüttengruber, B., Simböck, E., Khier, H., and Seiser, C. *Autoregulation of mouse histone deacetylase 1 expression*. Molecular and Cellular Biology (2003). 23(19):6993–7004.
- [107] Strachan, L., Murison, J. G., Prestidge, R. L., et al. *Cloning and biological activity of epigen, a novel member of the epidermal growth factor superfamily*. The Journal of biological chemistry (2001). 276(21):18265–18271.
- [108] Hershfield, M. S. *Genotype is an important determinant of phenotype in adenosine deaminase deficiency*. Current Opinion in Immunology (2003). 15(5):571–577.
- [109] Gibbs, S., Fijneman, R., Wiegant, J., et al. *Molecular characterization and evolution of the sprr family of keratinocyte differentiation markers encoding small proline-rich proteins*. Genomics (1993). 16(3):630 – 637.
- [110] Abel, T. and Zukin, R. S. *Epigenetic targets of HDAC inhibition in neurodegenerative and psychiatric disorders*. Current opinion in pharmacology (2008). 8(1):57–64.
- [111] Tronche, F., Kellendonk, C., Kretz, O., et al. *Disruption of the glucocorticoid receptor gene in the nervous system results in reduced anxiety*. Nature genetics (1999). 23(1):99–103.
- [112] Dashwood, M. R. and Loesch, A. *Endothelin-1 as a neuropeptide: neurotransmitter or neurovascular effects?* Journal of cell communication and signaling (2010). 4(1):51–62.
- [113] De Boer, E., Rodriguez, P., Bonte, E., et al. *Efficient biotinylation and single-step purification of tagged transcription factors in mammalian cells and transgenic mice*. Proceedings of the National Academy of Sciences of the United States of America (2003). 100(13):7480–7485.
- [114] Davis, H. E., Rosinski, M., Morgan, J. R., and Yarmush, M. L. *Charged polymers modulate retrovirus transduction via membrane charge neutralization and virus aggregation*. Biophysical journal (2004). 86(2):1234–1242.
- [115] Sommer, C. A., Stadtfeld, M., Murphy, G. J., et al. *Induced Pluripotent Stem Cell Generation Using a Single Lentiviral Stem Cell Cassette*. Stem Cells (2009). 27(3):543–549.

- [116] O'Connor, M. D., Kardel, M. D., Iosifina, I., et al. *Alkaline phosphatase-positive colony formation is a sensitive, specific, and quantitative indicator of undifferentiated human embryonic stem cells*. *Stem Cells* (2008). 26(5):1109–1116.
- [117] Hotta, A. and Ellis, J. *Retroviral vector silencing during iPS cell induction: an epigenetic beacon that signals distinct pluripotent states*. *Journal of Cellular Biochemistry* (2008). 105(4):940–948.
- [118] Wang, R., Liang, J., Jiang, H., Qin, L.-J., and Yang, H.-T. *Promoter-Dependent EGFP Expression during Embryonic Stem Cell Propagation and Differentiation*. *Stem Cells and Development* (2008). 17(2):279–290.
- [119] Wang, A., Kurdastani, S. K., and Grunstein, M. *Requirement of Hos2 histone deacetylase for gene activity in yeast*. *Science* (2002). 298(5597):1412–1414.
- [120] Hazzalin, C. A. and Mahadevan, L. C. *Dynamic Acetylation of All Lysine 4–Methylated Histone H3 in the Mouse Nucleus: Analysis at c-fos and c-jun*. *PLoS Biology* (2005). 3(12):e393.
- [121] Robert, F., Pokholok, D. K., Hannett, N. M., et al. *Global position and recruitment of HATs and HDACs in the yeast genome*. *Molecular Cell* (2004). 16(2):199–209.
- [122] Jelinic, P., Pellegrino, J., and David, G. *A Novel Mammalian Complex Containing Sin3B Mitigates Histone Acetylation and RNA Polymerase II Progression within Transcribed Loci*. *Molecular and Cellular Biology* (2011). 31(1):54–62.
- [123] Sun, J.-M., Chen, H. Y., and Davie, J. R. *Differential distribution of unmodified and phosphorylated histone deacetylase 2 in chromatin*. *The Journal of biological chemistry* (2007). 282(45):33227–33236.
- [124] Lenstra, T. and Holstege, F. C. P. *The discrepancy between chromatin factor location and effect*. *Nucleus* (Austin, Tex) (2012). 3(3).
- [125] Hezroni, H., Sailaja, B. S., and Meshorer, E. *Pluripotency-related, valproic acid (VPA)-induced genome-wide histone H3 lysine 9 (H3K9) acetylation patterns in embryonic stem cells*. *Journal of Biological Chemistry* (2011). 286(41):35977–35988.
- [126] Lin, Y.-y., Kiihl, S., Suhail, Y., et al. *Functional dissection of lysine deacetylases reveals that HDAC1 and p300 regulate AMPK*. *Nature* (2012). 482(7384):251–255.
- [127] Anokye-Danso, F., Trivedi, C. M., Jühr, D., et al. *Highly efficient miRNA-mediated reprogramming of mouse and human somatic cells to pluripotency*. *Cell Stem Cell* (2011). 8(4):376–388.
- [128] Karantzali, E., Schulz, H., Hummel, O., et al. *Histone deacetylase inhibition accelerates the early events of stem cell differentiation: transcriptomic and epigenetic analysis*. *Genome biology* (2008). 9(4):R65.
- [129] Lee, J.-H., Hart, S. R. L., and Skalnik, D. G. *Histone deacetylase activity is required for embryonic stem cell differentiation*. *Genesis* (2004). 38(1):32–38.

CURRICULUM VITAE

Name: Simon Weissmann

Date of birth: 29.06.1987, Vienna

Nationality: Austrian

Education

May 2011 – June 2012	Master thesis project “The Role of HDAC1 and HDAC2 in Transcription and Induced Pluripotency” at the Institute of Medical Biochemistry, University of Vienna, Group of Christian Seiser
2010	Completion of Bachelor studies and start of Master studies “Molecular Medicine” at the University of Vienna
2009	ERASMUS exchange semester at the University of Leicester, GB
2008 - 2009	Bachelor specialization in „Microbiology and Genetics“
2007 - 2008	Bachelor studies of general biology at the University of Vienna
1998 - 2006	Secondary school with extended courses in natural sciences “Sachsenbrunn”, Kirchberg am Wechsel, Lower Austria
1994 - 1998	Elementary school Zöbern, Lower Austria

Acknowledgements

Mein besonderer Dank gilt meinem Betreuer Christian Seiser, der in mir das Interesse an der Epigenetik geweckt hat. Danke für die Möglichkeit an diesen spannenden Projekten mitzuarbeiten. Danke für die fachliche Betreuung und die persönliche Unterstützung.

Ein spezieller Dank geht an Gordin Zupkovitz ohne dessen geduldige Hilfe, diese Arbeit nicht möglich gewesen wäre. Danke für all die Dinge die du mir in so kurzer Zeit beigebracht hast, beginnend bei molekularbiologischen Techniken bis hin zur Einführung in Welt der genomweiten Genregulation.

Ein besonderes Dziękuję geht auch an Ania die mir immer und überall geholfen hat und sowieso eigentlich eh alles weiß.

Danke auch an alle Lab7-Kollegen, für die angenehme Atmosphäre inner- und außerhalb des Labors. Vielen Dank: Astrid, Mirjam, Tina, Mircea, Juli, Dominik, Kathi, Manuela und Carina.

Des Weiteren danke ich auch Matthias Artaker, Roman Stocsits und der CSF-Sequencing Facility für die Unterstützung unserer Projekte.

Ein extra Dankeschön gilt auch Ania, Mirjam und Astrid für das genaue Korrekturlesen und Kommentieren meiner Arbeit.

Ein ganz spezieller Dank geht an meinen Eltern die mich nicht nur moralisch und finanziell, sondern auch durch kritische Diskussionen über Konduktivität und bovine Paradoxien unterstützt haben.

Danken möchte ich auch dem Rest meiner Familie, insbesondere meinen zwei Brüdern.

Danke MTJ.